

Dissertation zur Erlangung des Doktorgrades
der Fakultät für Chemie und Pharmazie
der Ludwig-Maximilians-Universität München

Translational control
by the multi-KH domain protein Scp160



Heidrun Schreck

aus

Engelskirchen

2010

Erklärung

Diese Dissertation wurde im Sinne von §13 Abs. 3 bzw. 4 der Promotionsordnung vom 29. Januar 1998 von Herrn Professor Dr. Ralf-Peter Jansen betreut.

Ehrenwörtliche Versicherung

Diese Dissertation wurde selbständig und ohne unerlaubte Hilfe erarbeitet.

München, den 03.05.2010

.....

Heidrun Schreck

Dissertation eingereicht am: 03.05.2010

1. Gutachter: Prof. Dr. Ralf-Peter Jansen
2. Gutachter: Prof. Dr. Klaus Förstemann

Mündliche Prüfung am: 08.07.2010

1. SUMMARY	1
2. INTRODUCTION	2
2.1. The mRNA lifecycle is coordinated by RNA-binding proteins	2
2.2. A glimpse of translation	4
2.3. Don't get lost in translation – translational control	6
2.3.1. Global control of translation.....	7
2.3.2. Target-specific translational regulation.....	9
2.3.3. Control of translation elongation and termination.....	10
2.4. hnRNP K-homology (KH) domains interact with RNA	11
2.5. Vigilins – a conserved family of multi KH-domain proteins	13
2.5.1. Human vigilin.....	13
2.5.2. Vigilin in <i>Xenopus laevis</i>	15
2.5.3. DDP1 is the vigilin homologue in <i>Drosophila melanogaster</i>	16
2.5.4. Scp160, the yeast homologue of vigilin	17
2.6. Scp160 is implicated in diverse cellular processes	17
2.6.1. Ploidy control.....	17
2.6.2. Scp160 associates with RNA	18
2.6.3. Regulation of telomeric silencing.....	18
2.6.4. A functional role in the mating response pathway	19
2.6.5. Translational control.....	19
3. AIMS OF THIS STUDY.....	21
4. RESULTS.....	22
4.1. Scp160 interacts with ribosomes	22
4.1.1. Scp160 copurifies with ribosomal proteins in a partially RNA-dependent manner.....	22
4.1.2. Scp160, Bfr1 and Stm1 bind to overlapping sets of ribosomes.....	23
4.1.3. Ribosome association of Scp160 is only partially dependent on KH domains 13/14 and Asc1	24
4.2. Scp160 associates with ribosome-containing cellular subfractions.....	25
4.2.1. Deletion of KH domains 13/14 induces a non-ribosome associated pool of Scp160	25
4.2.2. Mutation of conserved RNA binding domains causes partial loss of ribosome association.....	27
4.2.3. Scp160's subcellular localization remains unchanged upon diverse environmental changes.....	28
4.2.3.1. Pheromone treatment	29

TABLE OF CONTENTS

4.2.3.2. Heat shock	30
4.2.3.3. Hyperosmotic shock	31
4.2.3.4. Tunicamycin-induced ER stress.....	31
4.3. A possible role for Scp160 in translation	33
4.3.1. <i>scp160</i> deletion strains display reduced fitness and sensitivity against translation inhibitors.....	33
4.3.2. Translation initiation is slightly impaired in <i>scp160</i> deletion strains.....	34
4.4. A Tet-off system for the efficient depletion of Scp160	34
4.5. Translational profiling – elucidating the function of Scp160 in translation	36
4.5.1. Depletion of Scp160 causes subtle changes at the transcriptome level.....	38
4.5.2. Depletion of Scp160 induces translational state changes of a subset of mRNAs	40
4.6. mRNAs with significant translational state changes are bound by Scp160	44
4.6.1. Target mRNAs are enriched in immunoprecipitates of Scp160	44
4.6.2. Conserved residues in KH domains 13 and 14 are essential for target RNA binding.....	46
4.7. Scp160 is required for efficient translation of <i>PRY3</i> mRNA.....	47
4.7.1. <i>Pry3</i> -6HA protein levels are reduced in cells lacking Scp160.....	47
4.7.2. <i>Pry3</i> ΔGPI protein levels are reduced upon loss of Scp160.....	48
4.7.3. Enhanced degradation is not responsible for reduced levels of <i>Pry3</i> protein.....	50
4.8. Depletion of <i>PRY3</i> triggers polyploidization.....	51
4.9. Overexpression of <i>Pry3</i> does not rescue the polyploidy phenotype of <i>scp160</i> deletion strains	52
5. DISCUSSION.....	53
5.1. SCP160 BINDS TO RIBOSOMES.....	53
5.2. NO EVIDENCE FOR A REGULATORY SUBCELLULAR RE-LOCALIZATION OF SCP160.....	56
5.3. SCP160 MODULATES TRANSLATION OF A SPECIFIC SET OF MRNAs	57
5.4. A LINK BETWEEN TRANSLATIONAL REGULATION AND PLOIDY CONTROL. 62	
6. MATERIAL AND METHODS.....	65
6.1. Materials	65

TABLE OF CONTENTS

6.1.1. Consumables and chemicals	65
6.1.2. Commercially available kits.....	65
6.1.3. Equipment	66
6.1.4. Enzymes.....	67
6.1.5. Antibodies.....	67
6.1.6. Oligonucleotides	68
6.1.7. Plasmids.....	70
6.1.8. Strains	71
6.1.8.1. <i>E. coli</i>	71
6.1.8.2. <i>S. cerevisiae</i> strains.....	71
6.2. Methods	72
6.2.1. Standard methods.....	72
6.2.2. SDS-PAGE and Western blotting.....	72
6.2.3. Yeast-specific techniques	73
6.2.3.1. Culture of <i>S. cerevisiae</i>	73
6.2.3.2. Dot spots.....	73
6.2.3.3. Transformation of yeast cells.....	73
6.2.3.4. Knock-out and tagging of yeast genes	74
6.2.4. Preparation of nucleic acids and cell extracts.....	75
6.2.4.1. Preparation of RNA	75
6.2.4.2. Preparation of DNA	75
6.2.4.3. Alkaline lysis	76
6.2.4.4. Preparation of native whole cell extracts.....	76
6.2.5. Sucrose density gradients	76
6.2.5.1. Sucrose density gradient fractionation	76
6.2.5.2. RNA purification from gradient fractions.....	77
6.2.6. Subcellular fractionation.....	77
6.2.7. Tet-off depletion system	78
6.2.8. FACS analysis.....	78
6.2.9. Microarray analysis	79
6.2.9.1. Sample preparation and microarray hybridization.....	79
6.2.9.2. Microarray data analysis.....	79
6.2.9.3. Systematic classification of proteins	80
6.2.10. Quantitative real-time PCR (qPCR).....	80
6.2.11. Immunoprecipitation.....	80
6.2.11.1. Covalent coupling of α myc antibody to Protein G beads	80
6.2.11.2. Immunoprecipitation and preparation of RNA.....	81
6.2.12. Tandem Affinity Purification (TAP).....	81
6.2.12.1. Cell culture and lysis.....	81
6.2.12.2. Purification and TCA precipitation.....	82

TABLE OF CONTENTS

7. ABBREVIATIONS 83

8. REFERENCES..... 85

9. APPENDIX 94

10. CURRICULUM VITAE 95

11. ACKNOWLEDGEMENT 96

1. Summary

The control of mRNA translation mediated by RNA-binding proteins (RBPs) is a key player in modulating gene expression. In *S. cerevisiae*, the multi-KH domain protein Scp160 associates with a large number of mRNAs and is present on membrane-bound and, to a lesser extent, cytosolic polysomes. Its binding site on the ribosome is close to the mRNA exit tunnel and in vicinity to Asc1, which constitutes a binding platform for signaling molecules. The present study focused on the closer characterization of the Scp160-ribosome interaction and on the suggested function of Scp160 in modulating the translation of specific target mRNAs.

Using affinity purifications, the partial RNA-dependence of the Scp160-ribosome association was confirmed. In contrast to published results, ribosome association was found to be only slightly reduced but not abolished in the absence of Asc1 or the last two KH domains. Furthermore, the putative elongation regulator Stm1 was identified as a co-purifier of Scp160. In subcellular fractionation experiments, RNA-binding mutants of Scp160 were present in the ribosome-free cytosolic fraction and therefore partially deficient in ribosome association and/or mRNP formation. However, no physiological conditions were found that equally induce a shift of wildtype Scp160 towards the cytosolic fraction.

Within the scope of a translational profiling approach, microarray analyses of RNA isolated from sucrose density gradient fractions were performed and led to the identification of a set of mRNAs that shift their position within the gradients upon Scp160 depletion, indicating changes in their translation rates. Consistent with the membrane localization of Scp160, transcripts encoding secreted proteins were significantly enriched. Using immunoprecipitation and subsequent quantitative real-time PCR (qRT-PCR), the interaction of Scp160 with a subgroup of the identified targets was confirmed and it was shown that their binding is dependent on the conserved GXXG motifs in the two C-terminal KH domains of Scp160. Furthermore, data were obtained indicating that Scp160 can act as a translational activator on some of its target mRNAs, probably on the level of translation elongation. Finally, first evidence was provided that the translational misregulation of specific target transcripts may be involved in the polyploidization that is a hallmark of Scp160-deprived cells.

In summary, these data substantiate the assumption that Scp160 is involved in translational regulation of a specific, functionally related subset of mRNAs. This finding is in good accordance with the emerging view that RBPs co-regulate multiple transcripts in order to allow faster adaptation to environmental changes.

2. Introduction

2.1. The mRNA lifecycle is coordinated by RNA-binding proteins

On the post-transcriptional level, RNA binding proteins (RBPs) represent what transcription factors are on the level of transcription – they form a complex, multi-layered regulatory network that tightly controls all stages of the RNA lifecycle. In this section, a brief overview of the numerous processes that determine the fate of an mRNA in the budding yeast *S. cerevisiae* will be given, impressively demonstrating the prominent position of RBPs in the control of gene expression.

In the nucleus, ribonucleoprotein complexes, or short RNPs, start to form by the association of specific nuclear RBPs with nascent mRNAs even before transcription is completed (see Fig. 1). For example, the conserved four-protein complex THO associates with actively transcribed genes (Strasser et al., 2002; Abruzzi et al., 2004) in order to prevent the formation of RNA/DNA hybrids that promote hyperrecombination and transcriptional impairment. THO associates with Yra1, Sub2 and SR(serine/arginine-rich)-like proteins to form the TREX (TRanscription/EXport) complex which is involved in nuclear export of the nascent mRNP (Strasser et al., 2002). Interestingly, some of the factors that promote mRNA export are also involved in pre-mRNA splicing, for example Npl3 (Kress et al., 2008) and Sub2 (Zhang & Green, 2001). Other RBPs are required for co-transcriptional RNA processing, including the addition of the 7-methylguanosine (7mG) cap to the 5' end of the nascent transcript which protects it from degradation (Shatkin & Manley, 2000). Co-transcriptional events also include 3' end cleavage immediately downstream of the polyadenylation site in the 3'-untranslated region (UTR) (Zhao et al., 1999), leading to the release of the nascent RNA from the transcription complex. Subsequently, the poly(A) tail is added by a poly(A) polymerase and bound by the nuclear poly(A)-binding protein Nab2 (Mangus et al., 2003). By its interaction with the nuclear pore-associated protein Mlp1, Nab2 promotes export of mature mRNAs (Fasken et al., 2008). Mlp1 is in addition involved in the nuclear retention of unspliced transcripts (Galy et al., 2004). In general, mRNA processing in the nucleus underlies strict quality control mechanisms, leading to the degradation of aberrant transcripts that are produced when mRNP assembly is impaired (reviewed in Fasken & Corbett, 2009). Correctly processed and packaged, mRNPs are exported through nuclear pore complexes (NPCs), which is facilitated by the interaction of the Mex67/Mtr2 heterodimer with nucleoporins (Braun et al., 2002). At the NPC cytoplasmic face, the DEAD-box RNA helicase Dbp5 assists in remodeling the mRNP, e.g. by removing Mex67/Mtr2 (Lund & Guthrie, 2005) and Pab2 (Tran et al., 2007), and thus prevents mRNPs from returning to the nucleus (Stewart, 2007).

Once in the cytoplasm, many mRNAs immediately enter the translationally active pool. The nuclear cap-binding complex formed by CBC20 and CBC80 is replaced by eIF4E, the major cytoplasmic cap-binding protein, and nuclear Nab2 is exchanged for Pab1, the cytoplasmic poly(A)-binding protein (Mangus et al., 2003). Interactions between Pab1, translation initiation factor eIF4G and cap-binding protein eIF4E induce the translation-competent "closed loop" conformation of the mRNA (Wells et al., 1998) that promotes ribosomal 40S subunit recruitment and therefore translation initiation (see section 2.2.; Tarun et al., 1997).

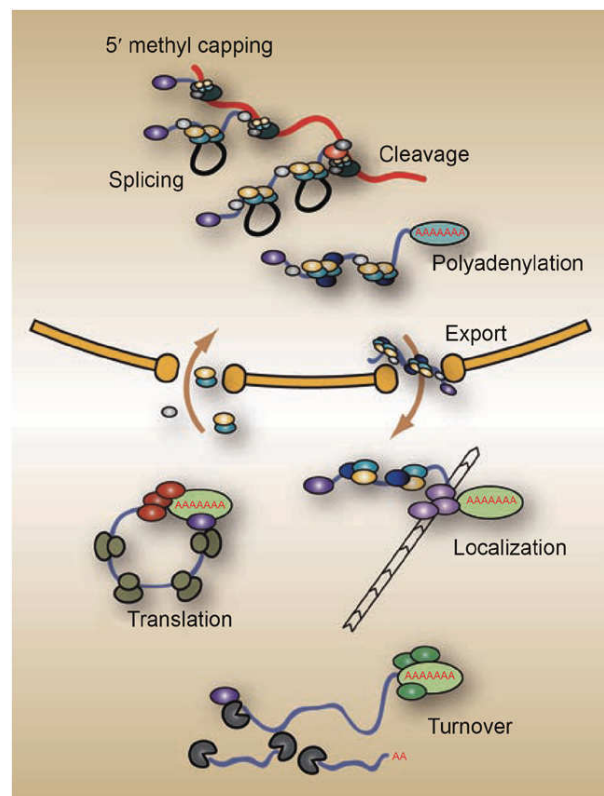


Fig. 1. The mRNA lifecycle is determined by combinatorial action of a plethora of RBPs. In the nucleus, pre-mRNA is processed in a co- and posttranscriptional manner by 5' end capping, splicing if required, 3' cleavage and polyadenylation. During these processes, quality control is exerted by the nuclear exosome. Correctly assembled mRNPs are exported through the nuclear pores and, in some cases, transported to specific subcellular regions. Translation of the transcripts often underlies control mechanisms. Eventually, mRNAs are degraded either through the normal decay pathway or through pathways specific for the removal of aberrant transcripts (figure from McKee & Silver, 2007).

However, translation of a large number of mRNAs is known to be spatially restricted. For example, one-tenth of randomly selected mRNAs of the *Drosophila* oocyte are specifically localized to its anterior pole (Dubowy & Macdonald, 1998), and in mammalian neurons, approximately 400 mRNAs are targeted to the dendrites (Eberwine et al., 2001). In many cases, it is known that the localized transcript is held in a translationally quiescent state upon nuclear

export to prevent ectopic expression (Huang & Richter, 2004). Localization of specific transcripts is dependent on "zipcodes" that are usually found in the 3' or 5' UTRs and that are recognized by RBPs that link the mRNA to the localization machinery (Paquin & Chartrand, 2008).

mRNAs have limited lifetimes, and regulation of their controlled degradation is another important mechanism in the modulation of gene expression. In most cases, degradation is induced by shortening of the poly(A) tail, which leads to the removal of the 5' cap structure (decapping) and thereby exposes the transcript to digestion by a 5'-3'-exonuclease (Parker & Song, 2004). Variations on this theme occur in nonsense-mediated decay (NMD) and nonstop decay (NSD) pathways, in which 3'-5'-degradation of aberrant mRNAs by the exosome plays an important role (Schmid & Jensen, 2008). mRNA degradation is believed to take place in P-bodies, cytoplasmic foci that contain the general repression/decay machinery (Parker & Sheth, 2007). P-bodies may not only serve degradation, but can also be used to store mRNAs for a subsequent return to the translation cycle (Brenques et al., 2005).

This overview illustrates that mRNAs are subject to diverse regulatory activities exerted by different classes of RBPs. Many of these control mechanisms rely on the combinatorial action of several factors, adding an additional layer of complexity which ensures that each individual transcript is appropriately regulated (Hogan et al., 2008). Taken together, this explains why there is wide variability in the degree to which mRNA and protein abundances correlate (Moore, 2005), and much more research will be required to obtain an exhaustive picture of the mechanisms that are involved in post-transcriptional control.

2.2. A glimpse of translation

Before going into details of translational control mechanisms, this section intends to give a short overview about eukaryotic translation. The translation process can be subdivided into three stages: initiation, elongation and termination, all of which require a specific subset of accessory factors (refer to Fig. 2).

The first step of initiation is the assembly of the ternary complex consisting of methionine-loaded initiator tRNA and GTP-bound eIF2. Together with initiation factors eIF3, eIF5, eIF1 and eIF1A, the ternary complex associates with the 40S small ribosomal subunit to form the 43S pre-initiation complex. On the side of the mRNA, initiation requires the association of the eIF4F complex with the cap structure at the 5' end of the transcript. The eIF4F complex is composed of the cap-binding factor eIF4E, the scaffolding protein eIF4G, and the RNA helicase eIF4A, whose activity is stimulated by its co-factor eIF4B (Rozen et al., 1990). Mediated by the

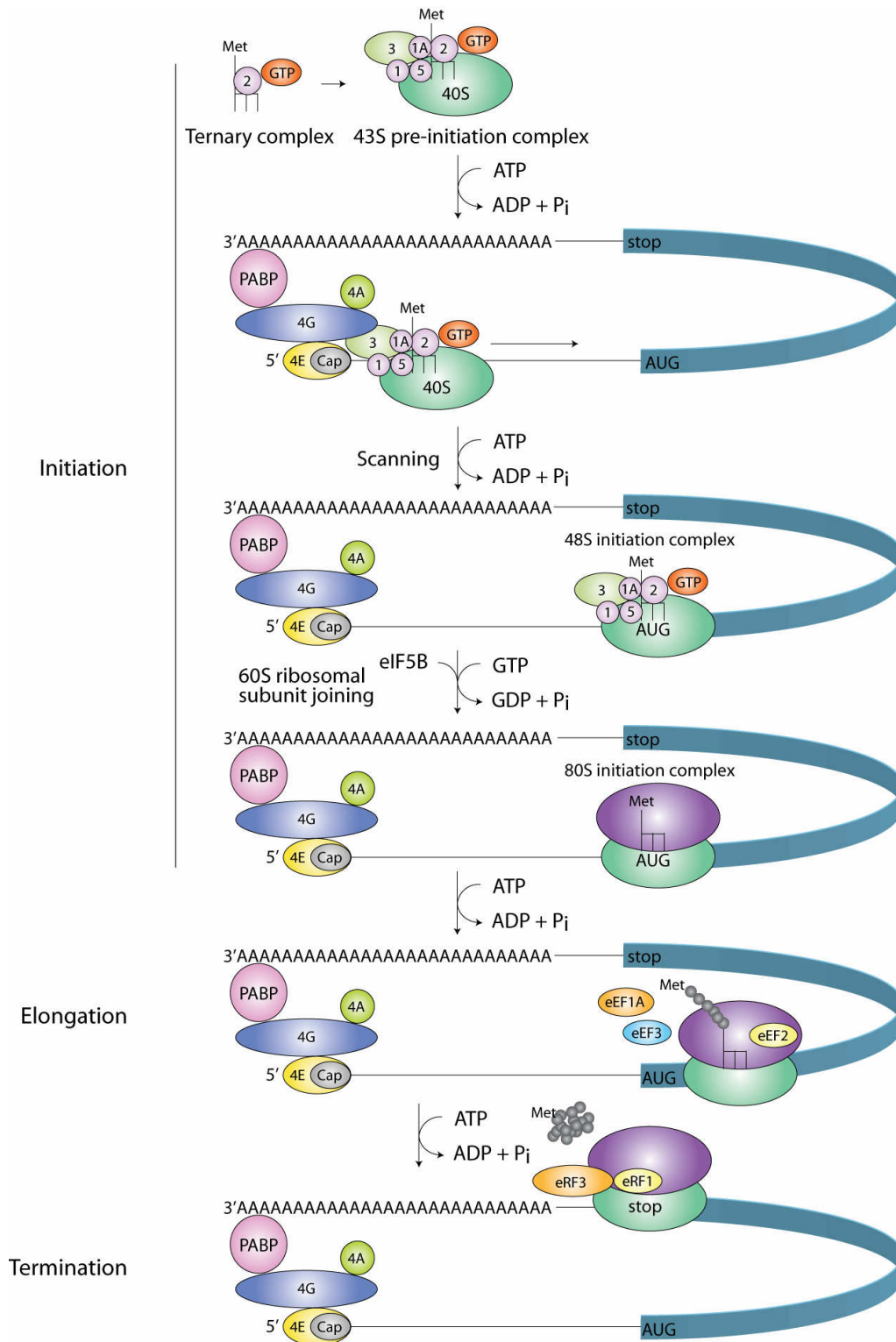


Fig. 2. A schematic view of eukaryotic translation. The translation process can be subdivided into three steps: initiation, elongation and termination. During initiation, the ternary complex binds to the 40S subunit and forms the 43S pre-initiation complex, which then associates with the mRNA. This 48S pre-initiation complex scans the transcript for the initiator AUG, where the 60S ribosomal subunit joins and elongation begins. Upon recognition of a stop codon, translation is terminated and the polypeptide chain released. For details, see text. Eukaryotic initiation factors (eIFs) are depicted as colored, numbered shapes; some eIFs have been omitted for simplicity. PABP refers to poly(A) binding protein; P_i – pyrophosphate (figure adapted from Gebauer & Hentze, 2004).

interaction between initiation factors eIF4G and eIF3, the ternary complex is loaded onto the mRNA whereupon it is referred to as the 48S pre-initiation complex. Assisted by the initiation factors eIF1, eIF1A and the helicase DHX29, the 48S complex scans the transcript for the AUG initiation codon where it is joined by the 60S large ribosomal subunit and starts translation elongation. For an extensive review on translation initiation, see Preiss and Hentze (2003).

As opposed to the large number of accessory factors that are required for initiation, only three factors are needed for polypeptide elongation in fungi: eEF1A, eEF2 and eEF3. eEF1A is responsible for the delivery of aminoacyl tRNAs to the ribosome, whereas eEF2 promotes the GTP-dependent translocation of the nascent protein chain from the A-site to the P-site (Taylor DJ, 2007). In contrast to eEF1A and eEF2, the ATPase eEF3 is only present in fungi, where it is essential for the binding of the ternary complex to the ribosomal A-site and is thought to facilitate the clearance of deacyl-tRNA from the E-site (Andersen et al., 2006).

The release factor eRF1 mediates termination by recognition of one of the three possible stop codons and subsequent binding to the ribosome in place of a tRNA. Together with association of eRF3, this stimulates the hydrolysis of GTP and the release of the peptide chain from the ribosome (reviewed by Mugnier & Tuite, 1999).

2.3. Don't get lost in translation – translational control

Translation is dependent on a sophisticated cellular machinery and is a highly energy-consuming process. A rapidly growing yeast cell, for example, contains nearly 200 000 ribosomes that occupy as much as 30-40% of the cytoplasmic volume (Warner, 1999). In fast growing *E. coli* cells, 30-50% of the energy gained from nutrient uptake is consumed by protein synthesis (Meisenberg G, 1998). Not to tightly monitor and regulate the translation process would therefore be detrimental to the cell, and indeed, control mechanisms have been found to act on virtually every level of translation. However, initiation is the step that is targeted by the vast majority of those mechanisms (Jackson et al., 2010).

Two general modes of translational regulation exist: First, global control which mainly occurs by the modification of translation initiation factors and thus affects translation of most transcripts (see section 2.3.1.), and second, target-specific control that is mediated by regulatory proteins recognizing specific structural features that are usually present in the UTRs (refer to section 2.3.2.; Gebauer & Hentze, 2004).

2.3.1. Global control of translation

Global translational regulation is for example mediated by various stress conditions such as nutrient depletion, heat shock or high osmolarity. Besides regulation at the transcriptional level, the elicited stress response generally involves translational repression of the majority of mRNAs. However, some transcripts that encode stress-relevant proteins are preferentially translated under these *a priori* repressing conditions. Taken together, the combined transcriptional and translational response enables the cell to adapt to the stress condition (Smirnova et al., 2005; Hinnebusch, 2005).

One of the best-characterized mechanisms of global translation repression is based on phosphorylation of eukaryotic initiation factor 2 (eIF2) (reviewed in Hinnebusch, 2005). Together with methionine-loaded initiator tRNA, GTP-bound eIF2 is part of the ternary complex that associates with the small ribosomal subunit to form the 43S pre-initiation complex (see Fig. 2). When the startcodon is recognized, GTP is hydrolyzed, leaving eIF2 in its GDP-bound form. To reactivate the ternary complex, GDP has to be exchanged for GTP which is mediated by eIF2B. This reaction is repressed when the three-subunit complex eIF2 is phosphorylated at a specific serine (Ser51) of its alpha subunit (eIF2 α); furthermore, the dissociation of phosphorylated eIF2 from eIF2B is blocked, so that eIF2B is sequestered (Fig. 3). The resulting reduction in the amount of active ternary complexes efficiently represses general translation initiation. In yeast, Gcn2 (general control non-derepressible 2) is the only kinase known to phosphorylate eIF2 α . Gcn2 activity is stimulated by uncharged tRNAs that accumulate during environmental stresses such as high salinity (Goossens et al., 2001), oxidizing conditions (Mascarenhas et al., 2008), nutrient starvation (Hinnebusch, 2005), or exposure to rapamycin (Cherkasova & Hinnebusch, 2003).

Interestingly, the transcription-factor encoding *GCN4* mRNA is preferably translated during these conditions due to a complex mechanism involving regulatory upstream ORFs (uORFs) (reviewed in Hinnebusch, 2005). Data from a recent large-scale study suggest that *GCN4* is not the only mRNA escaping eIF2 α phosphorylation-induced translational repression, but that in fact as many mRNAs may be regulated at the level of translation as at the level of transcription (Smirnova et al., 2005).

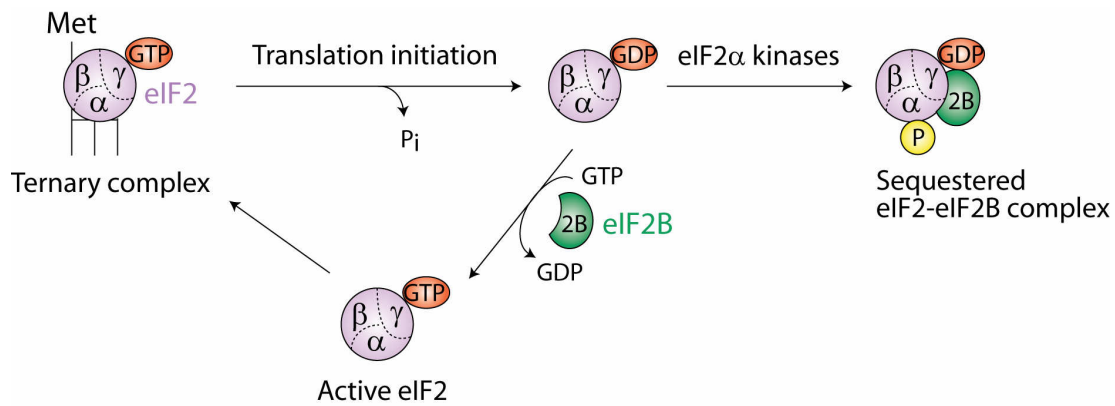


Fig. 3. Global translational control by eIF2 α phosphorylation. The three subunit-containing initiation factor eIF2 is part of the ternary complex in its GTP-bound form. During translation initiation, GTP is hydrolyzed. To regenerate active eIF2, bound GDP has to be exchanged for GTP; this reaction is catalyzed by the guanine nucleotide exchange factor (GEF) eIF2B. If eIF2 is phosphorylated on its alpha subunit, the dissociation rate of eIF2B is reduced so that the cellular pool of this exchange factor is depleted and eIF2 regeneration blocked. P_i – pyrophosphate (figure adapted from Gebauer & Hentze, 2004).

General translation rates are also regulated via the availability of the cap-binding protein eIF4E (reviewed in Rhoads, 2009). eIF4E interacts with the scaffold protein eIF4G and is required for cap-mediated recruitment of the 43S ribosomal complex to the mRNA (Gingras et al., 1999). The domain of eIF4G that is responsible for the association with eIF4E is shared by the 4E-binding proteins (4E-BPs), leading to a competition for eIF4E binding between eIF4G and 4E-BPs (refer to Fig. 4). Whereas interaction with eIF4G promotes translation initiation, association with a 4E-BP inhibits the binding of the 43S complex to the mRNA. The activity of 4E-BPs is regulated by phosphorylation: Only the hypophosphorylated form binds to eIF4E, whereas hyperphosphorylation releases the interaction (Pause et al., 1994). The 4E-BPs of budding yeast, Eap1 and Caf20, inhibit general translation initiation in response to stress conditions such as presence of cadmium and diamides in the growth medium or the occurrence of membrane stress (Deloche et al., 2004; Mascarenhas et al., 2008). In analogy to regulation exerted by phosphorylation of eIF2 α , some mRNAs experience enhanced translation in a situation in which 4E-BPs are activated. For example, cap-independent translation is promoted (Svitkin et al., 2005) and has been demonstrated to be required for physiological adaptation to stress (Gilbert et al., 2007).

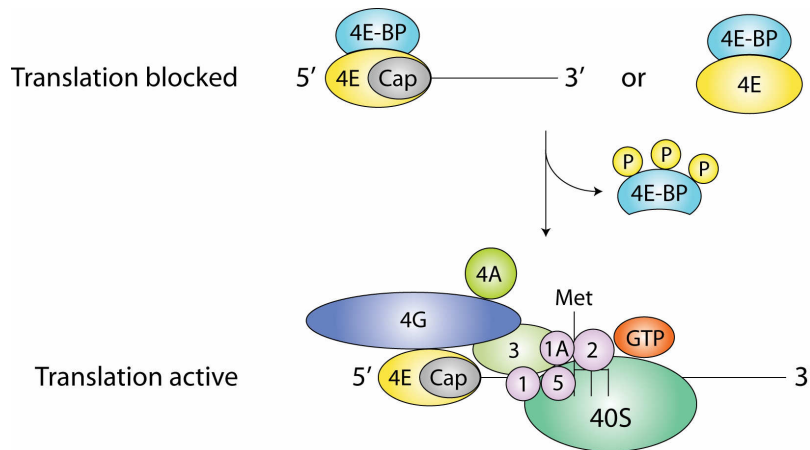


Fig. 4. Translational control by 4E-binding proteins (4E-BPs). 4E-BPs bind to the cap-binding protein eIF4E and thereby inhibit its interaction with eIF4G and the initiation machinery. This inhibitory association is released by phosphorylation of the 4E-BPs, upon which translation initiation can take place (figure adapted from Gebauer & Hentze, 2004).

2.3.2. Target-specific translational regulation

Target-specific regulation affects only a limited number of transcripts and is in general driven by the association of regulatory protein complexes. Several features of an mRNA can act as binding motifs, including cap-structure and poly(A) tail, secondary and tertiary RNA structures (e.g. hairpins and pseudoknots), and specific sequence motifs that are recognized by regulatory proteins (Gebauer & Hentze, 2004). Most known regulatory sequences are found within the 3' UTR, and it has been suggested that by adopting the closed-loop conformation (see figure 2; Wells et al., 1998), factors binding to the 3' UTR are brought in close proximity to the 5' end of the RNA, where they can modulate translation (Gebauer & Hentze, 2004).

In the last section, the function of the 4E-BPs has been described. Whereas these regulators control translation of a large number of transcripts, mRNA-specific 4E-BPs have been characterized that equally bind eIF4E and prevent its interaction with eIF4G, but that are tethered to sequence-specific RBPs (Groppo & Richter, 2009). For instance, the 4E-BPs Maskin and Neuroguidin interact with the RBP CPEB (Stebbins-Boaz et al., 1999; Jung et al., 2006), Cup associates with Bruno (Nakamura et al., 2004), and CYFIP1 with the Fragile X mental retardation protein (FMRP) and a small noncoding RNA (Napoli et al., 2008).

As a variation on this theme, a specific repressor of caudal mRNA, d4EHP (*Drosophila* eIF4E-homologous protein), has recently been identified that directly interacts with the 5' cap, thus interfering with eIF4E binding. The specificity of this interaction is mediated by the simultaneous

interaction of d4EHP with Bicoid, which binds to a recognition motif within the 3' UTR of caudal mRNA (Cho et al., 2005).

Cap- and poly(A) tail-independent translation inhibition is mediated by *D. melanogaster* Sex-lethal (Sxl). Sxl binds to recognition sites in both 5' and 3' UTRs of its target mRNA and recruits co-repressors to the 3' UTR, which prevents the stable association of the 40S ribosomal subunit with the mRNA (Gebauer et al., 2003). An even later step in initiation is targeted by heterogeneous nuclear ribonucleoproteins K and E1 (hnRNP K/E1). During early erythroid differentiation, both proteins bind to a recognition motif in the 3' UTR of *LOX* mRNA. Although 48S-complex formation still occurs upon hnRNPK/E1 association, joining of the large ribosomal subunit is prevented, presumably by interference with the respective initiation factor(s) (Ostareck et al., 1997; Ostareck et al., 2001).

2.3.3. Control of translation elongation and termination

Although initiation seems to be the most common target of translational control mechanisms, regulation of elongation and termination have also been reported (reviewed in Groppo & Richter, 2009).

In yeast, endoplasmic reticulum (ER) stress triggers the unfolded protein response (UPR) which results in an increase in the Hac1 transcription factor. Under non-stress conditions, unspliced *HAC1* mRNA contains ribosomes that are stalled due to base-pairing between sequences in the intron and complementary sequences in the 5' UTR (Ruegsegger et al., 2001). The UPR induces recruitment of *HAC1* to discrete foci of the ER where splicing via the stress sensor Ire1 occurs (Sidrauski & Walter, 1997), resulting in the alleviation of the stalled ribosomes and active translation (Ruegsegger et al., 2001). By modulating transcription, Hac1 induces the expression of genes that are essential to relieve ER stress, for example chaperones of the ER (Kaufman, 1999).

Another example for a post-initiation regulatory control mechanism is the response of mammalian cells to nonSTOP mRNAs that lack in-frame stop codons. In contrast to yeast, mammalian cells do not show enhanced degradation of nuclear-encoded nonSTOP mRNAs (Akimitsu et al., 2007). Although nonSTOP mRNAs were found to be associated with polysomes, indicating unperturbed initiation, ¹⁴C-leucine incorporation experiments suggested premature ribosome termination (Akimitsu et al., 2007). The authors propose that this ribosome fall-off is due to stalling of ribosomes at the poly(A) tail of the mRNA which prevents upstream translation events.

A third mechanism that has been suggested to affect elongation is translational control exerted by miRNAs. Several authors report that repressed mRNAs are associated with polysomes, but are less actively translated (e.g. Nottrott et al., 2006; Petersen et al., 2006; Maroney et al., 2006). This repression seems to be independent of normal initiation, since IRES-mediated translation is equally affected (Petersen et al., 2006). Therefore, decreased elongation rates or ribosome drop-off during elongation have been proposed to account for this type of miRNA-mediated control. However, the results are partly contradictory and the question as to which translation step is targeted by miRNAs – initiation or elongation – is currently a matter of active debate (reviewed in Jackson et al., 2010).

The multiple functions that RBPs fulfill in the regulation of the mRNA lifecycle are reflected in their often modular domain structure which necessarily comprises RNA-binding domains (RBDs). While a large number of these domains have been characterized (for a review, see Lunde et al., 2007), the next chapter will focus on a specific class – the KH domain – that is of particular importance for this work.

2.4. hnRNP K-homology (KH) domains interact with RNA

Besides RNA-recognition motif (RRM) and double-stranded RNA-binding domain (dsRBD), the so-called KH domain belongs to the most frequent domains that interact with RNA. First identified in heterogeneous nuclear ribonucleoprotein K (hnRNP K) and accordingly named hnRNP K homology (KH) domain (Siomi et al., 1993), KH domains are ubiquitous in archaea, bacteria and eukaryota (Siomi et al., 1993; Grishin, 2001). In various studies, it has been shown that KH domains are responsible for the recognition of single-stranded nucleic acids (Valverde et al., 2008), and that the corresponding RNA- or ssDNA-binding proteins are involved in a plethora of biological functions, from splicing to transcriptional regulation and translational control (Valverde et al., 2008).

A typical KH domain consists of approximately 70 amino acids that are structurally organized in a three-stranded antiparallel β -sheet packed against three α -helices (see Fig. 5). Based on their topology, KH domains can be grouped into two subfamilies: type I domains (typically present in eukaryotic proteins) have a $\beta_1\alpha_1\alpha_2\beta_2\beta_3\alpha_3$ organization, whereas type II domains (typically found in prokaryotic proteins) have a $\alpha_1\beta_1\beta_2\alpha_2\alpha_3\beta_3$ fold (Grishin, 2001). Between β_2 and β_3 (type I) or β_1 and β_2 (type II) strands, KH domains possess a variable loop that can be formed by three up to more than 60 amino acids (Valverde et al., 2008) and is involved in nucleic acid binding (see below). Near the center (between helices α_1 and α_2), KH domains contain a conserved and

functionally important signature sequence comprising the typical GXXG loop ((I/L/V)IGXXGXX(I/L/V)). Only in few cases of diverged KH domains, the GXXG loop is altered, interrupted or missing (Brykailo et al., 2007a). In type I domains, the nucleic acid-binding cleft is composed of the structural elements helix α_1 , GXXG loop, helix α_2 , strand β_2 and the variable loop between β_2 and β_3 (Fig. 5). Typically, this hydrophobic pocket accommodates four unpaired bases via Van der Waals forces, hydrophobic interactions and, to a lesser extent, electrostatic interactions (Valverde et al., 2008). Biochemical studies suggest that ssDNA and RNA are bound with a rather low micromolar affinity (Liu et al., 2001; Braddock et al., 2002). Therefore, one function of the frequently found array of multiple KH domains within the same protein may be to increase specificity and affinity by combination of multiple weak interactions (Lunde et al., 2007). For example, two KH domains are present in fragile X mental retardation protein (FMRP) (Ashley et al., 1993), three in hnRNP K (Siomi et al., 1993), and 14 in vigilin (section 2.5.; Dodson & Shapiro, 1997; McKnight et al., 1992). Cooperative function has for instance been demonstrated for the *E. coli* transcription elongation factor NusA whose two KH domains form an extensive area of interdomain contact and cooperatively bind an extended RNA segment (Beuth et al., 2005). However, multiple copies can also function independently, e.g. in FBP (Far-upstream element (FUSE)-binding protein), where KH domains 3 and 4 are separated by a flexible linker and individually bind to two different segments of ssDNA (Braddock et al., 2002b).

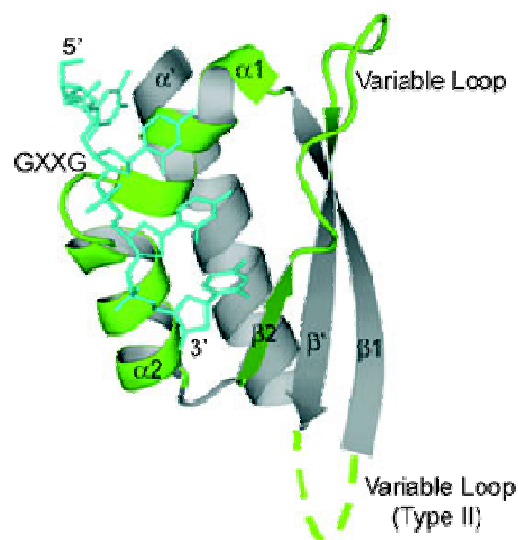


Fig. 5. Common structural features of KH domain-nucleic acid interactions. A typical binding cleft of KH domains comprises the secondary structural elements helix α_1 , GXXG loop, helix α_2 , strand β_2 , and variable loop (colored green). Four nucleotides (cyan sticks) can be accommodated within the binding pocket. Dotted green line: position of the variable loop in type II KH domains (figure from Valverde et al., 2008).

An extensively studied human KH domain-containing protein is FMRP, the lack of which leads to Fragile X mental retardation syndrome (D'Hulst & Kooy, 2009). Although in the majority of the cases, chromosomal fragility and transcriptional silencing of the FMRP-encoding gene is responsible for the disease (Jin & Warren, 2000), a single mutation within the conserved signature sequence of the second KH domain has been identified as cause for a severe peculiarity of the syndrome (De Boulle et al., 1993).

In yeast, the KH domain with the highest sequence identity (50%) to the second KH domain of human FMRP has been found in Scp160 (Currie & Brown, 1999). However, Scp160 contains 14 KH domains and is therefore unlikely to represent a yeast homologue of FMRP (Currie & Brown, 1999). Rather, Scp160 has been shown to belong to the highly conserved, multi KH domain-containing vigilin protein family which will be the focus of the next chapter.

2.5. Vigilins – a conserved family of multi KH-domain proteins

Vigilins, also known as high density lipoprotein-binding proteins, are a class of ubiquitous proteins that contain 14 related, but non-identical, KH domains. To date, vigilin homologues have been characterized in human (McKnight et al., 1992), chicken (Schmidt et al., 1992), *Xenopus laevis* (Dodson & Shapiro, 1997), *Drosophila melanogaster* (Cortes et al., 1999), *Caenorhabditis elegans* (Weber et al., 1997), *Danio rerio* (Chen et al., 2003), and *Saccharomyces cerevisiae* (Weber et al., 1997). Various biological functions have been assigned to the vigilin family members, including tRNA export (Kruse et al., 2000), formation of heterochromatin (Wang et al., 2005), and the selective protection of a specific transcript against endonuclease cleavage (Cunningham et al., 2000). In the following, the current knowledge about the so far best-characterized vigilins will be summarized.

2.5.1. Human vigilin

Human vigilin has first been described as a component of a cellular pathway that facilitates removal of excess cholesterol from cultured cells (McKnight et al., 1992). However, the presence of 14 consecutive KH domains (see Fig. 6) soon directed the attention to a potential function of vigilin in the cellular RNA metabolism.

Vigilin contains a functional SV40-type nuclear localization sequence (NLS) between KH domains 2 and 3 and localizes to both nucleus and cytoplasm, as shown by immunofluorescence microscopy (Kugler et al., 1996). More precisely, vigilin was found to be present in the "ribosome

factory" of the cell, the nucleolus, where it may associate with ribosomal precursors (Kruse et al., 2003). In affinity-purified nuclear multiprotein complexes, vigilin is present together with eEF1A, tRNA (Kruse et al., 1998) and the tRNA-specific nuclear export factor Exportin-t (Kruse et al., 2000), suggesting that it may be involved in the coordination of the export of newly synthesized ribosomes and tRNAs (Kruse et al., 2003).

In the cytosol, vigilin is as well complexed with eEF1A and tRNA (Kruse et al., 1998), but also associated with 80S ribosomes, and free- and membrane-bound polysomes (Vollbrandt et al., 2004). By *in vitro* studies, it has been demonstrated that the C-terminal domain of vigilin directly interacts with a subset of ribosomal 40S and 60S proteins (Vollbrandt et al., 2004). Yet, the ribosome-associated function of vigilin is unclear. Whereas its expression levels were found to be co-regulated with translational activity of both secretory and intracellular proteins (Kruse et al., 2003), indicating a general role in translation, siRNA-mediated knockdown had no effect on the overall rate of protein synthesis (Goolsby & Shapiro, 2003). However, depletion of vigilin presumably induces caspase-dependent apoptosis and is therefore lethal. It should be noted that the essential function of vigilin is independent of its potential role in chromosome partitioning during mitosis, since none-mitotic cells are equally susceptible to a vigilin knockdown (Goolsby & Shapiro, 2003).

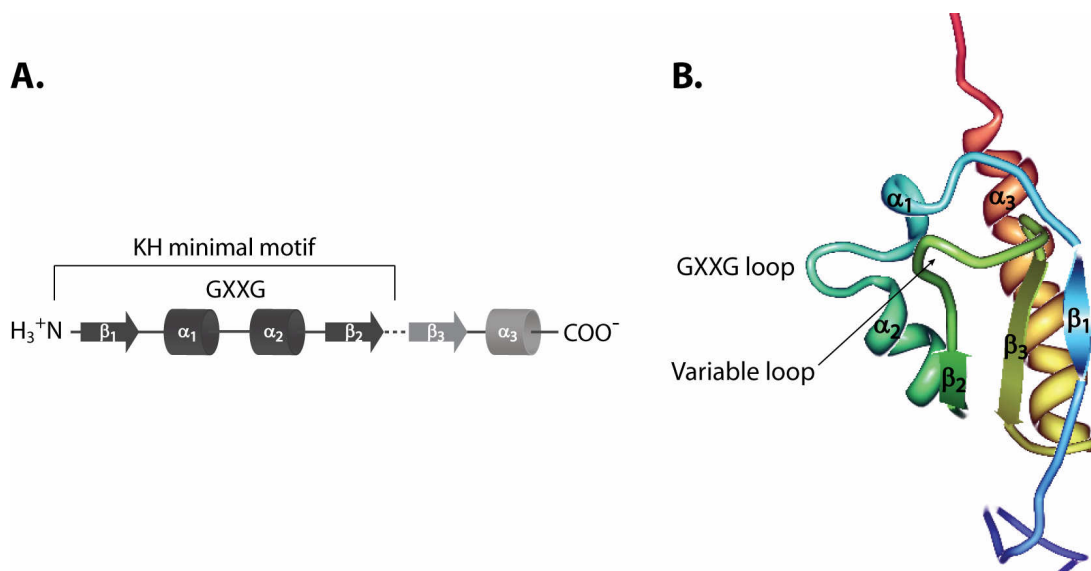


Fig. 6. KH domain 14 of human vigilin. (A) Schematic representation of the eukaryotic type I KH domain fold. The KH minimal motif consisting of two alpha helices and two beta strands encompasses the highly conserved GXXG motif. The dotted line between strands β_2 and β_3 marks the position of the variable loop (figure adapted from Valverde et al., 2008). (B) Solution structure of the 14th KH type I domain from human vigilin. The structural motifs are numbered as in (A); GXXG- and variable loop are indicated (structure unpublished; DOI: 10.2210/pdb2ctm/pdb).

Besides its functions in tRNA export and presumably translation, vigilin has been implicated in the induction of heterochromatin. Wang and coworkers showed that both vigilin and DDP1, the *D. melanogaster* vigilin homologue (see section 2.5.3), have a high affinity for inosine-containing RNAs (I-RNAs) (Wang et al., 2005). I-RNAs are produced by the editing enzyme adenosine deaminase (ADAR) which converts adenosine residues to inosine. In the nucleus, double-stranded RNAs are involved in heterochromatin formation via the RNAi pathway (Moazed et al., 2006), but can also be targeted and edited by ADAR (Gerber & Keller, 2001). Using affinity chromatography, vigilin was found to bind nuclear I-RNAs in a complex with ADAR, DNA-dependent protein kinase, RNA helicase A, the Ku70/Ku86 complex, histone variant H2AX and heterochromatin protein HP1 α (Wang et al., 2005). As part of this complex, vigilin recruits the histone methyltransferase SUV39H1 that methylates histone H3 on lysine 9, supports binding of HP1, and thus strongly promotes heterochromatin formation (Zhou et al., 2008). Taken together, the authors propose a model in which, first, bidirectional transcription of repetitive elements – for example retrotransposons, centromeric or telomeric sequences – produces dsRNA. Second, this dsRNA is edited by ADAR and subsequently recognized by vigilin, which in turn recruits the machinery that induces heterochromatin formation and thus silencing of nearby DNA sequences (Zhou et al., 2008).

2.5.2. Vigilin in *Xenopus laevis*

In contrast to human vigilin which has been implicated in several different processes, only one defined function has so far been assigned to the homologue in the African clawed frog: the stabilization of specific mRNAs.

mRNA turnover in the liver of *X. laevis* is regulated by the steroid hormone estrogen, which among others stabilizes the mRNA encoding vitellogenin (Brock & Shapiro, 1983) and destabilizes albumin mRNA (Pastori et al., 1991). Estrogen induces the expression of vigilin, which binds to a region of the vitellogenin mRNA 3' UTR (Dodson & Shapiro, 1994) that has been implicated in the control of vitellogenin mRNA stability (Nielsen & Shapiro, 1990). This region contains two copies of a consensus sequence that is recognized by PMR-1 endonuclease. Upon estrogen induction, these sequences are masked by vigilin, which protects vitellogenin mRNA from degradation. Albumin mRNA, in contrast, also contains the PMR-1 recognition motif, but is not bound by vigilin and is therefore degraded (Cunningham et al., 2000). By *in vitro* genetic selection, it was demonstrated that *X. laevis* vigilin preferentially associates with largely unstructured, single-stranded RNA stretches containing multiple (A)_nCU and UC(A)_n motifs.

Deletion analysis indicated that approximately 75 nucleotides are required for maximal binding (Kanamori et al., 1998), suggesting that more than one KH domain is involved.

2.5.3. DDP1 is the vigilin homologue in *Drosophila melanogaster*

As mentioned in section 2.5.1, not only human vigilin, but also the *D. melanogaster* vigilin protein DDP1 binds to I-RNAs with high affinity (Wang et al., 2005). This finding suggests that DDP1 may act in heterochromatin formation in the same way as has been described for vigilin, which indeed seems to be the case. It has been shown that DDP1 colocalizes with heterochromatin protein HP1 to heterochromatic regions in polytene chromosomes and in nuclei from larval neuroblasts (Cortes et al., 1999). HP1 is known to play a central role in organizing heterochromatin (Eissenberg & Elgin, 2000), and if DDP1 is mutated, HP1 deposition at the chromocenter of polytene chromosomes is strongly reduced, along with H3-K9 methylation which is a prerequisite for HP1 association (Huertas et al., 2004; Hall et al., 2002). Furthermore, DDP1 is associated with condensed mitotic chromosomes and is required for correct chromosome condensation and segregation (Cortes et al., 1999). These data suggest that DDP1 is involved in heterochromatin formation, and indeed, a mutant allele of DDP1 behaves as a dominant suppressor of heterochromatin-induced position effect variegation (Huertas et al., 2004). This phenomenon is based on the inactivation of a gene through its juxtaposition with heterochromatin, and its suppression by a DDP1 mutation indicates that this protein contributes to the formation of heterochromatin and gene silencing.

Apart from its heterochromatin-related function, DDP1 has been demonstrated to function in translational control of a specific transcript (Nelson et al., 2007). *D. melanogaster* Hsp83 mRNA contains a sequence element in its 3' UTR, the so-called Hsp83 degradation element (HDE), that functions in stimulating translation (Bashirullah et al., 1999). Using tandem RNA affinity purification (TRAP), Nelson and colleagues identified DDP1 to bind to the HDE along with Hrp48 and Poly(A) binding protein. In this regulatory complex, both DDP1 and Hrp48 function in translational enhancement (Nelson et al., 2007).

2.5.4. Scp160, the yeast homologue of vigilin

In the budding yeast, Scp160 has been characterized as member of the vigilin protein family (Weber et al., 1997). Although its primary sequence shows only about 20% identity with the vigilins of human, chicken and *C. elegans* (Weber et al., 1997), its array of 14 KH domains closely corresponds to the structure of vertebrate vigilins. However, whereas 12 KH domains of human vigilin contain a perfect GXXG motif, only seven of Scp160's KH domains contain a strictly conserved KH motif (domains 2, 8-12 and 14), while the remaining seven are diverged and display alterations in the GXXG motif or contain no GXXG motif at all (Figure 7; Weber et al., 1997).

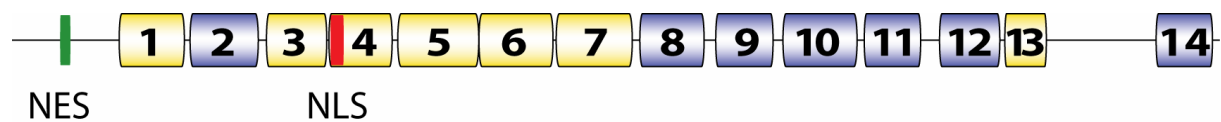


Fig. 7. Domain structure of Scp160. The schematic representation illustrates that Scp160 is essentially made up of 14 KH domains, seven of which contain conserved GXXG loops (marked in blue) whereas the remaining seven carry altered or no GXXG motifs (marked in yellow). The positions of the putative nuclear export (NES) and nuclear localization (NLS) sequences are indicated (see section 2.6.3).

In the next chapter, the current status of knowledge regarding the cellular functions of Scp160 – and therefore the starting point of the present study – will be reviewed.

2.6. Scp160 is implicated in diverse cellular processes

2.6.1. Ploidy control

Yeast strains in which Scp160 is deleted show an abnormal morphology with larger cell size and increased DNA content, along with irregular segregation of genetic markers. These observations indicate that Scp160 is a factor that is involved in the maintenance of cellular ploidy, and the protein has been named accordingly (*S. cerevisiae* protein controlling the ploidy) (Wintersberger et al., 1995). Interestingly, once established, this phenotype cannot be rescued by a plasmid-borne copy of Scp160. Since immunofluorescence microscopy illustrated that in addition to a cytoplasmic pool, Scp160 localizes to the nuclear envelope and to the ER, the authors hypothesized that Scp160 may be required for proper partitioning of this membranous network

during cell division (Wintersberger et al., 1995). Because yeast cells undergo closed mitosis, i.e. chromosome segregation takes place within the intact nucleus, unfaithful partitioning potentially induces ploidy aberrations. However, upon the finding that Scp160 contains nucleic acid-binding domains and associates with translating ribosomes, it has been suggested that the ploidy phenotype of the deletion strains may be induced indirectly by defects in the metabolism or translational control of target transcripts (see sections 2.6.2. and 2.6.5; Weber et al., 1997).

2.6.2. Scp160 associates with RNA

Using Northwestern blotting, Weber and coworkers (1997) demonstrated that purified Scp160 binds to all four ribohomopolymers, but exhibits the highest affinity for poly(rG). In subsequent competition experiments, rRNA was the most efficient competitor of poly(rC) binding, whereas double-stranded and single-stranded DNA competed less efficiently. tRNA did not compete with poly(rC) binding, indicating that in contrast to human vigilin (see section 2.5.1.), Scp160 may not be involved in tRNA-related processes. The assumption that Scp160 binds cellular mRNAs was supported by the finding that Scp160 is associated with polysomes as part of a RNase-sensitive protein complex (Lang & Fridovich-Keil, 2000). The final confirmation that Scp160 associates with mRNAs came from two studies in which Scp160-bound material was used for microarray analysis, revealing that Scp160 binds a rather large set of transcripts (Li et al., 2003; Hogan et al., 2008).

2.6.3. Regulation of telomeric silencing

As described in sections 2.5.1. and 2.5.3., vigilins are involved in the structural organization of heterochromatin both in human and *D. melanogaster*. Although the factors that mediate transcriptional silencing and heterochromatin formation in budding yeast are different from those in fission yeast and higher eukaryotes, Scp160 has also been found to play a role in silencing. Marsellach and coworkers (2006) showed that deletion of Scp160 relieves silencing at telomeres and at the mating-type locus, which goes along with decreased deposition of the silencing protein Sir3. Whereas Sir3 is required for heterochromatin formation and silencing at telomeres and the mating-type locus, it is not involved in the same processes at the rDNA locus; notably, silencing of the rDNA locus is not affected by deletion of Scp160. Interestingly, the contribution of Scp160 to silencing is independent of either its effect on cell ploidy or its binding to ribosomes (Marsellach et al., 2006). Although Scp160 contains a nuclear localization- as well as a nuclear export signal, there is so far no experimental evidence that full-length Scp160 enters the nucleus

(Brykailo et al., 2007b). Consistently, Scp160 was not found to associate with telomeric DNA in ChIP experiments (Marsellach et al., 2006). The authors rather suggest that the silencing function is connected to the localization of Scp160 to the nuclear envelope, since telomere clustering at the nuclear envelope – which facilitates telomeric silencing – is perturbed in *scp160Δ* cells.

2.6.4. A functional role in the mating response pathway

In the yeast mating response pathway, receptor stimulation by pheromones leads to the activation of a heterotrimeric G protein composed of an α subunit (Gpa1) and a tightly associated $\beta\gamma$ dimer. Upon activation, the $\beta\gamma$ dimer is released and activates downstream signaling proteins. Guo and colleagues (2003) demonstrated for the first time that also Gpa1 has a positive signaling function. Unexpectedly, in a genome-wide two-hybrid screen, Scp160 was identified as a putative binding partner of Gpa1 (Uetz et al., 2000). Further experiments showed that Scp160 associates preferentially with the activated form of Gpa1 and that it is essential for the transmittance of the pheromone signal by Gpa1 (Guo et al., 2003). These results raise the intriguing possibility that the RNAs that are targeted by Scp160 may act as a form of "second messenger" in signaling networks.

2.6.5. Translational control

Numerous findings indicate that Scp160 may be involved in translational control:

First, *scp160* deletion strains show increased sensitivity against translation inhibitors such as cycloheximide and hygromycin B (Baum et al., 2004).

Second, Scp160 is known to associate with cytosolic and membrane-bound polysomes (Frey et al., 2001), from which it is released by EDTA treatment as component of mRNP complexes. These large complexes contain the poly(A) binding protein Pab1 (Lang & Fridovich-Keil, 2000) and the RBP Bfr1. Bfr1, which has originally been implicated in the secretory pathway (Jackson & Kepes, 1994), colocalizes with Scp160 to ER and nuclear envelope and equally associates with polysomes. Interestingly, there is evidence that Bfr1 is required for polysome (but not ribosome) association of Scp160 (Lang et al., 2001). The binding site of Scp160 on the ribosome was localized to the ribosomal 40S subunit close to the mRNA exit tunnel (Baum et al., 2004), which is consistent with the idea that Scp160 actively contributes to the association of mRNAs with especially ER-bound ribosomes and/or controls translation of (specific?) transcripts (Frey et al., 2001). Scp160's association with the ribosome is partially dependent on its interaction with Asc1,

the yeast orthologue of mammalian receptor of activated C-kinase (RACK1) (Gerbasí et al., 2004; Baum et al., 2004). RACK1 integrates inputs from different signaling pathways on the ribosome and regulates translation by recruiting activity-modulating protein kinases (Nilsson et al., 2004).

Third, deletion of Scp160 is synthetic lethal with the eIF4E-binding protein Eap1 (Mendelsohn et al., 2003). Scp160 acts in concert with Eap1 in the so-called SESA network in order to inhibit translation of *POM34* mRNA in response to spindle pole body duplication defects (Sezen et al., 2009). However, this finding does not explain why Scp160 and Eap1 are synthetic lethal in otherwise wildtype cells, suggesting that the SESA network is only one part of a translational control system involving both proteins.

Finally, there is evidence that Scp160 is involved in the elongation step of translation, since it can form chemical crosslinks with elongation factor 1A (eEF1A) on the ribosome (Baum et al., 2004). In addition, the mammalian Scp160 homologue vigilin co-purifies in a complex with eEF1A and tRNA (refer to section 2.5.1.; Kruse et al., 1998; Kruse et al., 1996).

Taken together, these findings strongly suggest that Scp160 functions in the regulation of translation.

3. Aims of this study

At the starting point of this study, several lines of evidence implicated Scp160 in translational control: The increased sensitivity of Scp160-deprived cells against translation inhibitors, Scp160's association with membrane-bound and cytosolic polysomes, its binding site on the ribosome close to the signal adapter Asc1 (RACK1) and elongation factor eEF1A, as well as its synthetic lethality with the eIF4E-binding protein Eap1. However, genome-wide studies addressing the suggested function of Scp160 in translation were missing.

The present study focused on two major points: First, the interaction of Scp160 with ribosomes should be closer examined, and second, a translational profiling approach should be performed to identify mRNAs that are post-transcriptionally regulated by Scp160. To address the first question, affinity purifications of Scp160 should be used to identify so far unknown interaction partners as well as to recheck the suggested dependence of its ribosome interaction on RNA, Asc1 and the C-terminal KH domains. Further, fractionation experiments should be used to test if ribosome association is lost under specific conditions. In the second part of this work, changes in the transcriptome as well as changes in translation rates upon depletion of Scp160 should be determined by microarray analysis. Candidate mRNAs should be verified as direct targets of Scp160 by immunoprecipitation experiments, and their putative function with respect to the polyploidy phenotype of Scp160-deficient cells should be illuminated.

4. Results

4.1. Scp160 interacts with ribosomes

It has been demonstrated that the RNA-binding protein Scp160 associates with cytosolic and membrane-bound polysomes (Frey et al., 2001; Lang & Fridovich-Keil, 2000; Mendelsohn et al., 2003; Weber et al., 1997). These results are based on sucrose density fractionation studies, in which Scp160 has been shown to be present in the polysome-containing gradient fractions. To gain an independent picture of Scp160's ribosome association as well as to possibly identify to date unknown interaction partners, I isolated Scp160-containing complexes by Tandem Affinity Purification (TAP) (Rigaut et al., 1999).

4.1.1. Scp160 copurifies with ribosomal proteins in a partially RNA-dependent manner

Carboxyterminally TAP-tagged Scp160 was regarded as being functional, since the tagged strain did not display reduced fitness, as is the case for *scp160* deletion strains (not shown). The TAP procedure contains two subsequent purification steps, namely binding to IgG affinity resin through the protein A part of the tag and association with calmodulin beads through the calmodulin binding peptide moiety. The two parts of the tag are separated by a TEV protease cleavage site that is used to specifically cleave off bound complexes from the IgG beads (Rigaut et al., 1999). In my purifications of Scp160, I found that application of the whole purification procedure disrupted the association of Scp160 with its interactors (see Fig. 9, "CaM"), whereas applying only the IgG binding step together with a higher volume of wash buffer (see section 6.2.12.2.) resulted in specific co-purification of a number of proteins (Fig. 8, lane 3).

As shown in Fig. 8, TEV eluates of Scp160 purifications contain several co-purifying proteins, most of which can be assigned to components of the 80S ribosome as indicated by comparison with an 80S purification (lane 1). The interaction with these proteins is specific, since they are not present in a mock purification of an untagged wildtype strain (lane 2). Mass spectrometric analysis confirmed the presence of components of both small (Rps3, Rps0A, Rps0B, Rps5, Rps16A, Rps16B) and large (Rpl3, Rpl4A, Rpl5) ribosomal subunits. These results are in accordance with a large-scale survey, in which a set of ribosomal proteins has been found to co-purify with TAP-tagged Scp160 (Gavin et al., 2006). I further confirmed the association with the yeast homologue of mammalian RACK1, Asc1, which is involved in polysome binding of Scp160

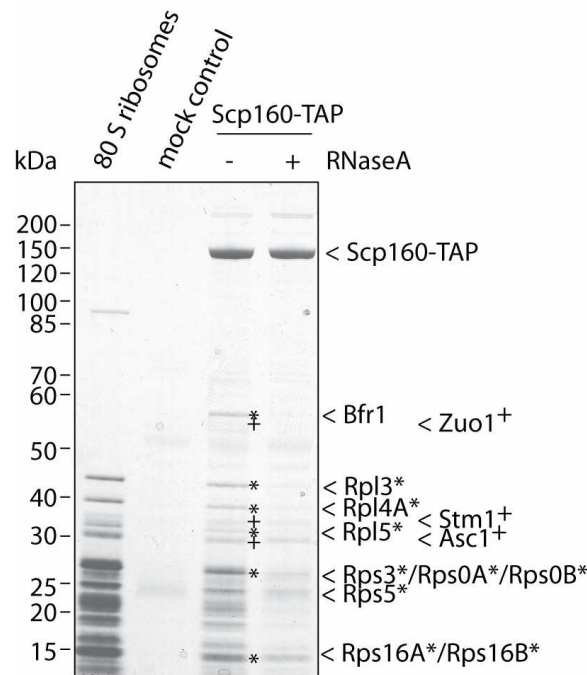


Fig. 8. Scp160 interacts with ribosomal proteins in a partially RNA-dependent manner. TAP-tagged Scp160 (strain RJY2946) was purified up to the TEV cleavage step and incubated for 10 min with or without 5 μ g RNase A. Co-purifying proteins were separated by SDS-PAGE and visualized by Coomassie staining. Bands of interest were excised and analyzed by mass spectrometry. For comparison, purified 80S ribosomes (courtesy of T. Becker) were loaded. Untagged wildtype extract (RJY358) served as mock control. Ribosomal proteins are marked with a star (*), ribosome-associated proteins are indicated with a cross (+).

(Baum et al., 2004), and Bfr1, which previously has been shown to associate with Scp160-containing complexes and polysomes (Lang et al., 2001). In addition, I identified two further proteins to be present in Scp160 purifications, namely Stm1 and Zuo1, which previously have been shown to associate with ribosomes (Van Dyke et al., 2006; Gautschi et al., 2001).

To test if the interaction of Scp160 with its co-purifiers is RNA-dependent, I treated IgG-bound material with RNase A prior to washing and TEV cleavage. Although all interactions were diminished, they were reduced at different degrees (Fig. 8, lane 4). Whereas association with Bfr1 was lost completely, ribosomal proteins including Stm1 were still found in the eluate.

4.1.2. Scp160, Bfr1 and Stm1 bind to overlapping sets of ribosomes

Having confirmed the interaction between Scp160 and Bfr1 and identified Stm1 as co-purifier of Scp160, I asked whether Scp160 can also be found in the reverse purifications (Bfr1 and Stm1 as baits, respectively). As expected, Scp160 was present in Bfr1-TAP TEV eluates as a prominent band (Fig. 9, left panel). Together with the fact that Scp160- and Bfr1 purifications show a very

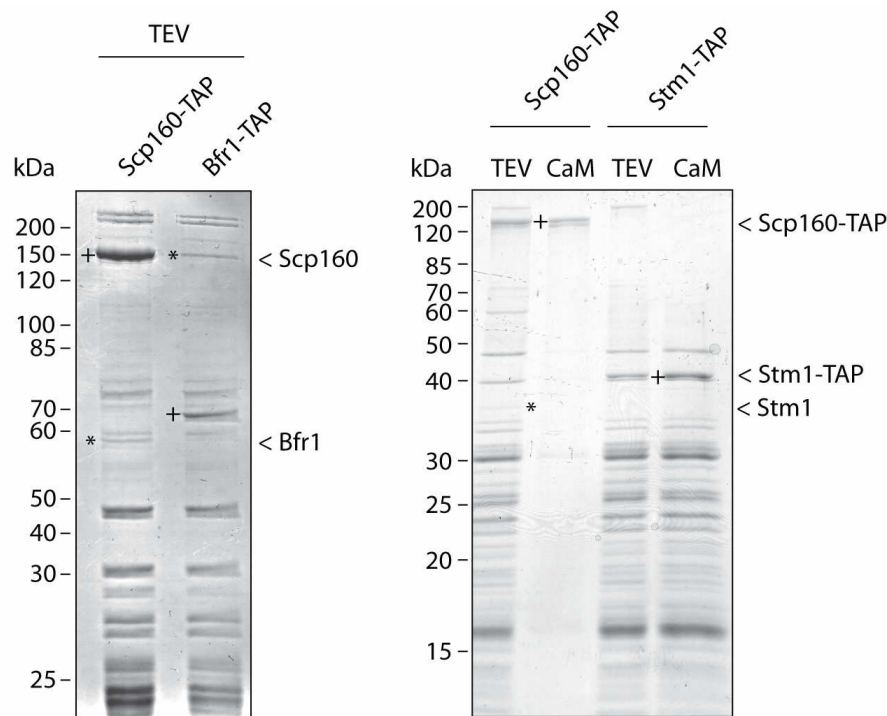


Fig. 9. Scp160, Bfr1 and Stm1 associate with overlapping sets of ribosomes. TAP-tagged proteins (from strains RJY2946, RJY3391 and RJY3179) were purified either up to TEV elution (TEV), or including binding to calmodulin beads (CaM). Co-purifying proteins were separated by SDS-PAGE and visualized by Coomassie staining. Co-purifiers are marked with a star (*), TAP-tagged proteins are labeled with a cross (+). 10% (left panel) and 12% (right panel) polyacrylamide gels were used.

similar pattern of co-purifying proteins, this suggests that both proteins localize to the same complexes. In contrast, in Stm1-TAP purifications, Scp160 was not visible as co-purifier on Coomassie level (Fig. 9, right panel). This could mean that although Stm1 is present in considerable amounts on ribosomes that are associated with Scp160, Scp160 in reverse is present on only a very small subset of ribosomes that contain Stm1.

4.1.3. Ribosome association of Scp160 is only partially dependent on KH domains 13/14 and Asc1

Several studies have shown that deletion of KH domain 14 reduces co-fractionation of Scp160 with polysomes (Li et al., 2004), whereas deletion of KH domains 13 and 14 disrupts this association (Brykailo et al., 2007a; Baum et al., 2004). Similarly, deletion of Asc1 has been shown to diminish polysome association of Scp160 (Baum et al., 2004). Since these results are based on co-fractionation in sucrose density gradients, I decided to use the TAP system in order to check ribosome binding in a more direct way.

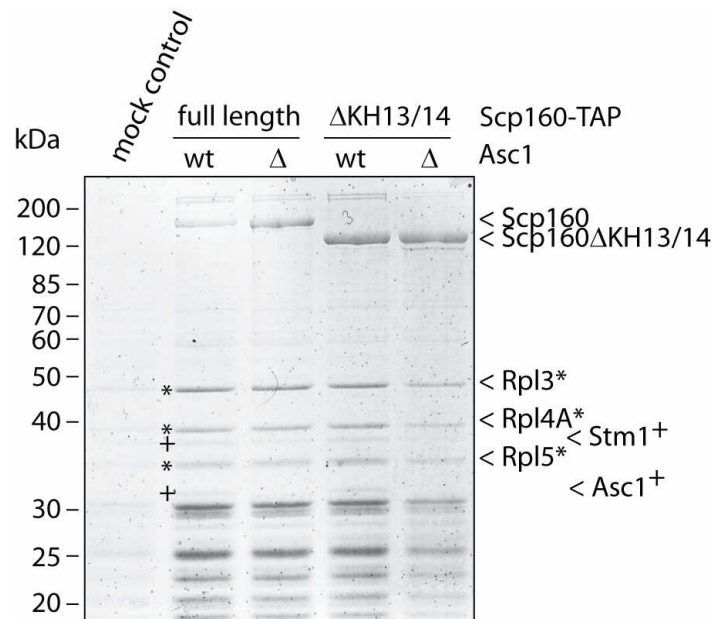


Fig. 10. Ribosome association of Scp160 is only partially dependent on KH domains 13/14 and Asc1. TAP purifications of full-length Scp160-TAP and Scp160 Δ KH13/14-TAP in both wildtype (strains RJY2946 and RJY3256) and *asc1 Δ (RJY3231 and RJY3258) background, were performed up to TEV cleavage. Co-purifying proteins were separated by SDS-PAGE and visualized by Coomassie staining. Ribosomal proteins are labeled with a star (*), ribosome-associated proteins are marked with a cross (+).*

Interestingly, both deletion of KH domains 13/14 and deletion of Asc1 induced only a slight reduction in the co-purification of ribosomal proteins (Fig. 10). Even in a strain carrying both KH domain 13/14 truncation and *asc1* deletion, significant amounts of ribosomal proteins are present in the TEV eluate (Fig. 10, lane 5). These results suggest that even if polysome association may be reduced under these conditions, Scp160 largely retains its ability to bind to ribosomes.

4.2. Scp160 associates with ribosome-containing cellular subfractions

4.2.1. Deletion of KH domains 13/14 induces a non-ribosome associated pool of Scp160

In subcellular fractionation experiments, Scp160 has been demonstrated to co-fractionate with ER membranes, but also with the cytosolic ribosome fraction. Ribosome-depleted cytosol, in contrast, is free of Scp160 (Frey et al., 2001). In my TAP experiments, I found that ribosome association of Scp160 truncations as well as of Scp160 in an *asc1* deletion background is slightly reduced (see Fig. 10). To test if this reduction induces changes in the subcellular localization of

Scp160, I carried out fractionation experiments as described by Frey and coworkers (Frey et al., 2001).

Briefly, three subsequent centrifugation steps applied to whole cell extracts result in three pellet fractions enriched in ER membranes and ribosomes (P6 – ER fraction, P18 – ER and heavy polysomes, P200 – cytosolic ribosomes) and a ribosome-free, cytosolic supernatant (S200) (Fig. 11A). Successful separation of these fractions was confirmed by immunoblotting against the ER-protein Sec61 (only present in P6), ribosomal protein Rps3 (in all pellet fractions, but not in the cytosolic fraction S200), and cytoplasmic phosphoglycerate kinase (Pgk1; only present in S200) (Fig. 11B). Probing with an anti Scp160 antibody showed that Scp160 colocalizes with ribosome-containing fractions (lanes 1-4; enrichment in the ER fraction P6, presence in ribosomal fractions P18 and P200). As expected, no signal was present in the cytosolic supernatant S200.

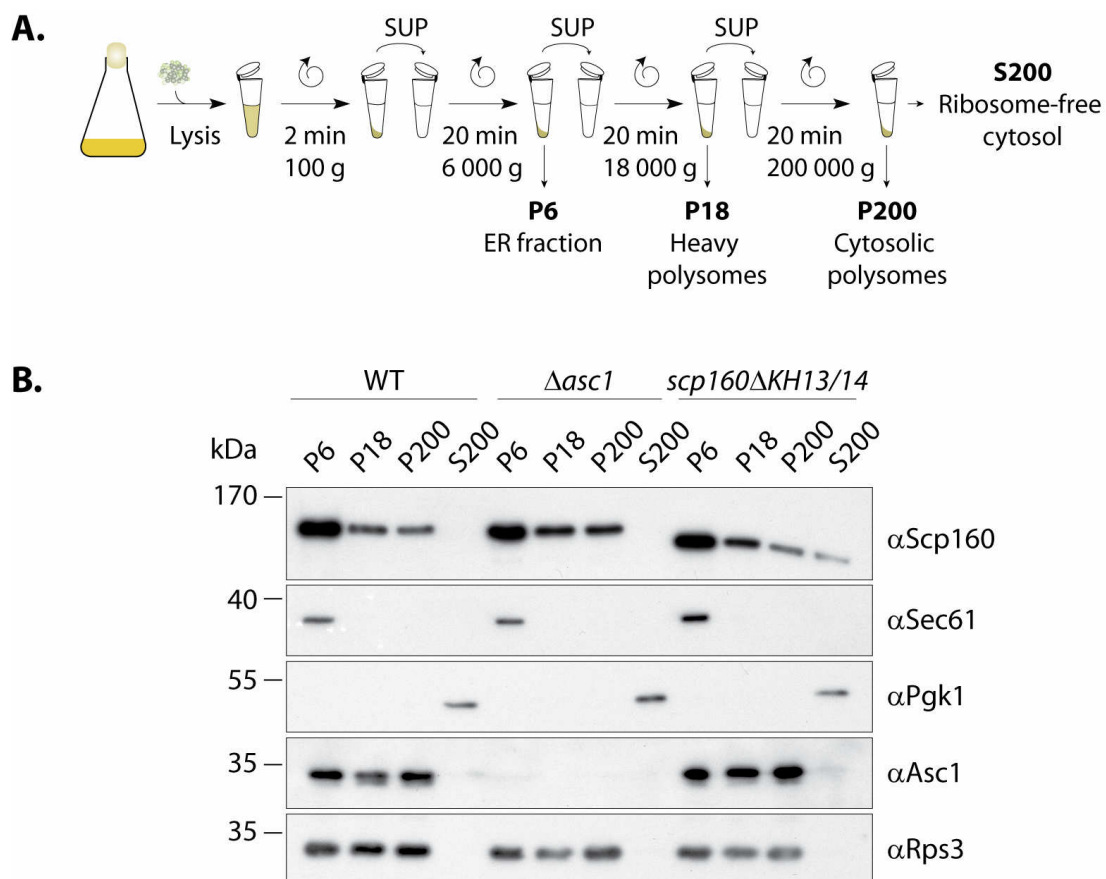


Fig. 11. Scp160's association with ribosome-containing cellular subfractions is independent of Asc1 and partially dependent on KH domains 13 and 14. (A) Schematic of the subcellular fractionation assay. Whole cell extracts derived from glass bead lysis were subjected to three subsequent centrifugation steps as indicated. **(B)** Fractionation assay of wildtype (RJY3515), *asc1* Δ (RJY3000) and *scp160\Delta KH13/14* (RJY3516) strains. Aliquots of the different centrifugation steps were separated by SDS-PAGE and probed for Scp160, the ER marker protein Sec61, the cytosolic marker protein Pgk1, and ribosomal proteins Asc1 and Rps3.

Interestingly, deletion of *asc1* did not change this fractionation pattern (lanes 5-8), whereas truncation of Scp160 by KH domains 13 and 14 induced the additional appearance of a non-ribosomal, cytosolic pool (lanes 9-12). This may reflect that KH domains 13 and/or 14 are involved in ribosome association or in Scp160's interaction with other high molecular complexes.

4.2.2. Mutation of conserved RNA binding domains causes partial loss of ribosome association

As described in paragraph 4.2.1., deletion of the two last KH domains causes an additional cytoplasmic pool of Scp160. To analyze if this effect is due to loss of the specific RNA-binding activity of these domains, I generated versions of Scp160 that contain point mutations within the conserved RNA-binding pockets of KH domains 13 and 14. Analogous mutations in other KH-domain containing proteins have been previously shown to interfere with RNA binding (Siomi et al., 1994; Jones & Schedl, 1995; Chmiel et al., 2006). As target sequence I chose the GXXG region that is the most conserved stretch in all KH domains described to date (refer to section 2.4 and Fig. 12). I introduced the following amino acid exchanges: glycine 1028 to aspartate, isoleucine 1031 to asparagine, glycine 1170 to aspartate, and glycine 1173 to aspartate (Fig. 12A). The resulting proteins, Scp160mutKH14 (with mutations G1170D and G1173D) and Scp160mutKH13/14 (with additional mutations G1028D and I1031N) were expressed as myc9-tagged versions from a low copy vector. Although their expression was higher than that of endogenous Scp160, they were detectable at similar levels as a wildtype myc9-tagged Scp160 expressed from the same vector (Fig. 12B).

In subcellular fractionation, plasmid-derived Scp160 distributed over the different fractions essentially as described before (Fig. 12C, compare to Fig. 11B). However, even in case of the wildtype construct (lanes 1-4), a small portion of Scp160 was present in the cytoplasmic fraction S200. This is probably due to the aforementioned overexpression of the constructs (Fig. 12B). In the point mutants (lanes 6-12), the cytoplasmic pool of Scp160 was increased, although the strongest signal was still detected in the ER fraction P6. These findings indicate that RNA-binding activity mediated by KH domains 13 and 14 contributes to the association of Scp160 with ribosomes or other large mRNP complexes. In this context, it is important to mention that in the further course of this study, I could confirm that the point mutants described here are deficient in the binding of target mRNAs (see section 4.6.2).

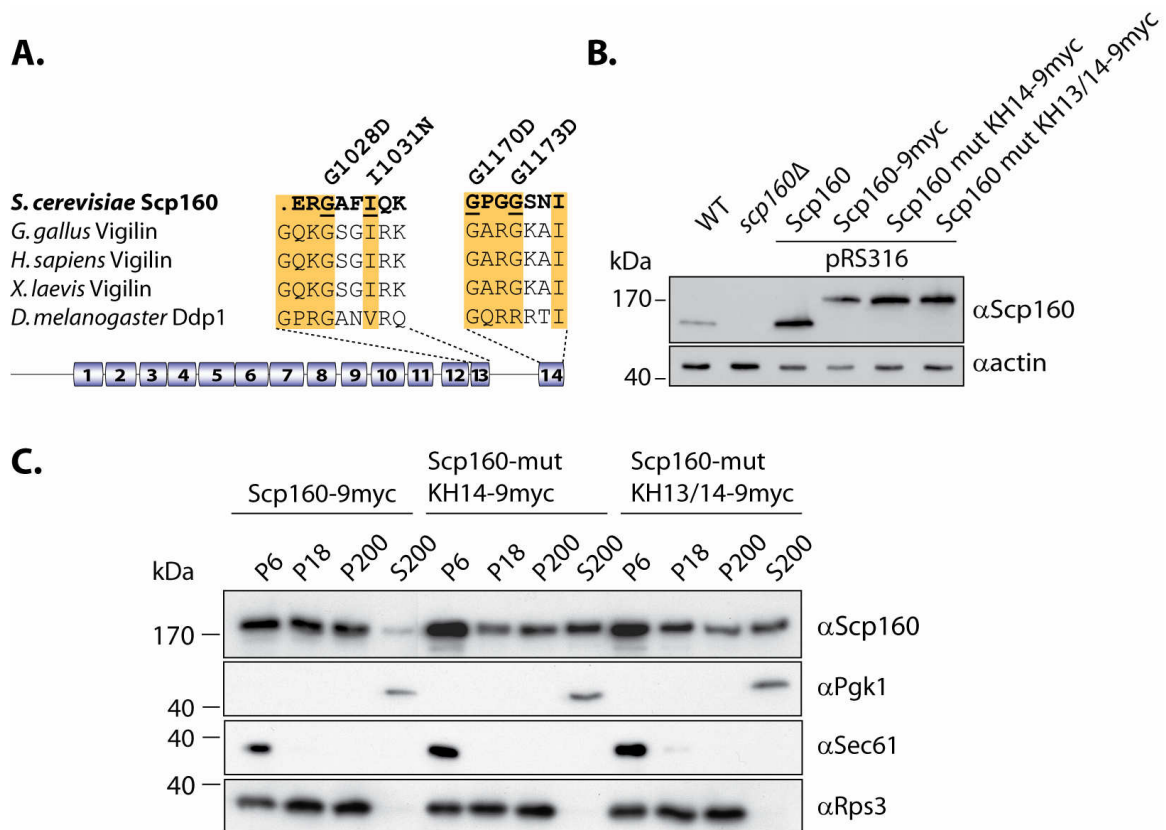


Fig. 12. Point mutations in the RNA binding pockets of KH domains 13 and 14 induce a non-ribosome associated pool of Scp160. **(A)** Sequence alignment of the GXXG regions of KH domains 13 and 14 of *S. cerevisiae* Scp160 and its orthologues in *G. gallus*, *H. sapiens*, *X. laevis* and *D. melanogaster*. GXXG motifs and the highly conserved isoleucins are boxed, residues that were mutated in this study are underlined. **(B)** Western blot of whole cell extracts using antibodies against Scp160 and actin (loading control). Compared to the expression of the endogenous gene (in strain RY358), Scp160 amounts are elevated if expressed from the centromeric plasmid pRS316 (strains HSY9, HSY11, HSY10 and HSY12). **(C)** Analysis of subcellular fractionation samples. Lysates were prepared from cells expressing wildtype Scp160 (HSY11), Scp160 with point mutations in KH domain 14 (G1170D and G1173D; HSY10) or in KH domains 13 and 14 (additionally G1028D and I1031N; HSY12). Subcellular localization of Scp160, Pgk1, Sec61 and Rps3 was examined by immunoblotting.

4.2.3. Scp160's subcellular localization remains unchanged upon diverse environmental changes

Scp160 has been suggested to function in translational control of specific mRNAs (Weber et al., 1997; Li et al., 2003; Frey et al., 2001), an assumption that has been confirmed recently for *POM34* mRNA in response to spindle pole body defects (Sezen et al., 2009). Considering the subcellular localization of Scp160, one can assume that target mRNAs may preferentially be translated at the ER. Furthermore, Scp160 interacts with the signal integrator Asc1 on the ribosome (Baum et al., 2004; Nilsson et al., 2004) and has been shown to act as an effector in the

4.2.3.2. Heat shock

As mentioned above, mRNAs translated at the ER are likely targets of Scp160. One subgroup of ER-localized transcripts encodes cell wall proteins that are directed to the extracellular surface of the plasma membrane through the secretory pathway (Lesage & Bussey, 2006). Assuming that Scp160 may control translation of those mRNAs, its ribosome association may be influenced by cell wall stress. Besides others, growth at elevated temperatures is a well-known condition that induces this kind of stress (Levin, 2005).

To test if higher temperatures induce changes in the subcellular localization of Scp160, I shifted wildtype cells from 30°C to 40°C and collected samples for fractionation assay and RNA preparation at two different timepoints (Fig. 14). Already after 10 min, the heat-shock protein-encoding *HSP42* mRNA (Wotton et al., 1996) was 50-fold induced as determined by qRT-PCR, indicating that the cells were responding to the heat stress as expected (Fig. 14, left panel). However, Western analysis of subcellular fractions showed that Scp160 retained its characteristic fractionation pattern also upon heat stress (Fig. 14, right panel).

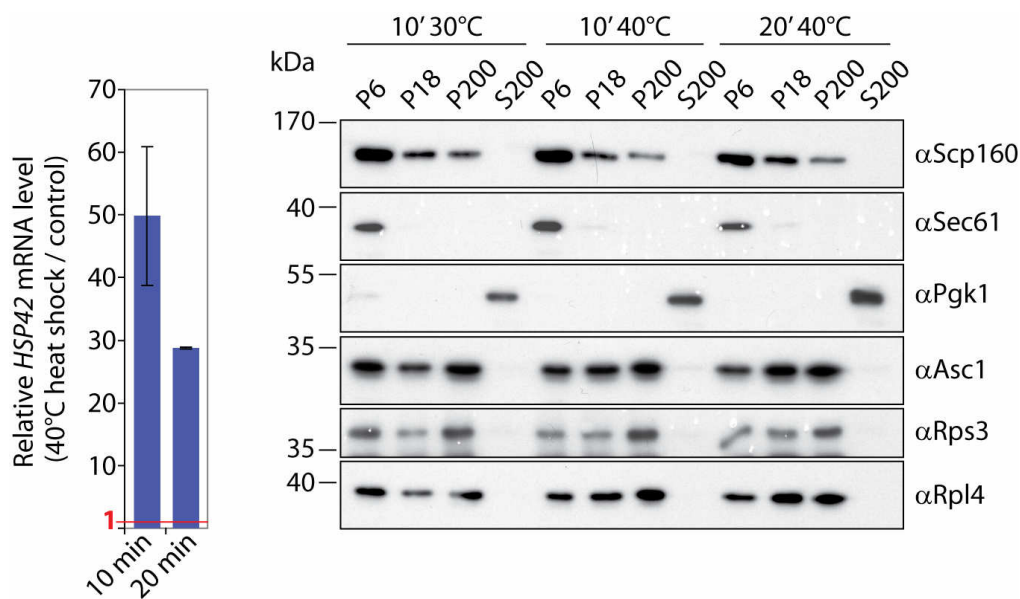


Fig. 14. Heat shock does not cause a shift in the subcellular localization of Scp160. Logarithmically growing wildtype cells (RJY358) were collected by centrifugation and resuspended in medium pre-warmed to 30°C or 40°C. Aliquots for subcellular fractionation and preparation of RNA were removed after the indicated times. Left panel: qRT-PCR analysis of the heat-shock inducible *HSP42* mRNA was used as control (duplicate analysis). Right panel: Fractionation samples were assayed by immunoblotting. Representative blots of two independent experiments are shown.

4.2.3.3. Hyperosmotic shock

Besides elevated temperatures, hyperosmotic shock is a stress condition that induces a cell wall integrity pathway-triggered response (Levin, 2005). Therefore - and for the reasons stated in section 4.2.3.2. -, hyperosmotic shock could induce changes in the localization pattern of Scp160.

To address this question, I subjected wildtype cells to high salt concentrations (0.4 M NaCl) and took aliquots for subcellular fractionation as well as qRT-PCR. The latter showed that the level of the hyperosmolarity-responsive *HOR2* mRNA (Hirayama et al., 1995) is more than 150-fold increased 15 min after onset of the salt stress (Fig. 15, left panel), which denotes that the osmosensing signal transduction pathway has been activated (Norbeck et al., 1996). However, also this cell wall stress-inducing condition did not exert any influence on Scp160's subcellular fractionation pattern (Fig. 15, right panel).

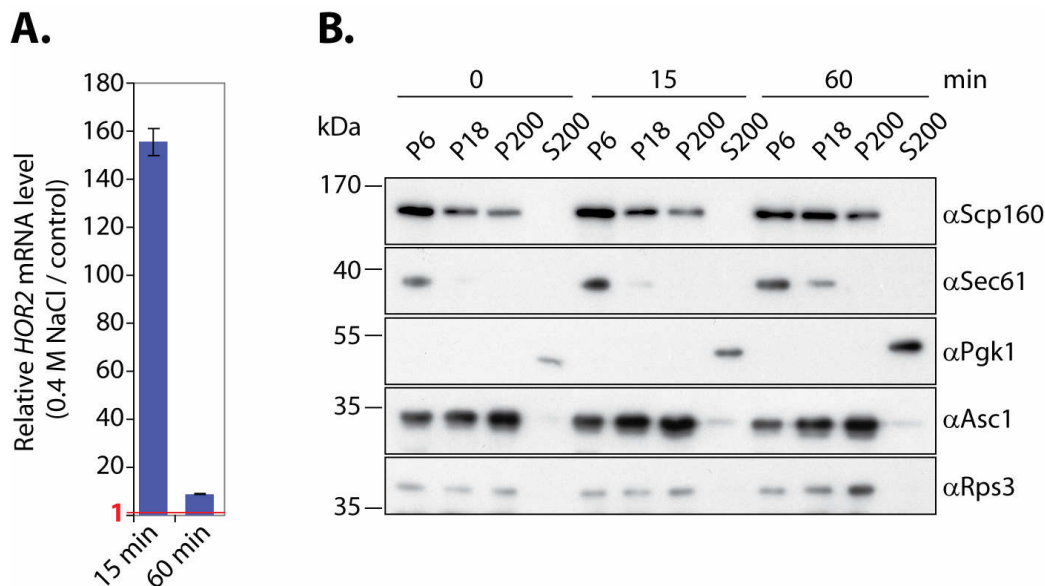


Fig. 15. Mild hyperosmotic shock does not lead to a redistribution of Scp160 within subcellular fractions. Logarithmically growing wildtype cultures (RJY358) were supplemented with 0.4 M NaCl. Samples for subcellular fractionation and RNA preparation were taken at the indicated time points. Left panel: As a control, relative *HOR2* mRNA levels were determined by qRT-PCR analysis (sample duplicates). *HOR2* is known to be induced by hyperosmotic conditions. Right panel: Representative Western blots of the fractionation samples.

4.2.3.4. Tunicamycin-induced ER stress

Accumulation of unfolded proteins in the ER causes stress and induces the unfolded protein response (UPR), which in turn upregulates expression of specific target genes that are involved in the release of the folding stress (Travers et al., 2000). Assuming that Scp160 is involved in the translational control of transcripts translated at the ER, I hypothesized that Scp160 may be

targeted by the UPR in order to diminish translation of its target mRNAs and therefore the load of unfolded polypeptides in the ER. ER stress can for example be induced by treatment with tunicamycin, a drug that inhibits N-linked glycosylation (Mahoney & Duksin, 1979).

To test this hypothesis, logarithmically growing cultures were supplemented with 1 $\mu\text{g}/\text{ml}$ tunicamycin. qRT-PCR analysis confirmed that this concentration of the drug was sufficient to trigger UPR, as mRNA levels of the known UPR target *LHS1* (Chapman et al., 1998) were more than three-fold induced upon treatment (Fig. 16, left panel). Samples were also subjected to subcellular fractionation and analyzed by immunoblotting (Fig. 16, right panel). Also upon induction of ER stress, Scp160 showed its normal distribution pattern.

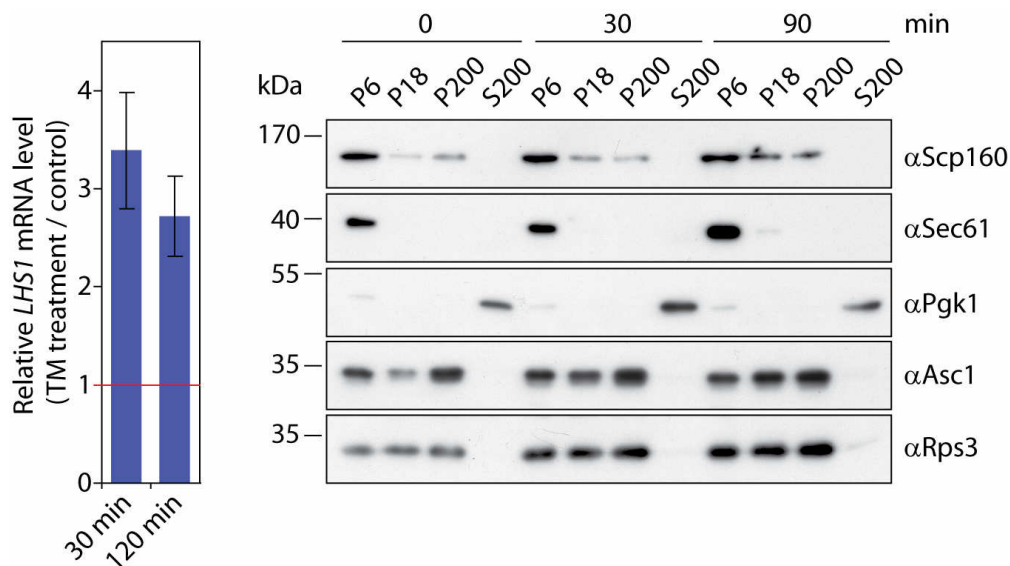


Fig. 16. Tunicamycin-induced ER stress does not lead to a shifted subcellular localization of Scp160. Logarithmically growing wildtype cells (RJY358) were incubated with 1 $\mu\text{g}/\text{ml}$ tunicamycin. Samples were taken at the indicated times and used for subcellular fractionation and preparation of RNA. Left panel: Upregulation of *LHS1* mRNA levels, as shown by qRT-PCR, served as control for the induction of the unfolded protein response (duplicate analysis). Right panel: Western analysis of the fractionation samples; representative blots of two independent experiments are shown.

4.3. A possible role for Scp160 in translation

4.3.1. *scp160* deletion strains display reduced fitness and sensitivity against translation inhibitors

Yeast strains with defects in the translation machinery generally display reduced fitness such as slow or thermosensitive growth (Cuesta et al., 1998). As an indirect test for a putative function of Scp160 in translation, I compared growth of *scp160* Δ and wildtype cells spotted in 10-fold serial dilutions on complete medium and incubated for three days at 20°C, 30°C and 37°C. At all temperatures tested, *scp160* deleted cells demonstrated slightly impaired growth (Fig. 17, left panel). As a more specific assay, the effect of two drugs that inhibit translation, hygromycin B and cycloheximide (CHX), on *scp160* Δ strains was tested. Serial dilutions of wildtype and *scp160* Δ cell suspensions were spotted on complete medium complemented with the respective drug, and growth was compared after three days incubation at 30°C. The deletion mutant showed a decrease in cell viability in this assay (Fig. 17, right panel), although growth was not as strongly impaired as has been reported before (Baum et al., 2004). My data suggest that Scp160 may be to some degree involved in general translation.

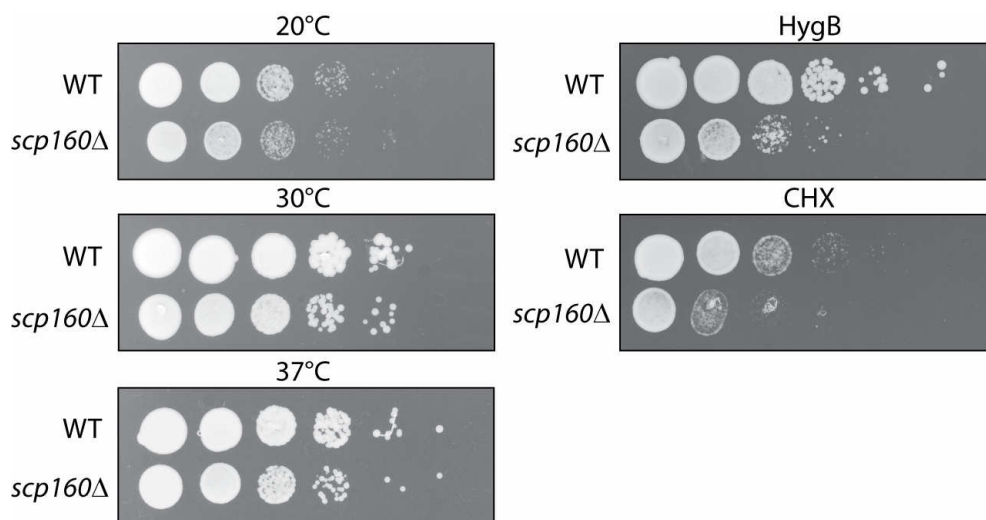


Fig. 17. *scp160* Δ cells display reduced fitness and increased sensitivity against translation inhibitors. Ten-fold serial dilutions of wildtype (RJY358) and *scp160* Δ (RJY3178) cell suspensions were spotted on YEPD plates and incubated for three days at the indicated temperatures (left panel). To test for defects in translation, cells were spotted on YEPD plates supplemented with 75 μ M hygromycin B (HygB) or 0.2 μ M CHX and incubated for three days at 30°C (right panel).

4.3.2. Translation initiation is slightly impaired in *scp160* deletion strains

Polysome profiling has been described as an ultimate phenotypic proof for translation defects (Lee et al., 2007). In order to assess if Scp160 causes changes in the proportion of actively translating ribosomes, polysome profile analyses were carried out for wildtype and *scp160* Δ strains. Whole cell extracts were centrifuged through linear sucrose gradients and absorbance profiles were continuously measured. From these graphs, areas corresponding to translating polysomes (P) and translationally less active monosomes (M) were determined. The P/M ratio was calculated for both strains and found to be significantly decreased in *scp160* Δ samples (2.6 ± 0.47 in *scp160* Δ versus 4.3 ± 0.08 in wildtype) (Fig. 18). These values reflect an increase in the monosome peak and a decrease in the polysome peaks of *scp160* Δ cells, which is indicative of a defect in translation initiation. Yet, further experiments indicated that this initiation defect constitutes an indirect or long-term effect of Scp160 loss (see next section).

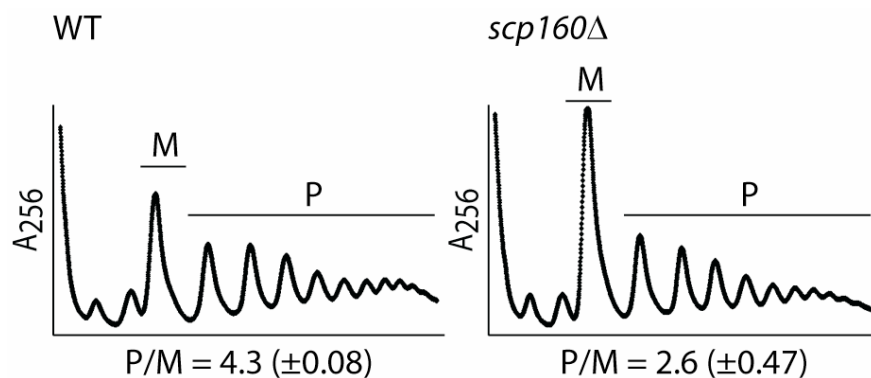


Fig. 18. *scp160* Δ cells are impaired in translation initiation. Lysates of wildtype (RJY358) and *scp160* Δ (RJY3178) cells were separated on 20-60% linear sucrose gradients, and gradient fractions were collected from top to bottom with continuous UV absorption measurement at 256 nm. From the recorded profiles, polysome (P) and monosome (M) areas were defined. Polysome-to-monomer ratios (P/M) report the global translation state. Data represent averages of three independent experiments; standard deviations are indicated in brackets.

4.4. A Tet-off system for the efficient depletion of Scp160

As described in the previous section, *scp160* deleted cells display reduced fitness, increased sensitivity against translation inhibitors, and reduced polysome-to-monomer ratios. These findings suggest a participation of Scp160 in translational processes. However, since deletion of Scp160 causes alterations in ploidy (Wintersberger et al., 1995), I was worried that these results are due to secondary effects caused by ploidy changes. Therefore, I generated a yeast strain in which *SCP160* expression is under control of a repressible Tet_{off} operator, which allows rapid

depletion of the protein upon addition of doxycycline (Gari et al., 1997). As verified by Western blot, repression of *SCP160* resulted in a considerable reduction of the protein after three hours (Fig. 19A). The protein was undetectable after five hours of depletion. In order to test if ploidy alterations occur during or directly after depletion, DNA content was determined by FACS analysis. FACS profiles of *Tet_{off}::SCP160* cells were recorded after 6, 12, 18, and 24 hours of Scp160 depletion and compared to the FACS profile of *scp160* Δ cells (Fig. 19B). A population of

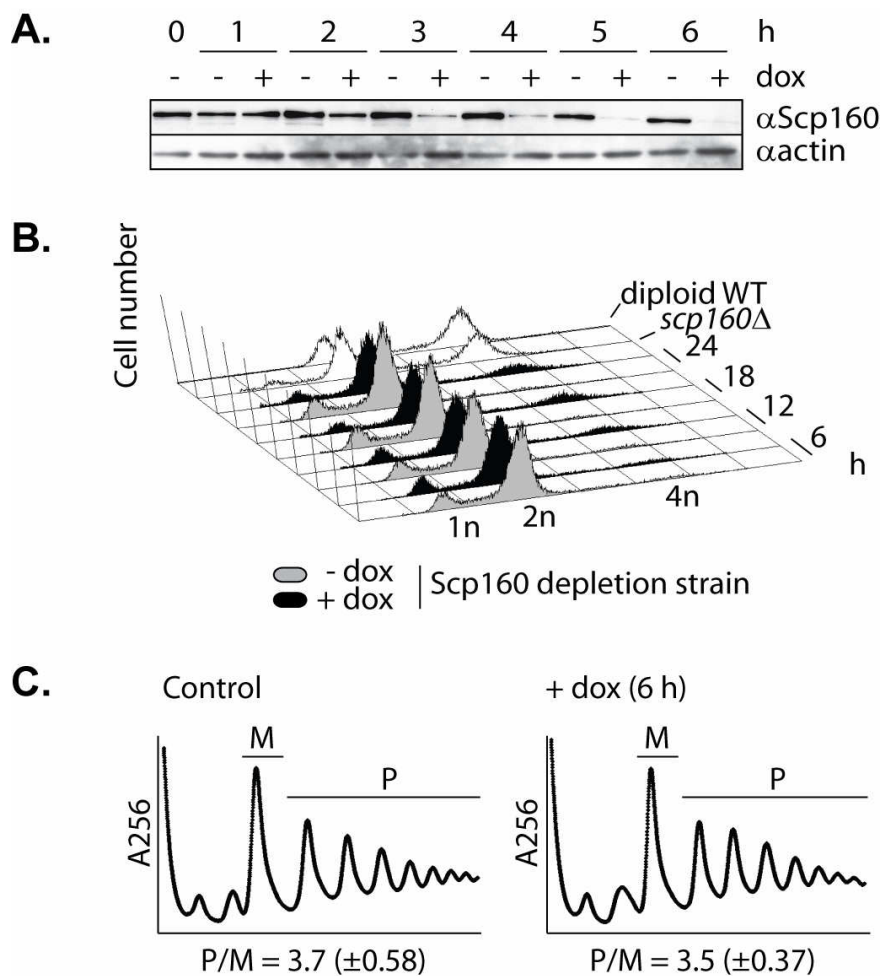


Fig. 19. Depletion of Scp160 results in an increase of ploidy, but does not affect global translation. (A) Western blot of a depletion time course. Logarithmically growing strain RJY3180 was incubated with 2 μ g/ml doxycycline 6 h in total. At times indicated, aliquots were removed to prepare cell extracts. Equivalent protein amounts were used for Western blotting. Depletion of Scp160 was monitored by probing the blot with an anti Scp160 antibody, actin served as loading control. (B) FACS analysis of Scp160-depleted cells. During a time course of 24 h, 2 OD_{600nm} units of cells were removed every 6 h, fixed and prepared for FACS analysis. An *scp160* Δ strain served as control. DNA contents corresponding to the haploid (1n), diploid (2n) or tetraploid (4n) state are indicated. (C) Global translation is not impaired by depletion of Scp160. Cell extracts were prepared of non-depleted and Scp160-depleted cells and separated by sucrose density centrifugation. Polysome-to-monosome ratios (P/M) were calculated as in Fig. 18. Data represent averages of three independent experiments; standard deviations are indicated in brackets.

haploid *scp160* Δ cells does not only contain cells with 1n or 2n DNA content but in addition 4n cells, indicating a failure to faithfully control ploidy. In contrast, only very few 4n cells can be detected in a population of cells depleted for Scp160 for six hours. I therefore chose a six hour depletion period of Scp160 for my further experiments.

Using the newly established depletion system, I repeated the polysome profile analyses (see section 4.3.2.). Polysome-to-monosome ratios were calculated and found to be unchanged by depletion of Scp160 (control: 3.7 ± 0.58 , depletion: 3.5 ± 0.37 ; Fig. 19C). In conclusion, Scp160 does not directly affect global translation initiation.

4.5. Translational profiling – elucidating the function of Scp160 in translation

Translational activity of a given transcript is commonly measured as the extent of its association with polysomes. As mentioned above, sucrose density gradient centrifugation can be used to separate cell extracts in translationally inactive or less active fractions (containing mRNPs, ribosomal subunits and monosomes; "light") and in fractions with high translational activity (polysomes; "heavy"). Using microarray analysis, specific translational profiles can be assigned to all mRNAs present in the samples. A large number of genome-wide studies dealing with the effects of diverse treatments such as glucose starvation or application of rapamycin have shown that this approach is highly valuable to identify both global translational changes as well as changes limited to smaller mRNA subsets (reviewed in Halbeisen et al., 2008). Therefore, I decided to apply a similar approach with the aim to identify transcripts that are differentially translated in dependence on Scp160.

The experimental setup comprised two parts. First, I aimed at identifying transcripts with changes in their translation rates and second, I wanted to assess genome-wide steady-state mRNA levels. The latter is essential for the interpretation of translation rate changes since reduced association of mRNAs with non-translating gradient fractions could either result from a shift towards translationally more active fractions or from increased degradation (Melamed & Arava, 2007).

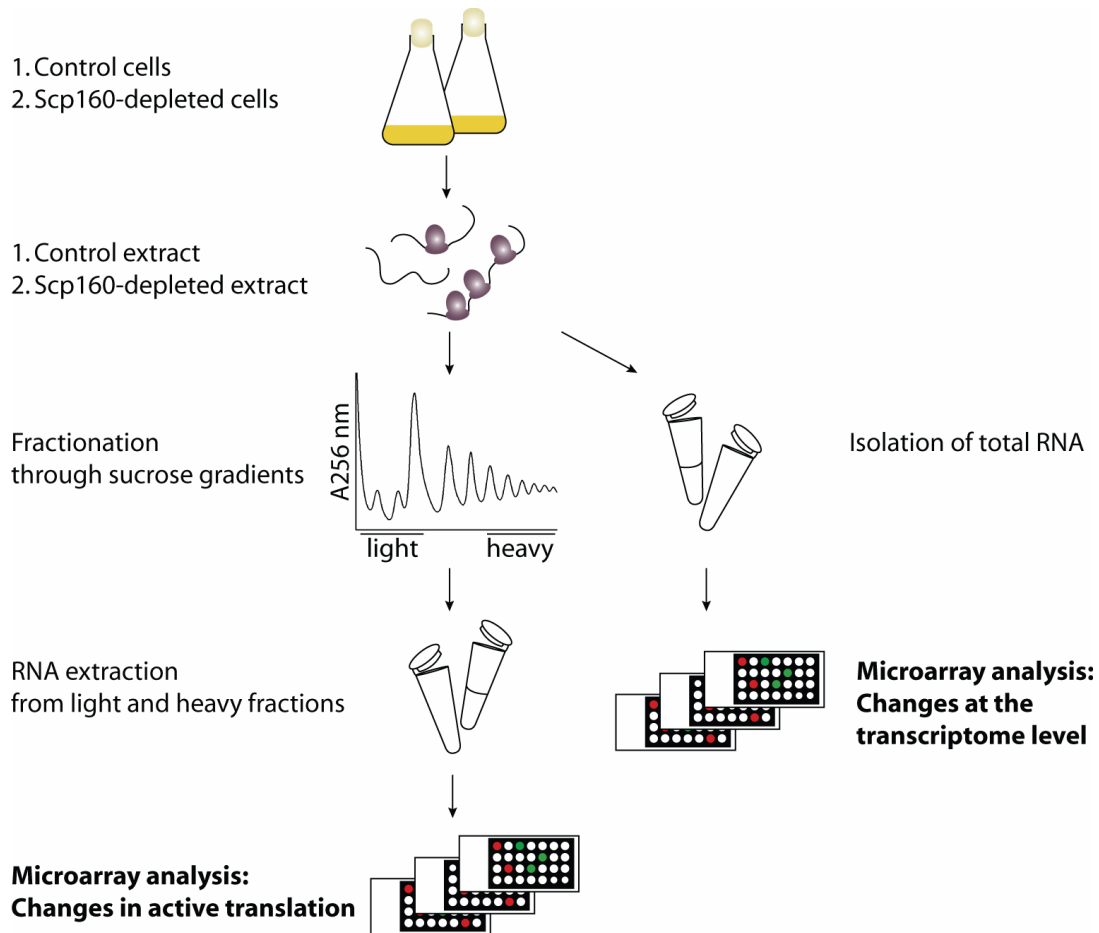


Fig. 20. Workflow of the translational profiling approach. Extracts from Scp160-depleted and non-depleted (control) cells were prepared and either directly used for isolation of total RNA (right) or fractionated by sucrose density centrifugation (left). RNA was extracted from fraction pools corresponding to mRNPs, ribosomal subunits and monosomes (light fractions) and heavy polysomes (heavy fractions). RNA samples were reverse transcribed and hybridized to DNA microarrays. Whereas analysis of total RNA should reveal changes in overall transcription and RNA stability, analysis of translationally inactive (light) and active (heavy) gradient fractions should reflect the translational state of the mRNAs.

A scheme of the experimental setup that was applied in this study is shown in Fig. 20. In order to prevent secondary effects caused by deletion of Scp160, I used cells in which Scp160 was depleted for 6 h by the above described Tet_{off} system (section 4.4.); mock-depleted cultures served as negative control. Whole cell extracts were prepared as described in section 6.2.5.1. and used for preparation of total RNA as well as for sucrose density centrifugation with subsequent RNA isolation from light and heavy fractions. Following reverse transcription, cDNA was hybridized to DNA microarrays. Data analysis was done in cooperation with Andreas Mayer from Prof. Patrick Cramer's laboratory at the Gene Center, LMU Munich.

4.5.1. Depletion of Scp160 causes subtle changes at the transcriptome level

To determine if loss of Scp160 leads to changes in the abundance of specific mRNAs, either through differing stability or changed transcription rates, microarray analyses were performed of total RNA from control and Scp160-depleted cells (see Fig. 20).

Using a standard p-value cutoff of 0.05 and a conservative fold change threshold of 2.5 in order to minimize the occurrence of false positives, I identified 60 mRNAs of which 49 were down- and 11 were up-regulated (see table 1). With a fold change threshold of 2.0, the abundance of 117 mRNAs was affected (89 down- and 28 up-regulated). This corresponds to 1.1% and 2.1% of the yeast transcriptome, respectively. Notably, most transcripts showed a decreased abundance in absence of Scp160 (82% and 76%, respectively). Among the five most downregulated mRNAs was *SCP160* (fold change of 0.11, corresponding to a 9-fold decrease compared to control cells), confirming the efficiency of the depletion. Li and coworkers identified *YOR338W* mRNA as being associated with Scp160-containing complexes, and found it to be 2.5-fold more abundant in *scp160Δ* cells as in wildtype (Li et al., 2003). In my study, I measured a 2.9-fold increased level of *YOR338W* upon depletion of Scp160, indicating that direct targets of Scp160 are likewise affected by deletion and depletion of Scp160.

Table 1. List of genes that are significantly up- or downregulated upon depletion of Scp160. Threshold: 2.5-fold change (≥ 2.5 or ≤ 0.4); data from duplicate microarray and qRT-PCR analysis.

ORF	Symbol	Fold change (depl. vs. control)	p-value	Fold change (depl. vs. control) qRT-PCR
YCR021C*	HSP30	0.04	4.05e-05	n/a
YER067W	---	0.05	2.10e-04	n/a
YER053C-A	---	0.10	1.49e-05	n/a
YPL014W	---	0.11	1.58e-06	n/a
YJL080C*	SCP160	0.11	2.13e-05	0.07
YDR171W*	HSP42	0.13	1.91e-05	0.92
YNR034W-A	---	0.14	6.38e-04	n/a
YER053C	PIC2	0.17	1.18e-05	n/a
YJL144W	---	0.18	5.27e-04	n/a
YER150W	SPI1	0.19	1.41e-05	n/a
YHR087W	---	0.21	6.21e-04	n/a
YFR015C	GSY1	0.23	1.67e-04	n/a
YHL036W*	MUP3	0.23	1.06e-06	0.95
YBR054W*	YRO2	0.24	1.15e-04	0.89
YPR157W	---	0.24	1.93e-04	n/a
YLL026W*	HSP104	0.25	1.26e-03	0.89
YGR249W*	MGA1	0.25	9.43e-04	0.83
YGR008C	STF2	0.26	1.26e-03	n/a
YMR104C	YPK2	0.27	2.66e-03	n/a
YLR327C*	TMA10	0.28	1.12e-03	1.01
YJL052W	---	0.28	8.97e-05	n/a
YGR052W	---	0.28	1.60e-04	n/a
YGR248W	SOL4	0.29	4.35e-04	n/a

RESULTS

YOR273C	TPO4	0.29	7.53e-04	n/a
YMR081C	ISF1	0.30	1.20e-03	n/a
YMR250W	GAD1	0.30	2.07e-04	n/a
YHL021C	---	0.30	1.93e-03	n/a
YEL011W	GLC3	0.30	4.97e-04	n/a
YDR258C	HSP78	0.31	5.47e-04	n/a
YJL052W	---	0.32	3.52e-04	n/a
YGR142W	BTN2	0.33	2.58e-04	n/a
YOR134W	BAG7	0.33	4.95e-04	n/a
YLR297W	---	0.33	3.06e-05	n/a
YCL040W	GLK1	0.34	1.32e-04	n/a
YPL240C*	HSP82	0.34	1.18e-03	0.96
YML128C	MSC1	0.34	1.10e-04	n/a
YBR214W	SDS24	0.35	7.63e-04	n/a
YLR142W	PUT1	0.35	1.80e-03	n/a
YER037W	PHM8	0.35	1.58e-04	n/a
YMR084W	---	0.36	2.51e-02	n/a
YBR169C*	SSE2	0.36	1.61e-04	0.77
YBR183W	YPC1	0.36	1.56e-04	n/a
YOR178C	GAC1	0.36	8.91e-03	n/a
YGR088W	CTT1	0.39	1.98e-03	n/a
YCR005C	CIT2	0.39	4.59e-05	n/a
YDR222W	---	0.39	8.83e-04	n/a
YOR173W*	DCS2	0.39	2.48e-03	0.79
YER130C	---	0.39	2.71e-05	n/a
YJL133C-A	---	0.39	4.26e-03	n/a
YMR085W	---	0.40	3.14e-04	n/a
YBR105C	VID24	2.53	1.29e-04	n/a
YBR296C	PHO89	2.55	4.75e-03	n/a
YDL038C	---	2.64	2.41e-03	n/a
YOL154W	ZPS1	2.76	8.23e-04	n/a
YOR338W	---	2.90	5.95e-04	n/a
YNL065W	AQR1	2.98	1.93e-04	n/a
YDL037C	BSC1	3.13	2.87e-03	n/a
YGR079W	---	3.14	8.13e-04	n/a
YGL209W	MIG2	3.34	7.68e-05	n/a
YKR075C	---	3.94	2.05e-04	n/a
YGR035C	---	6.15	1.50e-04	n/a

mRNAs subsequently tested by qRT-PCR are marked with a star (*). n/a – not tested.

Functional and locational classification of the proteins encoded by mRNAs with a more than 2.5-fold change was performed using the MIPS Functional Catalogue Database (Ruepp et al., 2004). With a p-value cutoff of 0.05 and considering only categories to which at least five mRNA targets could be assigned, I found a significant enrichment of transcripts encoding proteins that are localized to vacuole and cytoplasm (Fig. 21, upper panel). Regarding functional terms, mRNAs that code for proteins with functions in protein folding and stabilization, stress response and energy metabolism were overrepresented (p-value \leq 0.005, at least five mRNAs; Fig. 21, lower panel). These data suggest that depletion of Scp160 induces stress-related changes in the transcriptome.

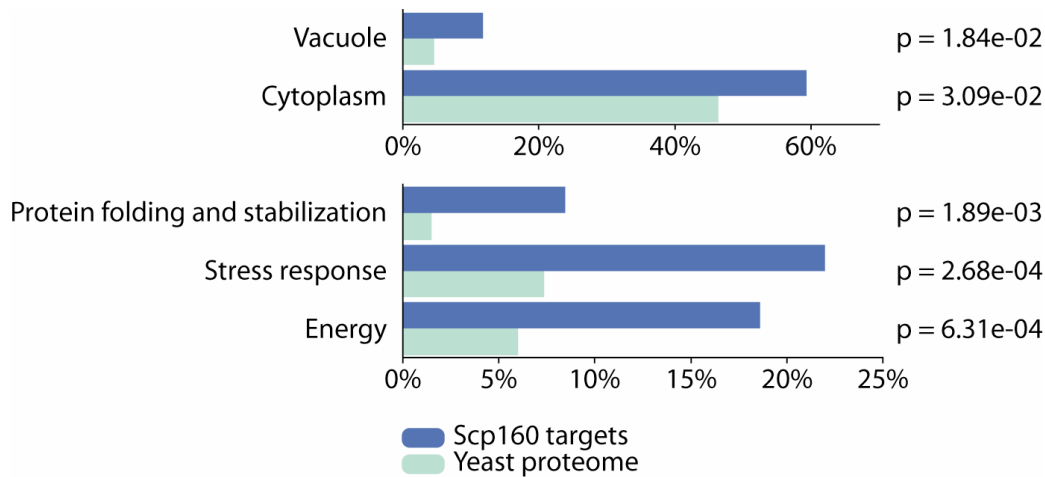


Fig. 21. Depletion of Scp160 induces changes in the abundance of stress-related mRNAs. Proteins encoded by mRNAs which are up- or downregulated more than 2.5-fold upon depletion of Scp160 were classified using the MIPS Functional Catalogue Database. Upper panel: Locational distribution analysis revealed an enrichment of vacuolar and cytoplasmic proteins (p -value cutoff: $p \leq 0.05$). Lower panel: Functional distribution analysis showed enrichment in distinct subgroups (p -value cutoff: $p \leq 0.005$).

In order to confirm the data derived from the microarrays, I performed qRT-PCR on control and Scp160-depleted samples for ten of the candidate mRNAs. Although downregulation of *SCP160* itself was in a similar range as measured by microarray analysis (microarrays: 9-fold decreased, qRT-PCR: 14-fold decreased), I could not corroborate the changes of the other transcripts tested (see table 1). This indicates that the data set gained from microarray analysis contains a high percentage of false-positives, probably due to the limited number of replicates (duplicate analysis). Deeper analysis of transcripts whose abundance is affected by loss of Scp160 was beyond the scope of this work since my focus was on Scp160's function in translational control. Careful validation by qRT-PCR of the so far not tested target mRNAs would be essential for potential further studies focusing on transcriptome changes induced by Scp160.

4.5.2. Depletion of Scp160 induces translational state changes of a subset of mRNAs

As described above, microarray analysis of RNAs isolated from translationally active and inactive gradient fractions was carried out to determine if depletion of Scp160 induces changes in the translational activity of specific mRNAs. From the resulting dataset, translational state changes were calculated (Fig. 22). I defined the translational state of an mRNA as the ratio of its abundance in heavy versus light fractions. The translational state of each mRNA was registered in

Scp160-depleted and control cells. From these values, ratios were calculated to obtain a translational state change (TSC) that reflects the shift in the distribution of a given mRNA within the sucrose gradient upon depletion of Scp160. Increases of the TSC value should indicate a shift from less efficient to efficient translation, whereas decreased TSC values should indicate an opposite shift. Using a cutoff of 1.8-fold (≥ 1.8 or ≤ 0.56), I identified 48 mRNAs with increased and 12 mRNAs with decreased polysome association (Table 2; 2 fold cutoff: 23 and 5 mRNAs, respectively). These results indicate that depletion of Scp160 affects the translational state of a small subset of mRNAs (1.1% of the transcriptome) even before ploidy defects are detectable. Notably, the majority (80%) of these mRNAs were shifted towards the heavy gradient fractions, indicating that Scp160 has the same effect on the translation of this group of targets.

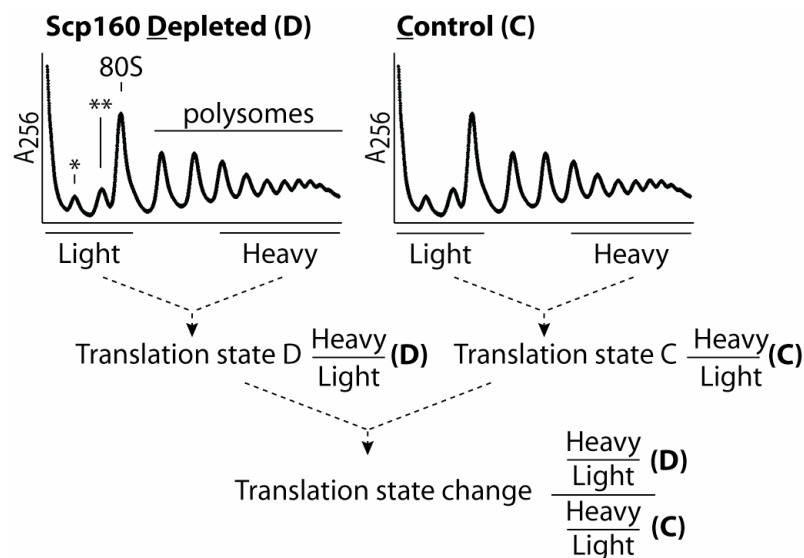


Fig. 22. Calculation of translation state changes. Sucrose gradient profiles of whole cell extracts of Scp160-depleted and control samples were monitored by absorbance at 256 nm. The positions of the small and large ribosomal subunits (* - 40S, ** - 60S), monosomes and polysomes are indicated. Light and heavy fractions of both samples were collected, and extracted mRNA was used for duplicate microarray analyses. For each individual mRNA, translation states were calculated as the ratio of the normalized signal in heavy and light fraction. Translation state changes were then calculated as the double ratio of the translation states in Scp160-depleted versus control sample.

Table 2. Genes with significant (≥ 1.8 or ≤ 0.56) translation state changes (TSC) upon depletion of Scp160 (data from duplicate microarray analyses).

ORF	Symbol	TSC depleted/control ^a	Polysomal RNA depleted/control ^b	Monosomal RNA depleted/control ^c	Total RNA depleted/control ^b
YPR159C-A	---	3.71	1.43	0.43	1.02
YHR213W	---	2.67	1.95	0.74	1.07
YJL078C*	PRY3*	2.66*	2.08*	0.75*	0.97*
YCR089W	FIG2	2.60	1.83	0.76	1.43
YLR139C	SLS1	2.60	2.08	0.82	1.43
YAL065C	---	2.59	1.57	0.65	1.12
YJR151C	DAN4	2.42	1.73	0.75	0.99
YNR044W*	AGA1*	2.41*	2.17*	0.93*	1.37*
YHR189W	PTH1	2.40	1.66	0.76	1.02
YCL021W-A	---	2.29	1.87	0.89	1.21
YDR420W	HKR1	2.23	2.23	0.97	1.14
YIR019C	MUC1	2.21	1.67	0.82	1.03
YPL085W	SEC16	2.18	1.57	0.74	1.15
YLR337C	VRP1	2.17	1.83	0.90	0.91
YNL271C	BNI1	2.17	1.71	0.83	1.06
YLR013W	GAT3	2.15	1.41	0.70	1.02
YMR175W-A	---	2.10	1.42	0.65	1.03
YAR050W	FLO1	2.09	1.58	0.77	1.03
YAR009C	---	2.07	2.27	1.10	0.89
YJL216C	---	2.05	1.34	0.65	1.38
YKR102W	FLO10	2.05	1.49	0.76	1.24
YOR181W	LAS17	2.01	1.52	0.78	1.05
YBL074C	AAR2	2.01	1.52	0.74	1.19
YOL019W-A	---	2.00	1.08	0.58	1.02
YMR070W	MOT3	1.97	1.71	0.93	1.45
YLR315W	NKP2	1.95	1.15	0.59	0.83
YOR316C-A	---	1.95	1.35	0.65	1.11
YBR072C-A	---	1.94	1.19	0.58	1.01
YNL277W-A	---	1.94	1.10	0.57	0.79
YNL068C	FKH2	1.91	1.65	0.88	1.05
YCR108C	---	1.91	1.20	0.62	0.97
YDL039C	PRM7	1.90	1.72	0.93	2.44
YCR068W	ATG15	1.90	1.56	0.87	0.97
YER132C	PMD1	1.89	1.49	0.84	1.15
YGR023W	MTL1	1.88	1.87	1.03	0.57
YBL044W	---	1.87	1.09	0.57	1.10
YNL093W	YPT53	1.87	1.03	0.58	0.49
YEL035C	UTR5	1.85	1.31	0.70	1.13
YLR390W-A*	CCW14*	1.84*	0.98*	0.56*	1.02*
YNL034W	---	1.84	1.26	0.69	1.26
YLR393W	ATP10	1.83	1.23	0.68	1.12
YDL195W	SEC31	1.83	1.34	0.74	1.02
YEL019C	MMS21	1.82	1.16	0.63	0.99
YLR136C	TIS11	1.82	1.27	0.72	0.56
YOR394C-A	---	1.81	1.54	0.85	1.20
YOR329C	SCD5	1.81	1.42	0.81	0.96
YGR014W*	MSB2*	1.81*	1.74*	0.99*	1.12*
YGR249W	MGA1	1.80	1.38	0.69	0.25
YDR034C-A	---	0.55	0.47	0.61	1.16
YGR109W-A	---	0.55	0.72	1.12	1.21
YDL156W	---	0.55	0.84	1.22	0.99
YFL024C	EPL1	0.52	1.05	1.62	1.12

YFL068W	---	0.52	0.61	1.15	1.14
YER014C-A	BUD25	0.52	0.52	0.79	1.05
YIR018C-A	---	0.51	0.48	0.74	1.14
YGL168W	HUR1	0.47	0.46	0.86	1.23
YFR035C	---	0.47	0.42	0.62	1.03
YGR240C-A	---	0.46	0.45	0.70	1.27
YGR035W-A	---	0.45	0.49	0.90	1.86
YDR524W-A	---	0.36	0.31	0.50	1.36

mRNAs tested by IP-qRT-PCR are in bold; mRNAs associated with Scp160 are marked with a star.

^a Changes in translation state (heavy/light (D) / heavy/light (C))

^b Changes in polysomal mRNA pool

^c Changes in monosomal and mRNP associated mRNA pool

^d Changes in total mRNA pool

A systematic classification of the mRNAs up- or downregulated in translation revealed that they are enriched for mRNAs encoding extracellular and cell wall proteins, as well as proteins involved in ER-to-golgi transport (Fig. 23, upper panel) as classified by the MIPS Functional Catalogue Database (Ruepp et al., 2004). The targets can be functionally grouped into proteins involved in cell-cell adhesion, cell polarity establishment and filament formation, sugar binding, endocytosis, and response to osmotic and salt stress (Fig. 23, lower panel). A common feature of many of these proteins is their targeting to the ER which occurs mainly co-translationally. This is in agreement with previously published data showing that Scp160 localizes to cytoplasmic as well as ER-attached polysomes (Frey et al., 2001; Weber et al., 1997; Lang & Fridovich-Keil, 2000).

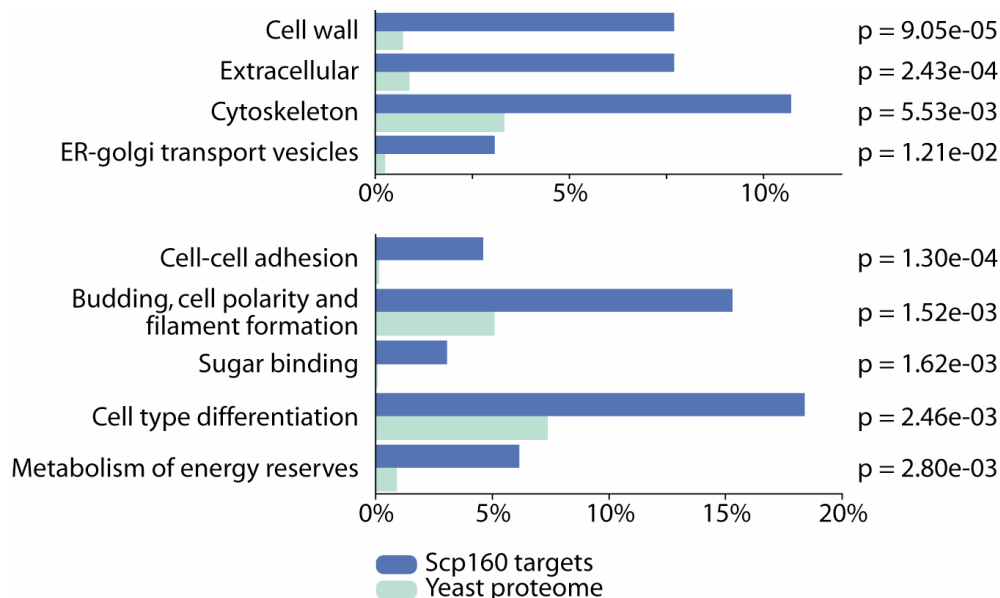


Fig. 23. Depletion of Scp160 changes translational states of a specific set of mRNAs. mRNAs with significant translation state changes (≥ 1.8 or ≤ 0.56) upon depletion of Scp160 were classified using the MIPS Functional Catalogue Database. Upper panel: Locational distribution analysis of the proteins encoded by the candidate mRNAs revealed clustering in specific classes (p-value cutoff: $p < 1.5e-02$). Lower panel: Functional distribution analysis of the same proteins showed enrichment in distinct subgroups (p-value cutoff: $p < 4.0e-03$).

4.6. mRNAs with significant translational state changes are bound by Scp160

4.6.1. Target mRNAs are enriched in immunoprecipitates of Scp160

The observed changes of the translational state of some mRNAs could be a direct consequence of the loss of Scp160, e.g. if it functions as translational regulator, or indirect by affecting the overall physiological state of the cell. A direct function on its target mRNAs is likely to be mediated by the RNA-binding activity of Scp160. In order to test this assumption, I applied immunoprecipitation of C-terminally myc9-tagged Scp160 in combination with quantitative real-time PCR (qRT-PCR) to detect co-purifying RNAs (Fig. 24). As specificity controls, I performed the same assay with two additional RNA-binding proteins that were likewise tagged with nine myc epitopes. She2 is an RNA-binding protein that associates with a defined set of localized mRNAs (Shepard et al., 2003). Khd1, like Scp160, belongs to the group of KH domain containing RNA-binding proteins and binds to a large set of mRNAs with diverse functions (Irie et al., 2002; Hogan et al., 2008; Hasegawa et al., 2008). Myc-tagged versions of all three proteins were functionally expressed in yeast and Western blot analysis confirmed that similar amounts of each protein could be immunoprecipitated (Fig. 24A). RNA was extracted from the pellet, reverse transcribed, and amplified with primers against 14 mRNAs showing significant translational state changes (≥ 1.8 or ≤ 0.56), but no differences in their total abundance (≥ 0.71 , ≤ 1.4 ; see table 2). I also included the nucleoporin-encoding *POM34* transcript in my analysis since it has recently been identified as a target of Scp160 (Sezen et al., 2009). Fig. 24B summarizes the results for the four mRNAs with significant enrichment in the Scp160 immunoprecipitates. Whereas She2 co-immunoprecipitated its known target mRNA *ASH1* but none of the other five mRNAs (Fig. 24B, black bars), Scp160 immunopellets (Fig. 24B, blue bars) were >7 fold enriched for *CCW14*, *AGA1* and *PRY3* and >2 fold enriched for *MSB2* and *POM34* mRNAs. These enrichment values do not directly reflect the degree of the translation state changes of these transcripts, since the TSCs of *AGA1* and *PRY3* are 2.4 and 2.7, respectively, whereas both *CCW14* and *MSB2* have a TSC of 1.8. A control mRNA, *CFT1*, whose translation rate did not change upon Scp160 depletion, neither co-purified with Scp160 nor with She2. *AGA1*, *PRY3*, and *POM34* were enriched in Khd1 immunopellets at similar levels (Fig. 24, orange bars), suggesting that they contain binding sites for KH domain type RNA-binding proteins. *CCW14* and *MSB2* mRNAs were also associated with Khd1, albeit enrichment was reduced in comparison to the Scp160 immunopellets to approximately 37% and 78%, respectively (p-values < 0.05). In summary, out of the 14 candidate mRNAs I found four to be

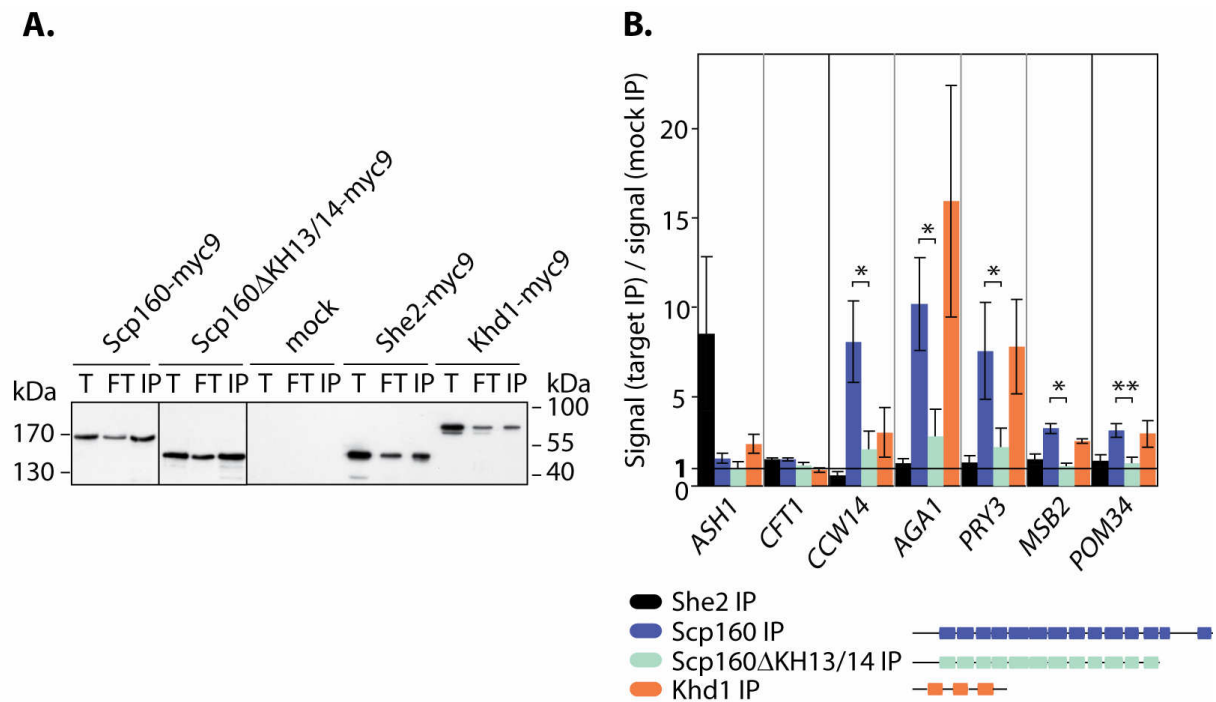


Fig. 24. Scp160 physically associates with target mRNAs. (A) Western blot of the immunoprecipitation of myc9-tagged Scp160 (strain RJY3515), Scp160 truncated for KH domains 13 and 14 (RJY3516), She2 (RJY3512) and Khd1 (HSY15) using anti myc antibody. T - total extracts, FT - flowthrough, IP - immunoprecipitate. (B) Scp160 binds *CCW14*, *AGA1*, *PRY3*, *POM34* and *MSB2* mRNAs. Immunoprecipitates were subjected to qRT-PCR and analyzed for bound *ASH1* mRNA (positive control in She2 IP), *CFT1* mRNA (negative control), and candidate mRNAs *CCW14*, *AGA1*, *PRY3*, *MSB2* and *POM34*. Specific enrichment was calculated as ratio of the signal in the target IP to the mock IP (untagged wildtype strain). Statistical significance (Student's t-test) compared to the KH domain truncation is indicated: *, P < 0.05; **, P < 0.01. Data are presented as mean \pm standard deviation, n = 3.

enriched more than 2-fold in the Scp160 immunoprecipitates (Fig. 24B): *CCW14*, encoding a cell wall glycoprotein (Moukadiri et al., 1997), *AGA1* that codes for a subunit of a-agglutinin in the cell wall (Roy et al., 1991), *PRY3* that encodes a member of the PRY family of GPI-anchored cell wall proteins (Yin et al., 2005), and *MSB2*, coding for an integral plasma membrane mucin linked to osmosensing (O'Rourke & Herskowitz, 2002). Consistently, these four mRNAs were also identified as associated with Scp160 ($\log_2 \geq 1.1$) in a recent large-scale survey (Hogan et al., 2008).

To investigate if binding of Scp160 to the mRNAs mentioned above is direct or mediated by an associated protein, I generated a carboxyterminally truncated version of Scp160 that lacks the last two KH domains (Scp160ΔKH13/14). Myc9-tagged Scp160ΔKH13/14 can be immunoprecipitated at similar levels than the full-length protein (Fig. 24A). However, none of the mRNAs co-purifying with Scp160 associates with the truncated version (Fig. 24B, light green bars), indicating that the last two KH domains are essential for RNA binding.

4.6.2. Conserved residues in KH domains 13 and 14 are essential for target RNA binding

In section 4.2.2., the generation of Scp160 point mutants with amino acid exchanges in the conserved RNA binding pockets of KH domains 13 and 14 has been described. These mutant versions of Scp160 have been shown to still localize to the ER and ribosomal fractions in subcellular fractionation experiments, but they are in addition present in a free, non-ribosome associated cytoplasmic pool (see Fig. 12). In order to obtain evidence that these point mutations are deleterious for RNA binding, I tested them in the above-described IP-qRT-PCR assay. Both mutants (either containing mutations in KH domain 14 only or additionally in KH domain 13; refer to Fig. 12) could be immunoprecipitated with similar efficiency as wildtype myc9-tagged Scp160 expressed from the same low copy vector (Fig. 25A). qRT-PCR revealed that Scp160mutKH14 binds significantly less of *CCW14*, *AGA1*, and *PRY3* mRNAs (Fig. 25B, blue bars) and that mutation of KH13 and KH14 (light green bars) reduces binding to less than 50%

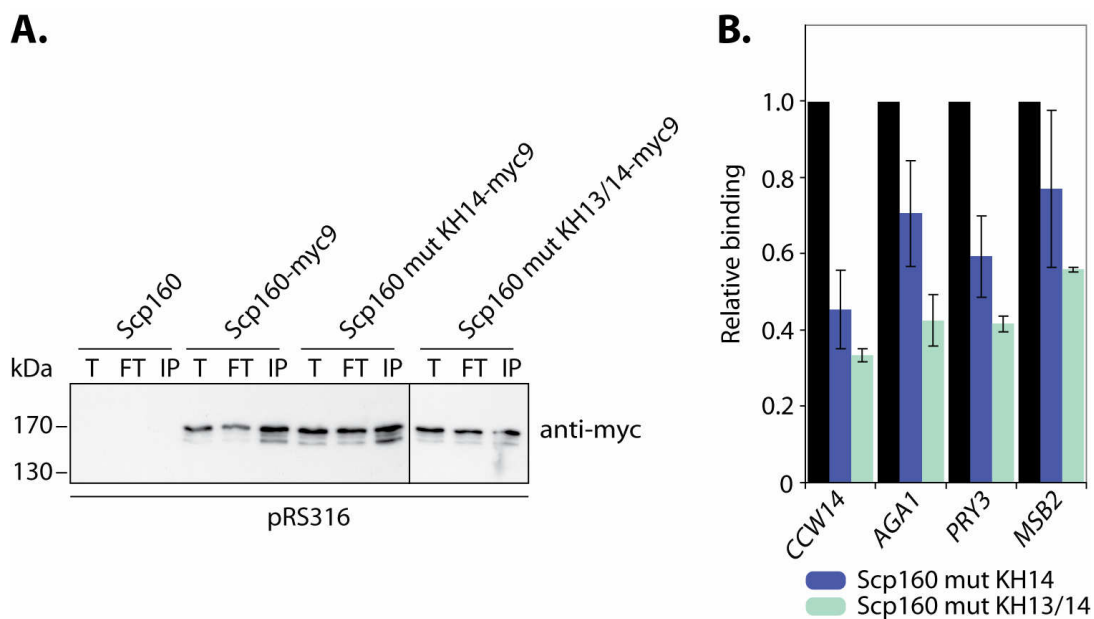


Fig. 25. Conserved residues in KH domains 13 and 14 are essential for target RNA binding. (A) Western blot of the immunoprecipitation of myc9-tagged Scp160 (HSY11), Scp160 with point mutations in KH domain 14 (HSY10) and Scp160 with point mutations in KH domains 13 and 14 (HSY12) using anti-myc antibody. As control, a strain expressing untagged wildtype Scp160 from pRS316 was used. T: total extracts, FT: flowthrough, IP: immunoprecipitate. (B) Target RNA binding of Scp160 point mutants is impaired. Immunoprecipitates of plasmid-derived myc9-tagged Scp160 (HSY11), Scp160mutKH14 (G1170D and G1173D) (HSY10) and Scp160mutKH13/14 (additionally G1028D and I1031N) (HSY12) were subjected to qRT-PCR and analyzed for bound *CCW14*, *AGA1*, *PRY3* and *MSB2*. Specific enrichment was calculated as in Fig. 24 and plotted as relative binding (target binding of wildtype Scp160-myc9 was arbitrarily set to 1). Data are presented as mean \pm standard deviation, n = 2.

of the wildtype. We conclude that mutations in amino acids that have been implicated in RNA binding by KH domains reduce the affinity of Scp160 for at least three mRNAs whose translational state depends on this protein. These mRNAs therefore represent likely target mRNAs for Scp160.

4.7. Scp160 is required for efficient translation of *PRY3* mRNA

So far, I have shown that *PRY3* mRNA significantly shifts towards the polysome fraction in response to depletion of Scp160 (section 4.5.2.), and that it is directly associated with Scp160 via KH domains 13 and 14 (sections 4.6.1. and 4.6.2.). My next experiments addressed the question if the gradient shift of *PRY3* indeed affects its translation rate.

4.7.1. Pry3-6HA protein levels are reduced in cells lacking Scp160

In order to test if the observed translational state changes reflect altered translation, I determined Pry3 levels before and after Scp160 depletion. For detection of Pry3, a variant with six HA epitopes fused to the carboxyterminus was expressed from its genomic locus. Lysates were prepared from cells six hours after doxycycline addition or after six hours incubation without

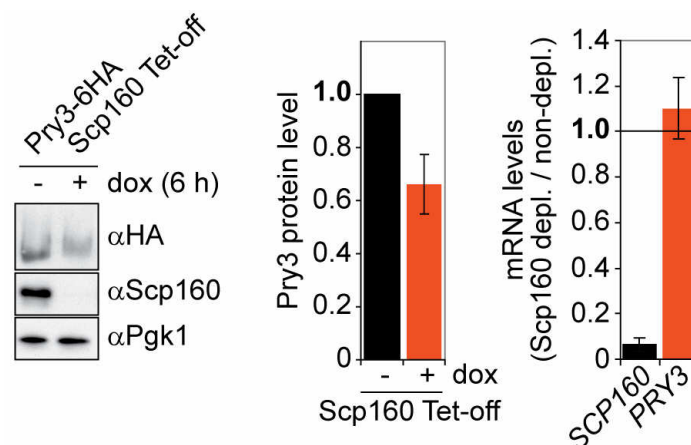


Fig. 26. Pry3-6HA protein levels are reduced upon depletion of Scp160. Whole cell extracts were prepared from strain RJY3498 6 h after addition of 2 $\mu\text{g}/\text{ml}$ doxycycline or after mock depletion. Left panel: Equivalent total protein amounts were used for Western blotting. Probing with anti Scp160 antibody shows the efficient depletion of Scp160, anti HA antibody the reduction of Pry3-6HA protein levels upon depletion of Scp160, and Pgk1 serves as loading control. One representative experiment is shown. Middle panel: Quantification of four experiments performed as in the left panel. Right panel: RNA was prepared from the same samples and used for qRT-PCR. Relative *PRY3* and *SCP160* mRNA levels were calculated as signal ratio between Scp160-depleted and non-depleted samples. All data are presented as mean \pm standard deviation, $n = 4$.

doxycycline (mock depletion). In contrast to Scp160 or phosphoglycerokinase (Pgk1), no defined bands but a smear at >200 kDa could be detected for Pry3-6HA (Fig. 26, left panel). Depletion of Scp160 led to a reduction of Pry3 levels to 66% (+/-11%) (Fig. 26, middle panel; four independent depletion experiments). In contrast, *PRY3* mRNA levels did not significantly change, whereas *SCP160* mRNA dropped to 6% (+/- 3%) of the original amount (Fig. 26, right panel). However, quantification of the protein levels was hampered by the smeary Western blot signal for Pry3, which was presumably caused by its GPI anchor (Eisenhaber et al., 2004).

4.7.2. Pry3ΔGPI protein levels are reduced upon loss of Scp160

To obtain more focused Pry3 signals on Western blots and therefore allow for more reliable quantification, I replaced the C-terminal 29 amino acids that include the GPI modification site at Gly 853 (Fig. 27A) as predicted by the GPI Fungal Prediction Server (Eisenhaber et al., 2004) by a myc9 tag (Pry3ΔGPI-myc9). FACS analysis demonstrated that this truncated version of Pry3 induced only minor changes in the DNA content of the resulting yeast strain (Fig. 27B), in contrast to the depletion of Pry3 (refer to Fig. 30).

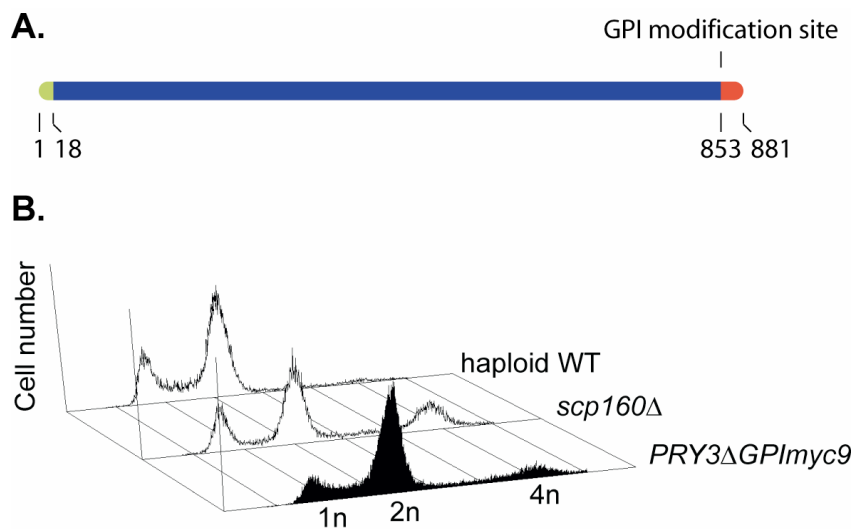


Fig. 27. Pry3 has a predicted GPI modification site. (A) Schematic drawing of the Pry3 primary structure illustrating the position of the predicted signal peptide (aa 1-18, shown in green), propeptide (aa 854-881, marked in red) and GPI modification site (Gly853). Refer to UniProtKB/Swiss-Prot data base entry P47033. Figure drawn to scale. **(B)** FACS analysis of the *PRY3ΔGPImyc9* strain (HSY19) reveals only minor DNA content aberrations.

Removal of the GPI modification site expectedly resulted in a more focused signal of Pry3, allowing better quantification (Fig. 28A and 28B, left panels). Pry3 Δ GPI-myc9 levels in *scp160 Δ were reduced to 53% (+/- 7%) compared to the wildtype control (Fig. 28A, middle panel). In cells depleted for Scp160, Pry3 Δ GPI-myc9 levels decreased to 87% (+/-12%; student's t-test: $p = 0.0022$) compared to non-depleted controls (Fig. 28B, middle panel). In both experimental setups, mRNA levels did not drop accordingly (Figs. 28A and 28B, right panels), suggesting a decrease in Pry3 translation or an increase in Pry3 degradation upon loss of Scp160.*

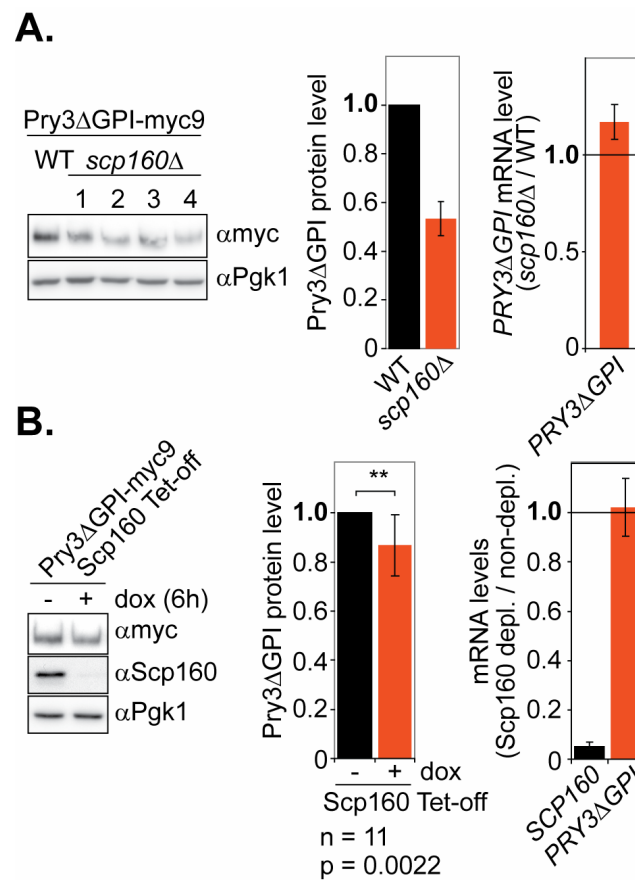


Fig. 28. Pry3 Δ GPI protein levels are reduced upon loss of Scp160. (A) Whole cell extracts were prepared from strain HSY19 (Pry3 Δ GPI-myc9 in WT background) and four independent clones of strain HSY20 (Pry3 Δ GPI-myc9 in *scp160* knock-out background). Left panel: Western blot of one representative experiment. Middle panel: Quantification of three independent experiments carried out as in the left panel. Right panel: RNA was prepared from the same strains and used for qRT-PCR. Relative PRY3 Δ GPI mRNA levels are represented as the signal ratio between *scp160 Δ and WT background. (B) Pry3 Δ GPI levels in Scp160-depleted cells. Whole cell extracts were prepared from strain HSY21 6 h after addition of 2 μ g/ml doxycycline or after mock depletion. Left panel: Representative Western blot showing the efficient depletion of Scp160 (anti Scp160) and the reduction of Pry3 Δ GPI-myc9 protein levels upon depletion of Scp160 (anti myc). Pgk1 serves as loading control. Middle panel: Quantification of n = 11 experiments performed as in the left panel. The decrease of the Pry3 Δ GPI-myc9 protein levels in the sample depleted for Scp160 is highly significant (Student's t-test, $p = 0.0022$). Right panel: RNA was prepared from the same samples and used for qRT-PCR. Relative PRY3 and SCP160 mRNA levels were calculated as the signal ratio between the Scp160-depleted and non-depleted samples. All data are presented as mean \pm standard deviation, n = 3.*

4.7.3. Enhanced degradation is not responsible for reduced levels of Pry3 protein

To rule out that enhanced degradation upon loss of Scp160 is responsible for the reduction in Pry3 protein levels, I performed cycloheximide chase experiments to determine the half-life of Pry3 Δ GPI-myc9 in Scp160-depleted, *scp160 Δ , and control cells. Western blotting against Pry3 Δ GPI-myc9 in lysates from cells that had been incubated with the translation inhibitor cycloheximide (CHX) demonstrated that the decay of Pry3 Δ GPI-myc9 is not accelerated after Scp160 depletion. Half-lives of Pry3 Δ GPI-myc9 in *scp160 Δ or Scp160-depleted cells ($t_{1/2}$ =8 min or 11 min, respectively) were not significantly reduced as compared to wildtype ($t_{1/2}$ = 7 min) or mock-depleted ($t_{1/2}$ = 14 min) cells (Fig. 29). In conclusion, these data confirm that enhanced**

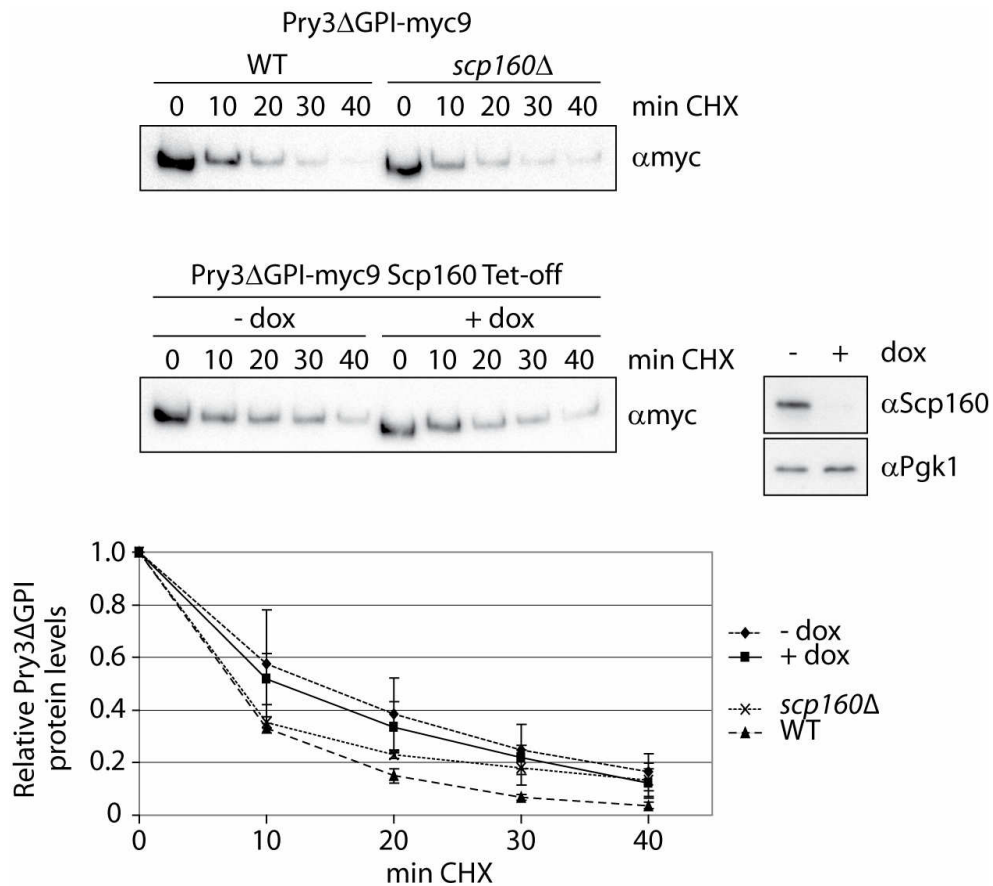


Fig. 29. Stability of Pry3 Δ GPI-myc9 is not affected in cells lacking Scp160. Cycloheximide (CHX) chase analyses were performed to assess the stability of Pry3 Δ GPI-myc9 in wildtype (HSY19), *scp160 Δ (HSY20) and Scp160 depletion (HSY21) background. Logarithmically growing cultures were supplemented with 0.5 mg/ml CHX; aliquots were taken at indicated time points and immediately processed for Western blotting. Upper panels: Representative Western blots probed with either anti-myc antibody to detect Pry3 Δ GPI-myc9 or anti Scp160 and anti Pgk1 antibodies to test for successful depletion of Scp160. Lower panel: Quantification of five replicates (Scp160 depletion) and three replicates (WT versus *scp160 Δ). Data are presented as mean \pm standard deviation.**

degradation is not the cause for the reduced Pry3 protein levels. It is therefore likely that Scp160 causes translational downregulation of Pry3, which suggests that Scp160 is required for proper translation of this GPI-anchored protein.

4.8. Depletion of *PRY3* triggers polyploidization

A hallmark of *scp160* Δ cells is an increased ploidy in a subpopulation of these cells (Wintersberger et al., 1995). Since Scp160 is an RNA-binding protein, the defect in ploidy control could be due to translational misregulation of one or several of its target mRNAs. Among the four mRNAs that I confirmed to directly bind to Scp160 (see sections 4.6.1. and 4.6.2.), *PRY3* mRNA is the one with the strongest translational state change (2.7; see table 2). As demonstrated in chapter 4.7, efficient translation of *PRY3* mRNA requires Scp160. Therefore, I asked if a decrease in the Pry3 level results in polyploidization.

A strain for the galactose-inducible expression of *PRY3* was constructed by replacing the endogenous *PRY3* promoter by the *GAL1* promoter. When *pGAL1-PRY3* cells were grown under repressing conditions, *PRY3* mRNA levels dropped to 21% of wildtype levels as measured by qRT-PCR (Fig. 30). Most interestingly, loss of Pry3 was associated with an increase of the subpopulation of haploid cells with 4n DNA content, which is reminiscent of the FACS profile of *scp160* Δ cells (Fig. 30).

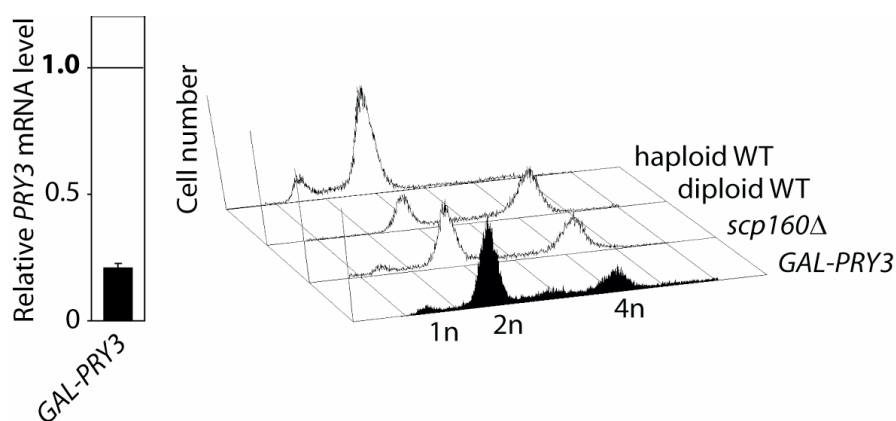


Fig. 30. Depletion of *PRY3* mRNA induces polyploidization. Left panel: qRT-PCR analysis of relative *PRY3* mRNA levels in uninduced *GAL-PRY3* cells (RJY3487) compared to wildtype (RJY358) indicates a reduction to 21%. Right panel: FACS analysis of the same sample reveals a significant fraction of cells with tetraploid DNA content similar to the *scp160* Δ (RJY3178) phenotype.

To test if overexpression of Pry3 also induces ploidy changes, I introduced a plasmid harboring the *PRY3* ORF under control of the inducible *GAL1* promoter into a wildtype strain that still contained an intact *PRY3* copy. In contrast to the depletion of *PRY3*, induction of its overexpression by growth in galactose-containing medium did not effect any changes in ploidy, as determined by FACS analysis (not shown).

4.9. Overexpression of Pry3 does not rescue the polyploidy phenotype of *scp160* deletion strains

In the last sections, I showed that loss of Scp160, which goes along with ploidy increase, causes a reduction of Pry3 protein levels, and that depletion of *PRY3* equally induces polyploidization. Therefore, Pry3 is a likely candidate of an Scp160-controlled factor that regulates ploidy.

In order to test if depletion of Pry3 is the major cause of ploidy misregulation, I performed rescue experiments. Pry3 was expressed in *scp160*Δ cells from a plasmid with the strong constitutive *GPD1* promoter to determine if Pry3 overexpression reverts the polyploidization phenotype in *scp160*Δ cells. Although expression of Pry3 from the *GPD1* promoter resulted in >50 fold increase of *PRY3* mRNA, the number of cells with 4n content in an *scp160*Δ *GPD-PRY3* strain were not reduced as compared to *scp160*Δ (Fig. 31). This suggests that correct translation of *PRY3* is required for ploidy regulation but that it is not the only target of Scp160 whose misregulation ultimately leads to polyploidization.

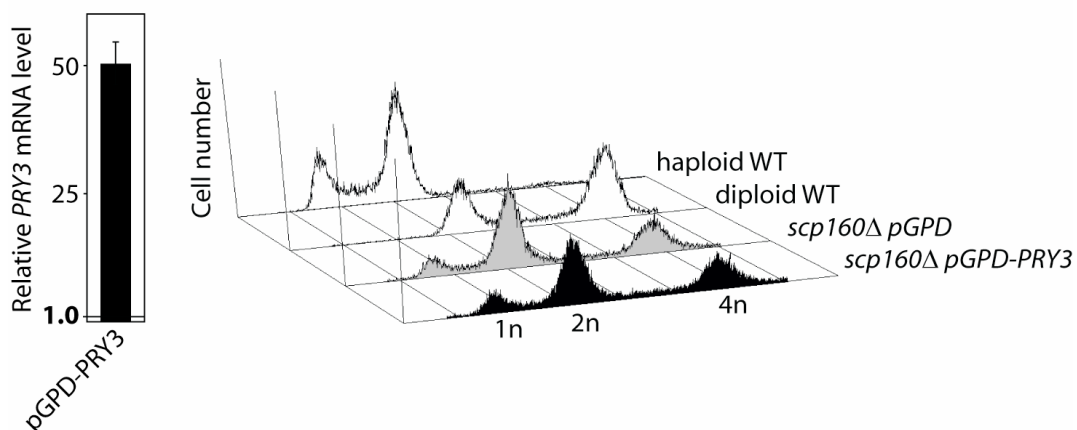


Fig. 31. Overexpression of Pry3 does not rescue the polyploidy phenotype of *scp160*Δ cells. Left panel: qRT-PCR analysis demonstrating 50-fold overexpression of *PRY3* under control of the constitutive *GPD1* promoter (plasmid HSP11) compared to cells transformed with a control plasmid (HSP12). Right panel: FACS profiles of haploid (RJY358) or diploid (RJY925) wildtype cells and *scp160*Δ cells (RJY3178) with or without Pry3 overexpression. No significant difference is visible between both *scp160*Δ strains.

5. Discussion

Since the first characterization of Scp160 as an RNA-binding protein (Weber et al., 1997), major achievements have been made in the research field of post-transcriptional regulation. Paralleled by the optimization of array technologies, sophisticated assays have been developed that target the mechanisms by which RBPs control gene expression (Sanchez-Diaz & Penalva, 2006). During the last years, a number of different cellular functions have been assigned to Scp160 (see chapter 1.6) and large-scale analyses revealed that it binds a large number of transcripts (Hogan et al., 2008; Li et al., 2003). However, Scp160's ribosome-associated function – and a large part of its cellular pool localizes to polysomes (Lang & Fridovich-Keil, 2000) – still remains elusive.

In my work, I focused on two main aspects: first, the further characterization of Scp160's binding to ribosomes, and second, the identification of mRNAs whose translational activity is dependent on Scp160.

5.1. Scp160 binds to ribosomes

Sucrose density fractionation experiments have demonstrated that Scp160 associates with free and membrane-bound polysomes (Frey et al., 2001) as part of a large, RNase-sensitive mRNP complex (Lang & Fridovich-Keil, 2000). Whereas fractionation experiments are well-suited to determine polysome association of Scp160, affinity purifications may be more precise in determining whether its interaction with ribosomes is lost or partially maintained under specific conditions. The question whether RNase-treatment of cell extracts disrupts the ribosome association of Scp160 completely (Lang & Fridovich-Keil, 2000) or whether a fraction of Scp160 remains in a complex with 80S ribosomes (Frey et al., 2001) has so far not conclusively been answered. In TAP purifications of tagged Scp160, co-purification of 40S and 60S ribosomal proteins is in large part RNase-sensitive (Fig. 8). This indicates that an important part of the association with ribosomes is mediated indirectly via mRNA and potentially rRNA. A truncated version of Scp160 lacking the C-terminal KH domain 14 is compromised in its polysome association and was reported to be deficient in the formation of RNPs, as judged from size fractionation experiments (Li et al., 2004). Correspondingly, truncation of KH domains 13 and 14 was reported to disrupt polysome association (Baum et al., 2004). In TAP purifications, in contrast, co-purification of ribosomal proteins with Scp160 Δ KH13/14 was only marginally decreased (Fig. 10). The disruption of Scp160-mRNP complexes by RNase-treatment (Lang & Fridovich-Keil, 2000) and the equivalent effect of a C-terminal truncation (Li et al., 2004) suggest that KH13/14 are implicated in RNA binding. This question was directly addressed in this work

(see sections 4.6.1. and 4.6.2.). As the C-terminally truncated version of Scp160 still associates with ribosomes (Fig. 10), this strengthens the notion that additional factors mediate this interaction. In this respect, it should be noted that Scp160 was found to bind ribosomal RNA (rRNA) *in vitro* (Weber et al., 1997), suggesting that direct physical interactions with ribosomal components are also involved. Furthermore, Asc1 has been suggested to interact with Scp160 on the ribosome. Both proteins bind in close proximity to each other next to the mRNA exit channel on the small ribosomal subunit, as demonstrated by chemical crosslinking experiments (Baum et al., 2004) and cryo-electron microscopy (Sengupta et al., 2004). In cells lacking Asc1, polysome association of Scp160 has been shown to be hampered (Baum et al., 2004). However, I have found that in an *asc1*Δ strain, Scp160 still co-purifies with ribosomes to almost the same extent as in wildtype cells (Fig. 10). The combined *asc1* deletion and truncation of KH13/14 demonstrated the strongest reduction of ribosome association (Fig. 10). Taken together, affinity purifications of Scp160 indicate that its association with ribosomes is based on different, cooperating interactions.

In an attempt to identify new interaction partners of Scp160, prominent bands of TAP-purified samples were analyzed by mass spectrometry. Besides ribosomal proteins, the ribosome-associated proteins Asc1 and Stm1, the RBP Bfr1 and the nascent-chain chaperone Zuo1 were found (Fig. 8). Apart from Stm1, these interactors have also been identified in a recent large-scale study (Gavin et al., 2006), confirming the specificity of the purification protocol.

Asc1, the yeast orthologue of mammalian receptor for activated C-kinase (RACK1) (Gerbasí et al., 2004), presumably acts as a binding platform for diverse signaling molecules on the ribosome. Due to its propeller-like structure of seven WD40 repeats, each of which could potentially interact independently with binding partners (Rodríguez et al., 1999), RACK1 is believed to integrate inputs from different signaling pathways (Nilsson et al., 2004). For example, RACK1 recruits activated protein kinase C (PKC) to the ribosome, leading to translation stimulation by phosphorylation of eIF6 and subsequent subunit joining (Ceci et al., 2003). As discussed above, Scp160 binds to the ribosome in close proximity to Asc1 (Baum et al., 2004). Although my results do not confirm the proposed dependency of the Scp160-ribosome interaction on Asc1 (Fig. 10), the spatial co-localization of both proteins may indicate a functional interaction.

The Brefeldin A Resistance protein Bfr1, originally suggested to function in the secretory pathway (Jackson & Kepes, 1994), has been found to associate with Scp160-containing, polysome-associated mRNP complexes (Lang et al., 2001; Sezen et al., 2009; Hogan et al., 2008). In line with that, Scp160 is a main co-purifier in Bfr1 immunoprecipitates (Fig. 9). Consistently with studies reporting the RNA-dependency of these interactions (Lang et al., 2001; Sezen et al.,

2009), the Bfr1 signal is completely lost in RNase-treated TAP purifications (Fig. 8). Immunofluorescence microscopy showed that both proteins localize to the ER and the outer nuclear envelope, which comprises a major part of the yeast ER (Lang et al., 2001). Interestingly, loss of Bfr1 has not only been reported to induce abnormal large cells with increased DNA content (Jackson & Kepes, 1994) similar to the *scp160* knockout, but also to disrupt the interaction of Scp160 with polysomes (Lang et al., 2001). Furthermore, a recent extensive microarray study of RBP targets has shown that Scp160 and Bfr1 associate with a largely overlapping set of mRNAs (Hogan et al., 2008), indicating an intimate functional relationship between these two proteins.

Stm1 has been characterized as a ribosome-associated protein that is important for protein synthesis under nutritional stress conditions (Van Dyke et al., 2006). When bound to the ribosome, Stm1 may facilitate the release of the ATP-hydrolyzed conformation of eEF3, thereby permitting efficient translation elongation (Van Dyke et al., 2009). Interestingly, Scp160 did not co-purify with TAP-tagged Stm1 in Coomassie-detectable amounts (Fig. 9), suggesting that most Stm1-containing ribosomes are not associated with Scp160, whereas Stm1 is a prominent co-purifier of Scp160-containing ribosomes. This result is somewhat contradictory to studies indicating that Stm1 is present on ribosomes with a close to 1:1 stoichiometry (Van Dyke et al., 2006). However, the same group published results showing that overexpression of Stm1 enhances its effect on protein synthesis (Van Dyke et al., 2009), a finding that is hard to reconcile with endogenous Stm1 being present on every ribosome.

Zuotin (Zuo1) is a ribosome-associated DnaJ-like chaperone that promotes the folding of nascent polypeptide chains as part of the ribosome-associated complex (RAC) (Yan et al., 1998). RAC is also involved in the correct sorting of signal-sequence containing nascent polypeptides (Wiedmann et al., 1994) and has recently been implicated in cap-independent translation (Raychaudhuri et al., 2006), suggesting that it may fulfil additional regulatory functions in addition to assisted protein folding.

Taken together, the finding that Scp160 associates with ribosomes together with other factors that have a potentially regulatory function suggests that translation of its target mRNAs is subject to complex regulatory mechanisms.

5.2. No evidence for a regulatory subcellular re-localization of Scp160

Due to its mRNA-binding activity and ribosome association, it has been speculated that Scp160 positions specific transcripts at the ER, where they are translated (Frey et al., 2001). Consequently, Scp160-mediated translational control could involve the modulation of target mRNA partitioning between cytosolic and membrane-bound fractions. In spindle pole body duplication-defective cells, the Scp160-containing SESA complex has indeed been demonstrated to inhibit *POM34* mRNA translation by shifting it to the cytosolic fraction (Sezen et al., 2009). If this mode of action were generally exerted by Scp160, one would expect to see changes in its subcellular localization pattern as soon as a significant fraction of its target mRNAs is differentially controlled.

In accordance with the results from TAP purifications, deletion of *asc1* did not induce changes in the typical enrichment of Scp160 in the membrane- and ribosome-containing fractions (Fig. 11), indicating that an earlier study suggesting the association of Scp160 with polysomes to be dependent on Asc1 has to be critically reviewed (Baum et al., 2004). Li and coworkers (2004) reported that a truncated version of Scp160 lacking KH domain 14 is compromised for polysome association, not competent to form RNPs, and is equally distributed between pellet and soluble fractions in differential centrifugation assays. In agreement with these data, I found Scp160 Δ KH13/14 to be present in the ribosome-free cytosolic fraction (Fig. 11). However, the majority still pelleted with membranes and, to a lesser extent, with membrane-free ribosome-containing fractions. The same is true for RNA binding-impaired versions of Scp160 carrying point mutations in the conserved GXXG motifs of KH domain 14 or KH domains 13/14 (Fig. 12).

These findings support the above-stated notion that besides RNA-mediated interactions, ribosome association of Scp160 depends on additional factors. Furthermore, it should be noted that Scp160 may associate with membranes also independently of ribosomes. For example, treatment with EDTA, which disrupts ribosomes, only partially releases Scp160 from the membrane fraction (Frey et al., 2001; Weber et al., 1997). In addition, deletion of the last two KH domains does not have any significant effect on telomeric silencing, and therefore, given that its localization to the nuclear envelope is a prerequisite for Scp160-mediated silencing, the truncated version must still sufficiently localize to this membrane compartment (Marsellach et al., 2006). It should also be considered that Scp160's co-fractionation with ribosome-containing fractions could partially be due to its association with ribosome-free mRNPs of high density.

Although I could confirm that RNA binding-impaired mutant versions of Scp160 partially localize to an additional cytoplasmic pool, I was not able to find a condition under which

wildtype Scp160 shows a reproducible shift in its subcellular localization pattern (Figs. 13-16). This means that either the cellular answer towards the tested stimuli does not involve Scp160, or that the putative Scp160-mediated response does not involve a significant shift in its localization. In fact, differential regulation of only a limited number of mRNAs would probably not induce a measurable shift of Scp160 itself, as it is the case for the translational regulation of *POM34* mRNA (Sezen et al., 2009).

5.3. Scp160 modulates translation of a specific set of mRNAs

Scp160's interaction with ribosomes (Figure 8; Lang & Fridovich-Keil, 2000; Baum et al., 2004), its association with a plethora of mRNAs (Li et al., 2003; Sezen et al., 2009; Hogan et al., 2008), as well as the reduced fitness of *scp160*-deleted cells and their increased sensitivity against translation inhibitors (Figure 6; Baum et al., 2004) strongly suggest that Scp160 is involved in translational control. Although this role has been proposed for Scp160 already by several authors (Weber et al., 1997; Baum et al., 2004; Frey et al., 2001; Lang & Fridovich-Keil, 2000; Mendelsohn et al., 2003), comprehensive studies tackling this question are missing to date. Therefore, I followed a systematic approach to identify mRNAs that are translationally controlled by Scp160.

To prevent secondary effects due to ploidy changes in *scp160* knock-out cells (Wintersberger et al., 1995), I used a Tet-off system (Gari et al., 1997) for the efficient depletion of Scp160 (Fig. 19). In contrast to other regulatable expression systems such as the GAL cassette (see for example Janke et al., 2004), the Tet-off system does not require major changes in the growth conditions, but can be shut down simply by the addition of doxycycline to the culture medium. In microarray studies, it was shown that doxycycline itself has no significant effect on global gene transcription (Wishart et al., 2005), confirming the advantages of this system.

The translational profiling described here encompassed the analysis of changes at the transcriptome level as well as changes in active translation upon depletion of Scp160 (Fig. 20), resulting in a comprehensive picture of the influence of Scp160 on transcription, mRNA stability and translation.

At the transcriptome level, depletion of Scp160 affected the abundance of 60 mRNAs, the majority of which (82%) showed a decreased level in the absence of Scp160 (Table 1). Classification of the proteins encoded by these transcripts demonstrated an enrichment of proteins involved in polypeptide folding and stabilization, stress response and energy metabolism (Fig. 21), indicating that loss of Scp160 preferentially affects stress-related transcripts. Since

doxycycline *per se* has been reported not to induce any significant changes in the transcriptome (Wishart et al., 2005), I suspected that the depletion of Scp160 evokes a general stress response. However, this scenario is contradicted by the fact that the identified stress-related mRNAs were downregulated upon loss of Scp160, and not, as expected in response to a stress situation, more abundant. Since qRT-PCR failed to confirm the microarray results of all mRNAs tested besides *SCP160* itself (table 1), it is questionable if the apparent effect on stress-related transcripts is real. Currently, the discrepancy between microarray and qRT-PCR data cannot be explained, but it should be noted that in a related study in which mRNA abundances were measured upon depletion of Scp160 by a GAL system, Northern analysis also failed to confirm microarray data (Frey, 2002). However, since my microarray results confirmed that *YOR338W* mRNA levels are increased in cells lacking Scp160 (Li et al., 2003), it seems likely that they are only partially erroneous and should be in depth validated by qRT-PCR, which was beyond the scope of this work.

Microarray analysis of polysome gradient fractions upon depletion of Scp160 revealed that the distribution of 60 mRNAs changed significantly between free mRNPs and polysomes (Table 2). Notably, 80% of these mRNAs were shifted towards the heavy gradient fractions, indicating an increased polysome load on these mRNAs and a similar function of Scp160 in the regulation of these targets. Considering that Scp160 is thought to bind probably more than 1000 mRNAs (Hogan et al., 2008), only a very small subset is affected in its ribosome load. However, some mRNAs may have been missed due to the activity of residual Scp160. The fact that the vast majority of these transcripts shows no significant changes on the transcriptome level demonstrates that their differential polysome association is due to regulatory mechanisms other than transcription rates and modulation of mRNA stability. Classification of the encoded proteins revealed a specific enrichment of cell wall and extracellular proteins as well as proteins of the membranous compartment involved in vesicle transport (Fig. 23). These findings are in good agreement with a previous large-scale study of Scp160-associated mRNAs, in which Scp160 has been found to bind mRNAs encoding proteins of cell wall, plasma membrane, ER and nucleolus (Hogan et al., 2008). Most of these transcripts are expected to be translated at the ER, which is consistent with the localization of Scp160 to this cellular compartment (Frey et al., 2001). My results also fit well into the emerging view of RBPs organizing nascent RNA transcripts into functional groups that are coordinately regulated, especially at the level of mRNA stability and translation (Keene, 2007). The most striking example for a group of RBPs that bind transcripts encoding proteins with common localizations and functions are the five Puf (Pumilio family) proteins in yeast: Puf1 and Puf2 preferentially interact with mRNAs encoding membrane-associated proteins, Puf3 nearly exclusively binds to cytoplasmic mRNAs encoding mitochondrial

proteins, Puf4 preferentially associates with transcripts coding for nucleolar ribosomal RNA-processing factors, and Puf5 binds to mRNAs encoding chromatin modifiers and components of the spindle pole body (Gerber et al., 2004). In analogy, it is tempting to speculate that Scp160 translationally co-regulates its target mRNAs in response to stimuli that affect cell wall and membrane-related functions.

Biochemical analysis of 14 target mRNAs revealed that only four of these mRNAs can be demonstrated to co-purify with Scp160, as indicated by qRT-PCR analysis of Scp160 immunoprecipitates (Table 2, Fig. 24). This again coincides with previous results from Hogan and co-workers (Hogan et al., 2008), whose set of Scp160-bound mRNAs includes my verified targets and is widely in accordance with my data concerning mRNAs that could not be verified as being associated with Scp160. Both results indicate that weaker interaction partners might be lost during purification, which is a known drawback of protocols that do not include a cross-linking step (Hieronymus & Silver, 2004). Alternatively, mRNAs that were not enriched in the IP-qRT-PCR assay may not directly associate with Scp160. The observed changes in their translational profile might consequently be due to indirect effects caused by translational changes in primary (Scp160-bound) target mRNAs.

Three of the Scp160 target mRNAs tested (*AGA1*, *PRY3* and *POM34*) were enriched to a similar extent in Scp160 and Khd1 immunoprecipitates, whereas enrichment of *CCW14* and *MSB2* mRNAs was more pronounced in the case of Scp160 (Fig. 24). Khd1 has originally been described as a protein required for efficient localization and translational repression of *ASH1* mRNA (Irie et al., 2002; Hasegawa et al., 2008). However, it has lately been found to bind a set of more than 1000 mRNAs (Hasegawa et al., 2008; Hogan et al., 2008). Many of these mRNAs encode bud-localized proteins or proteins localized to the cell periphery, like cell wall and cell membrane proteins (Hasegawa et al., 2008; Hogan et al., 2008). Thus, Khd1 and Scp160 show similar preferences concerning the functional subsets of their RNA targets, which is also reflected by the observation that the overlap between the two sets of target mRNAs is significantly higher than expected from a random distribution (Hogan et al., 2008). In this regard it is interesting to note that Khd1 and Scp160 are two of the three known multi-KH domain containing proteins in budding yeast; however, Pbp2, the third member of this group, has been found to interact with fewer than ten target mRNAs and therefore likely plays a different role (Hogan et al., 2008). Taken together, my results indicate that Scp160 and Khd1 have similar target binding specificities and are in good accordance with published data.

As discussed in section 5.1, the C-terminal KH domains 13 and 14 have been implicated in RNA binding. To obtain direct evidence for this assumption, I tested a truncation mutant lacking both

KH domains in the IP-qRT-PCR assay and found that it is severely compromised in the binding of *CCW14*, *AGA1*, *PRY3*, *MSB2* and *POM34* mRNAs (Fig. 24). Although I have not tested other Scp160-bound mRNAs for their dependence on KH13 and KH14, it is tempting to speculate that their binding is also reduced or abolished in the Scp160 Δ KH13/14 mutant. In order to exclude that the RNA binding deficiency of this truncated protein is due to misfolding, I additionally tested Scp160 mutants that carry amino acid exchanges in conserved residues of both KH domains. As expected, these mutants also showed a strong reduction in target mRNA binding (Fig. 25). Corresponding amino acid exchanges in various KH domain-containing proteins like Khd1 (Hasegawa et al., 2008), *E. coli* NusA protein (Zhou et al., 2002) or human FMR1 (Siomi et al., 1994) similarly resulted in loss of RNA binding and functional impairment. It has been reported that a specific cysteine in KH13 (Cys1067) is required for cross-linking Scp160 to Asc1 (Baum et al., 2004). Therefore, it has been proposed that KH13 and KH14 are involved in ribosome binding whereas KH1-12 function in selecting specific mRNAs for targeting to ribosomes (Baum et al., 2004). My results designate in contrast that KH13/14 mediate Scp160's association with target mRNAs, suggesting that these KH domains fulfil a double function.

When cells are deprived of Scp160, 60 potential target mRNAs showed significant alterations in their abundance in mRNP and polysome fractions, the majority of which shifted towards the heavy gradient fractions (see above). In principle, this redistribution would be expected to reflect increased association with polysomes and therefore translational upregulation (Melamed et al., 2009). To test if this applies to *PRY3* mRNA, which is one of the transcripts with the most pronounced enrichment in the heavy fractions upon depletion of Scp160, I performed quantitative Western blotting on epitope-tagged Pry3 protein. Against my expectations, I found that Pry3 protein levels are reduced in Scp160-depleted cells (Figs. 26 and 28). This reduction was not caused by enhanced degradation, as demonstrated by cycloheximide chase assays (Fig. 29). These results indicate that Scp160 does not act as a translational repressor of *PRY3* mRNA, but in contrast is required for its efficient translation.

How can the mRNA shift towards the heavy gradient fractions be reconciled with the apparent decrease in *PRY3* translation? Two scenarios explaining these findings can be envisioned. First, the mRNA shift may not result from a differential polysome association of *PRY3*, but from a relocalization of *PRY3*-translating polysomes from the ER to the cytosol. Second, it is known that increased polysome association of an mRNA is not always due to a higher translation rate, but can also reflect slower ribosomal transit and therefore less efficient protein synthesis.

The first scenario is based on the fact that no detergent was used during sample preparation for sucrose density centrifugation. Therefore, some of the ER-bound polysomes may have been lost

before application onto the sucrose gradient. If, in the absence of Scp160, *PRY3*-containing polysomes were shifted from the ER membrane to the cytosol, *PRY3* mRNA would show an apparent enrichment in the heavy fractions. In the cytosol, translation of *PRY3* mRNA may be blocked by a mechanism which – since affecting polysomes – would have to be different from the interaction with signal recognition particles (SRPs). To test if polysome relocalization occurs, I used qRT-PCR to determine if *PRY3* mRNA is shifted between membrane and cytosolic fractions in dependence of Scp160. Preliminary data indicate that no such shift occurs (not shown), therefore arguing against the first scenario.

The second scenario is based on studies demonstrating that under certain conditions, translationally inactive polysomes can form. This has for example been described in mitotic cells where ribosomal slowdown on bulk mRNA elicits the formation of unusually stable polysomes (Kedersha et al., 2005; Sivan et al., 2007). Furthermore, regulation of translation elongation is well established upon oxidative stress (Ayala et al., 1996) or treatment with hormones and mitogens (Rhoads, 1999). Although the underlying molecular mechanisms are not entirely understood, both eEF2 and eEF1 seem to be involved in the regulation of elongation, the latter being of specific interest in the context of this study:

It has been shown that in rabbit, three eEF1 subunits (eEF1A, eEF1B α , eEF1B δ) are phosphorylated by protein kinase C (PKC) and S6 kinase *in vitro* or after stimulation, for example by insulin (Chang & Traugh, 1998). These modifications enhance elongation by stimulating the GDP-to-GTP exchange rate on eEF1A (Peters et al., 1995). In this regard, it is interesting to note that Scp160 binds to the ribosome in close proximity to eEF1A and Asc1, the yeast homologue of the PKC target RACK1 (Baum et al., 2004; Nilsson et al., 2004). In human cells, eEF1A has also been identified to be present in vigilin-containing RNPs, suggesting that this interaction may be conserved (Kruse et al., 1998). To determine if Scp160 regulates translation elongation through the action of eEF1, it would be interesting to test if its presence influences the phosphorylation state of this factor.

Besides eEF1, the ribosome-associated protein Stm1 is a potential candidate that could be involved in Scp160-mediated enhancement of translation elongation. Stm1 is thought to stimulate the release of the ADP-bound conformation of eEF3, which enhances elongation efficiency (Van Dyke et al., 2009). If Stm1 is absent, polysomes are notably increased due to hampered elongation (Van Dyke et al., 2009). Although speculative, the presence of Stm1 on Scp160-associated ribosomes (see Fig. 8 and section 5.1) could provide a link between Scp160 and increased translation elongation.

The working hypothesis that Scp160 enhances elongation on its target mRNAs is in good accordance with findings indicating that the *D. melanogaster* Scp160 homologue DDP1 has a stimulatory function in the translation of Hsp83 mRNA (see section 2.5.3.; Nelson et al., 2007). Although the mechanism of this translational enhancement is unknown – i.e. which step in translation is targeted –, the fact that expression of DDP1 fully complements an *scp160Δ* yeast strain suggests that both proteins play a similar role in the translation of specific mRNAs.

5.4. A link between translational regulation and ploidy control

Deletion of Scp160 induces increased ploidy (see section 2.6.1.), suggesting an as yet unclear function in the maintenance of the correct DNA content (Wintersberger et al., 1995). In my experiments, I identified *PRY3* mRNA as a target of Scp160-mediated translational enhancement. Most interestingly, I found that downregulation of *PRY3* expression induces polyploidization in a similar way as deletion of Scp160 (Fig. 30), suggesting a link between translational control exerted by Scp160 and polyploidization.

The function of the cell wall protein Pry3 is largely unknown. Pry3 belongs to the CAP (CRISP-Ag5-PR) protein superfamily that includes CRISP (cysteine-rich secretory proteins) extracellular glycoproteins (Gibbs et al., 2008). The family comprises fungal proteins (including *S. cerevisiae* Pry1-3), mammalian glioma Pr-1 (GLIPR1) proteins, *C. elegans* LON-1, and plant pathogenesis-related PR proteins (Gibbs et al., 2008; Morita et al., 2002). Whereas plant PR proteins function in systemic acquired resistance against pathogens (Uknes et al., 1992), the function of most other members of this family is not clear. It is interesting to note that *C. elegans* lon-1 mutants exhibit an endoreduplication phenotype, resulting in polyploid nuclei of hypodermal tissue (Morita et al., 2002), which is reminiscent of the increase in ploidy observed in cells with reduced Pry3 levels. How the cell wall protein Pry3 is involved in ploidy control remains unknown. *C. elegans* lon-1 is presumably an integral membrane protein and has been proposed to function as an extracellular ligand (Morita et al., 2002), suggesting that Pry3 may also be involved in an extracellular signaling event. However, the DNA content of cells in which the GPI modification site of Pry3 has been removed is almost unchanged (Fig. 27), indicating that Pry3 may have additional functions that are independent of its attachment to the cell wall.

My results indicate that in the absence of Scp160, insufficient translation leads to lower Pry3 levels, which contributes to the de-regulation of genomic stability or ploidy control. Since overexpression of *PRY3* from a strong heterologous promoter does not revert the polyploidy (4n) phenotype of cells lacking Scp160 (Fig. 31), there might be additional proteins whose

translational de-regulation contributes to the genomic instability phenotype of *scp160* Δ cells. For instance, Scp160 has been attributed to function in the SESA network of proteins, which regulates translation of a specific set of mRNAs including *POM34* (Sezen et al., 2009). The SESA network downregulates translation of *POM34* and thus rescues mutants with defects in spindle pole body duplication (e.g. *ndc1-1*) and ploidy control (Sezen et al., 2009; Chial et al., 1999).

However, the function of Scp160 in translational control of specific mRNAs alone cannot explain the ploidy phenotype of the deletion strain, since cells expressing a truncated version of Scp160 lacking KH domains 13 and 14 have normal FACS profiles (Baum et al., 2004). This observation indicates that in addition to RNA binding which is mainly mediated by KH domains 13 and 14, Scp160 has another function that contributes to ploidy maintenance. Interestingly, *Scp160* Δ KH13/14 is still fully functional with respect to telomeric silencing (Marsellach et al., 2006), raising the possibility that Scp160's suggested role in the structural organization of heterochromatin is the second key player in Scp160-mediated ploidy control. In this context, it is important to note that although a nuclear function of mammalian vigilin and *D. melanogaster* DDP1 in heterochromatin formation and maintenance is well established (see sections 2.5.1. and 2.5.3.; Zhou et al., 2008; Huertas et al., 2004), it is questionable how far Scp160 acts in the same way. For example, it has to date not been possible to show a nuclear localization of full-length Scp160 (Brykailo et al., 2007b). Consistently, Scp160 was not found to associate with telomeric DNA in ChIP experiments, leading to the hypothesis that it exerts its effect on telomeric silencing from its position at the nuclear membrane (Marsellach et al., 2006). It is therefore unclear if and how Scp160 directly affects chromosome segregation or other nuclear processes that are involved in ploidy maintenance.

Working Model:

In conjunction with published data, my study supports the following working model. As part of large mRNPs containing transcripts destined for translation at the ER, Scp160 localizes to ER membranes. My preliminary data indicate that Scp160 is not required for the localization of its target mRNAs to the ER, suggesting that it rather co-localizes in a passive manner. At the ER membrane, Scp160 enhances translation of its target mRNAs under standard growth conditions, probably by stimulating elongation. The regulatory mechanism may involve the action of Asc1, eEF1A, and perhaps other protein factors. Upon specific signal cues, Scp160 could differentially regulate translation of its target transcripts, which may involve the signal integration capacity of Asc1. Defects in translational regulation due to lack of Scp160 presumably contribute to an increased cell ploidy phenotype, along with defects in yet-to-be identified functions of Scp160.

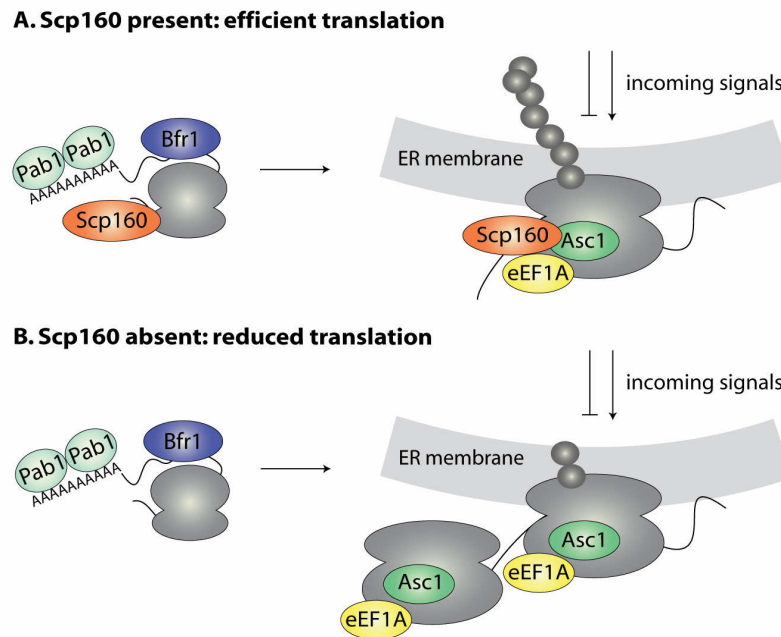


Fig. 32. Model for translational regulation mediated by Scp160. (A) Scp160 localizes to the ER as part of large mRNP complexes containing mRNA, the RBP Bfr1 and the Poly(A)-binding protein Pab1. At the ER, Scp160 enhances translation elongation of its target mRNAs. In this process, elongation factor eEF1A could be involved as well as the signal integrator Asc1. **(B)** If cells are deprived of Scp160, target mRNAs are still transported to the ER. However, elongation is less efficient, leading to stalled polysomes and decreased protein production.

In summary, my data substantiate the assumption that Scp160 is involved in translational regulation of a specific, functionally related subset of mRNAs. Although results obtained for one of the target transcripts suggest a function of Scp160 in enhancement of translational elongation, it will be required to test further candidate mRNAs in order to confirm this notion. Furthermore, the underlying molecular mechanisms as well as potential regulatory aspects are as yet unknown and will be the focus of our future investigations.

6. Material and methods

6.1. Materials

6.1.1. Consumables and chemicals

Consumables and chemicals were purchased from the following companies:

Acros Organics (Geel, Belgium), Applichem (Darmstadt), Applied Biosciences (Darmstadt), Apollo Scientific Limited (Bredbury, UK), Axon (Kaiserslautern), Becton Dickinson (Heidelberg), Beckman Coulter (Krefeld), Biaffin (Kassel), Biomol (Hamburg), Biorad (Munich), Biozym (Hess. Oldendorf), Chemicon (Temecula, Canada), Fermentas (St. Leon-Rot), Formedium (Norwich, UK), GE Healthcare (Munich), Gilson (Bad Camberg), Invitrogen (Karlsruhe), Macherey & Nagel (Düren), Medac (Hamburg), Medigenomix (Munich), Membra Pure (Bodenheim), Merck Biosciences (Darmstadt), Millipore (Molsheim, France), Mobitec (Göttingen), MP Biomedical (Illkirch, France), NEB (Frankfurt), Neolab (Heidelberg), Nunc (Wiesbaden), Peske (Aindling-Arnhofen), Promega (Mannheim), Qiagen (Hilden), Roche (Mannheim), Roth (Karlsruhe), Santa Cruz (Santa Cruz, USA), Sarstedt (Nümbrecht), Semadeni (Düsseldorf), Serva (Heidelberg), Sigma (Taufkirchen), Stratagene (Amsterdam, The Netherlands), VWR (Ismaning).

6.1.2. Commercially available kits

Name	Supplier
Colloidal Blue Staining Kit	Invitrogen
QuikChange [®] Site-Directed Mutagenesis Kit	Stratagene
QIAquick [®] Gel Extraction Kit	Qiagen
QIAquick [®] PCR Purification Kit	Qiagen
QIAprep [®] Spin Miniprep Kit	Qiagen
CloneJET [™] PCR Cloning Kit	Fermentas
Quick Ligation Kit	New England Biolabs (NEB)
High Capacity cDNA Reverse Transcription Kit	Applied Biosystems
Power SYBR [®] Green PCR Master Mix	Applied Biosystems
NucleoSpin RNA Clean-up Kit	Macherey-Nagel

6.1.3. Equipment

Name	Supplier
Research Pipettes P10, P20, P200, P1000	Eppendorf
Ultracentrifuge L-80; rotor SW40	Beckman Coulter
RC M120 Ex Micro-Ultracentrifuge; rotor RP120-AT	Thermo Fisher Scientific
T1 Thermal Cycler	Biometra
Sonifier 200	Branson
Thermomixer Compact	Eppendorf
Cooling centrifuge 5415R	Eppendorf
BioPhotometer	Eppendorf
Tabletop centrifuge Biofuge <i>pico</i>	Haereus
Multifuge 3 L-R	Haereus
Vibrax VXR basic	Ika
Gel documentations system	Mitsubishi
Research PCR cycler PTC-200	MJ
Akku-Jet	Neolab
Shaking incubator	New Brunswick
Semi-dry blotting device	Peqlab
Universal Analytical balance	Sartorius
Vortex Genie 2	Scientific Industries
Sorvall Evolution RC; rotors SLC6000, SS-34, SLA-1500	Thermo Fisher Scientific
Light microscope ICS/KF 2	Zeiss
Gel electrophoresis chamber	Starlab
FACS Calibur™ flow cytometer	Becton Dickinson
Biocomp Gradient Station	Fredericton
Mini Hybridization Oven	MWG Biotech
Mini-PROTEAN® Tetra Cell	Bio-Rad
Optimax TR developing machine	MS Laborgeräte
LAS-3000 mini system	Fujifilm

6.1.4. Enzymes

Name	Supplier
Taq Polymerase	Axon
CIAP (Calf Intestine Alkaline Phosphatase)	Fermentas
Restriction endonucleases	Fermentas
Quick-T4-DNA-Ligase	New England Biolabs (NEB)
Herculase [®] II Fusion DNA Polymerase	Stratagene
RNase A	Roche
Zymolyase 20T	Seikagaku America

6.1.5. Antibodies

Name	Source	Dilution	Company
Primary Antibodies			
Protein A (PAP)	coupled with HRP	1:5000 (Western)	Sigma
Dhh1	rabbit	1:5000 (Western)	gift from Karsten Weis
Sec61	rabbit	1:10000 (Western)	gift from Matthias Seedorf
Asc1	rabbit	1:30000 (Western)	gift from Matthias Seedorf
Rps3	rabbit	1:10000 (Western)	gift from Matthias Seedorf
Rpl4	chicken	1:2000 (Western)	gift from Birgitta Beatrix
Scp160	rabbit	1:30000 (Western)	gift from Matthias Seedorf
myc 9E10	mouse	1:2000 (Western)	Evan et al., 1985
myc 9E11	mouse	used for IP	Evan et al., 1985
actin	mouse	1:2500 (Western)	Chemicon
Pgk1	mouse	1:10000 (Western)	Invitrogen
Secondary antibodies			
anti-mouse-IgG-HRP	goat	1:5000 (Western)	Dianova
anti-rabbit-IgG-HRP	goat	1:5000 (Western)	Dianova
anti-rat-IgG-HRP	goat	1:5000 (Western)	Dianova
anti-chicken-IgY-HRP	rabbit	1:5000 (Western)	Davids Biotechnologie

6.1.6. Oligonucleotides

In the following list, only oligos used for plasmid generation, site-directed mutagenesis and qRT-PCR are listed. Oligos used for gene knock-outs, taggings and checking of transformants were generated according to standard protocols (Janke et al., 2004; Knop et al., 1999; Gauss et al., 2005; Puig et al., 2001).

Name	5'-3' Sequence
RJO 2583	CGCAAAGGATCCATGTCTGAAGAACAAACCGC
RJO 2584	CGCAAAGGATCCATGTCTGAAGAACAAACCGC
RJO 2702	GCTCGATGGAGAATTCAAAATAG
RJO 2703	CTATTTTGAATTCTCCATCGAGC
RJO 3200	CAAACGATTCGGCTAAGAAGG
RJO 3201	CCGGCATATGTAGCAGATGGT
RJO 3297	CCCAAGCTTATGCTGGAGTTTCCAATATCAG
RJO 3298	CCCAAGCTTCTAGAAGGCGAACAGAACAGC
RJO 3332	CAAGGCTTCTTCCACCGAAT
RJO 3333	GGAAGCTTGCTTGCTCGAAG
HSO 3	AAAGGACATTGTCGGTGCTG
HSO 4	AAGCTTCAATAGCGGCTTCG
HSO 38	TAGGATCCCATTTGATCCTTCTTCTCATTC
HSO 39	GCAAGCTTAGTTATGCTTTTCACCGCC
HSO 46	CGAATCGAGATCTTATCCGGTTCIGCTGCTAGTGGTG
HSO 47	CAATCGAAGATCTTTAGCTAGTGGATCCGTTCAAG
HSO 48	TTTTTGAAATCCTTAAGAAGACAGATCTAAGCTCTTTGAAACCAATTT
HSO 49	AAATTGGTTTCAAAGAGCTTAGATCTGTCTTCTTAAGGATTTCAAAA
HSO 50	GATTCAATATGATTGTTGACCCAGGTGATTCTAACATCAAAAAG
HSO 51	CTTTTGTGATGTTAGAATCACCTGGGTCAACAATCATATTGAATC
HSO 52	GAATATGTTTCAAGAACGTGATGCTTCAATCAAAAAGTTGAGAATG
HSO 53	CATCTCAACTTTTGTGATTGAAAGCATCACGTTCTGAAACATATTC

Oligonucleotides for qPCR analyses

Name	5'-3' Sequence	qPCR target
RJO 2207	GTGGCTCATTTCAGCCATT	ASH1
RJO 2208	GGACGACCTAGTCGATTCCA	
RJO 3188	TTGGCCAACGACTTTTATCAGA	CFT1
RJO 3189	CGCAATGCTTTTCCGTCTATC	
RJO 3332	CAAGGCTTCTTCCACCGAAT	CCW14
RJO 3333	GGAAGCTTGCTTGCTCGAAG	
RJO 3330	ACAACCCACTTCTTCCACAGC	AGA1
RJO 3331	TCGATTCACAGAGGTAGATGG	
RJO 3198	CAAACGAAGGCACCTCTTCC	PRY3
RJO 3199	TTGCACCTAGGCTTGTGCTG	
HSO 29	TGGTCACGGGTTGACAAATAA	MSB2
HSO 30	TTCCAACCCAGGGAGTTTGTG	
RJO 3326	CCTGGGGGTAGACATGCAAT	POM34
RJO 3327	TGTGCCATTTGGCTGATCTT	

HSO 80	AAGGGAAGGAAGGAAAAACGA	HUR1
HSO 81	TGTGGACGAGGAAAAAGAATGA	
RJO 3334	TGATCCCGATACTGGAAATCAA	HKR1
RJO 3335	CGAATTTGTATGAAGGGGTGTG	
HSO 88	CTGCCCTCCCTGGAATACAA	SLS1
HSO 89	GGAGTCTGGCTGATGTGTGG	
HSO 82	GCCCCCAGCACCAGTATTAG	PTH1
HSO 83	AGGTTCTCTGCCGATTCCAA	
RJO 3194	CCACCACCAAGTCCATCTACG	VRP1
RJO 3195	GCGTTCGATCCACCTGTAGAA	
RJO 3369	CGCGTCTGAAAATAGCGACA	FLO10
RJO 3370	GCCACGAGGCTGTTGAGATA	
RJO 3328	TCAGCACCAAAGCCAACAAC	FIG2
RJO 3329	CCAAGTTGAGGATGCAGCAG	
RJO 3336	AGAGTCGACCATCCCCAAAG	DAN4
RJO 3337	AACATGCTAATCCCTGCATCG	
RJO 3192	TCCAATCACTGGTGAGCCTTT	SEC16
RJO 3193	ATGGGAGAGGATGGTGATGG	
RJO 3196	GCAACAGCGTTTGCAGATTC	NKP2
RJO 3197	TGGCATTTGICTCCTGCACTC	
HSO 56	TGGCGAAACCAACAAAGAAA	HSP42
HSO 57	GGAAGGCGCTTGTAGGTGAG	
HSO 85	CATTTGAAGTCCCAGGTGCAG	HOR2
HSO 86	ATCACGGGTACCGGAAGTTG	
HSO 87	TTCCACCAGGTGAACAGCAG	LHS1
HSO 88	GTGTCCCTCCGGCTGCAATA	
HSO 54	TCCGCCITGGATATGGTACA	HSP30
HSO 55	CCCCACTTGTAGGTGGACTTG	
HSO 89	TTACCCAAAGAGGGCGAATC	MUP3
HSO 90	AAGAGCCCAATAGCGACCAA	
HSO 91	TTCCCATGGCCAATTATTCA	YRO2
HSO 92	GCAGCAATCAACCAGCAGAC	
HSO 58	AGGTACTIONCGCCATCCCAGA	HSP104
HSO 59	GATCATGGAGTTGGCACCAG	
HSO 60	ACGGTGAACATGATGCGAAG	MGA1
HSO 61	GGCTGCTGAGGCTGGACTAT	
HSO 93	GGACAGTCCACGAAGCAAAGT	TMA10
HSO 94	GCCTTTCCCATAGCCTCCTC	
HSO 62	GGGCTGCTTTGGCTAAGTTG	HSP82
HSO 63	TTGGTGTICTGGCATTCTGG	
HSO 64	GAGCTTCACTGGGGTCAAGG	SSE2
HSO 65	CCGTTGTGTAAGCGTTCTCG	
HSO 66	CGATCGTGTACAGGGACGAC	DCS2
HSO 67	ATAGTGCTGGGGGATGATGG	
RJO 3200	CAAACGATTTCCGCTAAGAAGG	SCP160
RJO 3201	CCGGCATATGTAGCAGATGGT	

6.1.7. Plasmids

Name	Short description	Reference
pCM182	pTet CEN TRP	Gari et al., 1997
RJP 1463	pCM182- <i>SCP160</i> CEN TRP (RJP 1463)	This study
HSP 4	pRS316- <i>prSCP160-SCP160</i> CEN URA3	This study
HSP 8	pRS316- <i>prSCP160-SCP160mutKH14myc9</i> CEN URA3	This study
HSP 9	pRS316- <i>prSCP160-SCP160myc9</i> CEN URA3	This study
HSP 10	pRS316- <i>prSCP160-SCP160mutKH13/14myc9</i> CEN URA3	This study
HSP 11	p415- <i>prGPD1-PRY3</i> CEN LEU2	This study
HSP 12	p415- <i>prGPD1</i> CEN LEU2	This study

The centromeric plasmid pCM182 (Gari et al., 1997) was used to clone wild-type *SCP160* under the control of the repressible tetracycline operator. The *SCP160* ORF was amplified by proof-reading PCR from vector pMS342 (gift from M. Seedorf) using oligos RJO2583/RJO2584 and cloned as BamHI-PstI fragment into pCM182. The resulting plasmid RJP1463 was sequenced and confirmed to complement a genomic *scp160* deletion in terms of cell ploidy.

For the generation of plasmids carrying *SCP160* variants under control of its own promoter *pSCP160* (HSP4-HSP10), proof-reading PCR was performed on genomic DNA with primer pair HSO38/RJO2702, yielding a fragment encompassing 681 nt of the *SCP160* promoter region and the first 1836 nt of the *SCP160* ORF, and primer pair RJO2703/HSO39, producing a fragment spanning the last 1783 nt of the *SCP160* ORF and 286 nt of the *SCP160* terminator. These PCR products were cloned into plasmid pRS426 (Sikorski & Hieter, 1989) using restriction sites BamHI/EcoRI and EcoRI/HindIII, respectively, that were either introduced via the PCR oligos (HSO38 and HSO39) or naturally present in the *SCP160* ORF (EcoRI). To construct plasmid HSP4, *SCP160* promoter, ORF and terminator were subcloned into pRS316 (Sikorski & Hieter, 1989) using BamHI/SalI. The introduction of the myc9 tag was done as follows. First, oligos HSO46/HSO47 were used with plasmid pYM19 (Janke et al., 2004) to generate a PCR fragment containing the myc9 nucleotide sequence flanked by BglII restriction sites. Then, the stop codon of *SCP160* in HSP4 was converted to a BglII site by site-directed mutagenesis (HSO48/HSO49) (Quik Change II XL Site-Directed Mutagenesis Kit, Stratagene). To generate HSP9, the myc9 fragment was then introduced in frame after the *SCP160* ORF making use of the BglII sites. The correct orientation of the insert was confirmed by sequencing. Using HSP9 as template, site-directed mutageneses were performed to introduce point mutations into the last two KH domains of *Scp160*. By employing oligos HSO50/HSO51, the nucleotide sequence of KH domain 14 was altered to exchange both glycines of the GXXG motif by aspartates (G1170D and G1173D), giving rise to plasmid HSP8. In addition, with oligos HSO52/HSO53, mutations

were introduced into KH domain 13 that induce a replacement of the second glycine of the GXXG motif by aspartate (G1028D) and of the conserved isoleucine C-terminal of the GXXG motif to asparagine (I1031N), resulting in plasmid HSP10.

Plasmids HSP11 and HSP12 were constructed as follows. First, the GAL1 promoter of p415 GAL1 was replaced with the GPD promoter of pYM-N14 making use of the SacI/XbaI restriction sites, resulting in HSP12. Then, the *PRY3* open reading frame was introduced as HindIII fragment that was generated by PCR of genomic DNA using oligos RJO3297 and RJO3298, giving HSP11.

6.1.8. Strains

6.1.8.1. *E. coli*

Name	Essential Genotype
TOP10	<i>F-mcrA</i> Δ (<i>mrr-hsdRMS-mcrBC</i>) φ 80 <i>lacZ</i> Δ M15 Δ <i>lacX74</i> <i>recA1</i> <i>araD139</i> Δ (<i>ara-leu</i>) 7697 <i>galU galK rpsL</i> (Str ^R) <i>endA1 nupG</i> (Invitrogen)

6.1.8.2. *S. cerevisiae* strains

All yeast strains that were generated for this work are based on either haploid (RJY 358) or diploid (RJY 925) W303 wildtype cells.

Name	Essential Genotype
RJY 358	<i>MATa</i> , <i>ade2-1</i> , <i>trp1-1</i> , <i>can1-100</i> , <i>leu2-3,112</i> , <i>his3-11,15</i> , <i>ura3</i> , <i>GAL</i> , <i>psi+</i>
RJY 925	<i>MATa/MATalpha</i> , <i>ade2-1</i> , <i>trp1-1</i> , <i>can1-100</i> , <i>leu2-3,112</i> , <i>his3-11,15</i> , <i>ura3</i> , <i>GAL</i> , <i>psi+</i>
RJY 361	<i>MAT a</i> , <i>his1</i>
RJY 362	<i>MAT alpha</i> , <i>his1</i>

Strains generated in this work:

RJY 2946	<i>MAT a</i> , <i>SCP160-CBP-TEV-ProtA::K.I.TRP1</i>
RJY 3000	<i>MAT a</i> , <i>asc1::HIS3MX6</i>
RJY 3178	<i>MAT a</i> , <i>scp160::HIS3MX6</i>
RJY 3179	<i>MAT a</i> , <i>STM1-CBP-TEV-ProtA::K.I.TRP1</i>
RJY 3180	<i>MAT a</i> , <i>scp160::HIS3MX6</i> , pCM182- <i>SCP160</i> (RJP 1463)
RJY 3231	<i>MAT a</i> , <i>SCP160-CBP-TEV-ProtA::K.I.TRP1</i> , <i>asc1::HIS3MX6</i>
RJY 3256	<i>MAT a</i> , <i>SCP160(KH1-12)-CBP-TEV-ProtA::K.I.TRP1</i>
RJY 3258	<i>MAT a</i> , <i>SCP160(KH1-12)-CBP-TEV-ProtA::K.I.TRP1</i> , <i>asc1::HIS3MX6</i>
RJY 3391	<i>MAT a</i> , <i>BFR1-CBP-TEV-ProtA::K.I.TRP1</i>

RJY 3487	<i>MAT a, natNT2-pGAL1-HA3-PRY3</i>
RJY 3498	<i>MAT a, scp160::HIS3MX6, PRY3HA6::natNT2, pCM182-SCP160</i> (RJP 1463)
RJY 3512	<i>MAT a, SHE2myc9::K.I.TRP1</i>
RJY 3515	<i>MAT a, SCP160myc9::K.I.TRP1</i>
RJY 3516	<i>MAT a, SCP160ΔKH13/14myc9::K.I.TRP1</i>
HSY 9	<i>MAT a, scp160::HIS3MX6, pRS316-prSCP160-SCP160</i> (HSP 4)
HSY 10	<i>MAT a, scp160::HIS3MX6, pRS316-prSCP160-SCP160mutKH14myc9</i> (HSP 8)
HSY 11	<i>MAT a, scp160::HIS3MX6, pRS316-prSCP160-SCP160myc9</i> (HSP 9)
HSY 12	<i>MAT a, scp160::HIS3MX6, pRS316-prSCP160-SCP160mutKH13/14myc9</i> (HSP 10)
HSY 14	<i>MAT a pRS314</i>
HSY 15	<i>MAT a, KHD1myc9::K.I.TRP1</i>
HSY 19	<i>MAT a, PRY3ΔGPImyc9::kanMX4</i>
HSY 20	<i>MAT a, scp160::HIS3MX6, PRY3ΔGPImyc9::kanMX4</i>
HSY 21	<i>MAT a, scp160::HIS3MX6, PRY3ΔGPImyc9::kanMX4, pCM182-SCP160</i> (RJP 1463)

6.2. Methods

6.2.1. Standard methods

Many of the following microbiological and biochemical, as well as molecular biological methods such as restriction digests, dephosphorylation of fragments, ligations and separation of DNA in agarose gels are based on standard techniques (Ausubel, 2000; Sambrook, 2001). Commercially available kits were used according to the manufacturer's instructions. Point mutations were inserted by site directed mutagenesis using the QuickChange[®] Site-directed Mutagenesis Kit (Stratagene). Plasmids were sequenced by Eurofins MWG Operon (www.eurofinsdna.com). For all methods described, deionised water was used.

6.2.2. SDS-PAGE and Western blotting

SDS-PAGE was performed according to Laemmli (Laemmli, 1970) using a Mini-PROTEAN[®] Tetra Cell (BioRad). Proteins were transferred onto PVDF membrane using a semi-dry blotting device (Peqlab) for 1-2 h at 1.5 mA/cm². Optimal blotting duration was determined empirically and differed with different target proteins (for efficient blotting of Scp160, 2 h were found to be required). After transfer, the membrane was blocked with blocking buffer (2% milk-powder in PBS containing 0.1% Tween (PBS-T)). Alternatively, membranes were allowed to air-dry and stored at 4°C. Reactivation of the PVDF membrane was achieved by incubation with methanol; then, membranes were rinsed with water, followed by the normal blocking procedure. Blocked

membranes were incubated 1 h to overnight at 4°C with the first antibody diluted in blocking buffer. Excess of first antibody was removed by washing the membrane at least three times for 10 min with PBS-T buffer at RT. Incubation with secondary antibodies diluted 1:5000 in blocking buffer was done for 1-2 h at RT. Visualization of immuno-decorated proteins was performed using an ECL-Kit (Applichem), followed by exposure of the membrane to light-sensitive films (GE Healthcare) and subsequent developing using an Optimax TR developing machine. Alternatively, signals were detected with an LAS-3000 mini system equipped with a CCD camera. Image processing and signal quantification was performed with Image Reader and Multi Gauge softwares (Fujifilm).

6.2.3. Yeast-specific techniques

6.2.3.1. Culture of *S. cerevisiae*

Yeast strains were cultured in either full medium (YPD) or synthetic complete (SDC) medium. Full medium contained 11 g/l yeast extract, 22 g/l tryptone and 55 mg/l adenine. Synthetic complete media contained 6.7 g/l yeast nitrogen base (Formedium), 55 mg/l adenine and complete synthetic mix (CSM) as specified by the manufacturer. Media were supplemented with 2% glucose. For the preparation of solid medium, agar was added at 22 g/l before autoclaving.

6.2.3.2. Dot spots

Yeast cells from a fresh plate were resuspended in sterile water to OD₆₀₀ 2.0. From this cell suspension, six 10-fold dilutions were prepared and 5 µl were spotted on the respective plates.

6.2.3.3. Transformation of yeast cells

For high-efficient transformation, competent yeast cells were prepared according to the protocol of (Knop et al., 1999). Briefly, 50 ml of the appropriate medium were inoculated to an OD₆₀₀ of 0.25 from a dense overnight culture of the respective strain and grown at 30°C to an OD₆₀₀ of 0.5-0.7. Cells were harvested by centrifugation (4000 g, 5 min), washed once with 25 ml sterile water and once with 5 ml LitSorb (0.1 M lithium acetate, 10 mM Tris/HCl pH 8.0, 1 mM EDTA, 1 M sorbitol; pH 8.0). The cell pellet was then resuspended in 360 µl LitSorb and 40 µl of salmon sperm DNA (heated for 5 min at 95°C and rapidly cooled on ice) was added. After gentle mixing, 50 µl aliquots were directly stored at -80°C. For transformation with PCR fragments, 20 µl of

purified PCR product and 420 μ l of LitPEG (0.1 M lithium acetate, 10 mM Tris/HCl pH 8.0, 1 mM EDTA, 40% (w/v) PEG 3350; pH 8.0) were added to one aliquot of competent cells and incubated at RT for 30 min. 54 μ l of DMSO were added and samples were put to 42°C for 15 min, before cells were spun down and plated on adequate selective medium. Cells transformed with fragments containing the kanMX marker were allowed to recover for 3 h at 30°C in YEED before plating.

Plasmids were introduced by a one-step transformation protocol. One inoculation loop of cells were scraped from a fresh plate, washed with sterile water and resuspended in 100 μ l of one-step buffer (0.2 M lithium acetate, 40% (w/v) PEG 3350, 100 mM DTT). 10 μ l 2 mg/ml salmon sperm DNA and 100-500 ng plasmid DNA were added and samples were incubated at 45°C for 30 min. Then, cells were pelleted by centrifugation and plated on selective medium.

6.2.3.4. Knock-out and tagging of yeast genes

The chromosomal deletion of yeast genes as well as the C- or N-terminal insertion of epitope tags were performed by a PCR-based strategy (Janke et al., 2004; Knop et al., 1999; Gauss et al., 2005). The introduction of C-terminal TAP tags was carried out as described elsewhere (Puig et al., 2001). Briefly, PCR products were generated from special cassette modules that consist of a selection marker and, for tagging applications, an additional sequence encoding the tag. The PCR primers used for this purpose contain sequences homologous to the respective tagging cassette, allowing for efficient amplification of the module, as well as sequences homologous to the flanking regions of the genomic target site. PCR products were purified using the QIAquick® PCR Purification Kit (Qiagen) and used for transformation of competent yeast cells. Transformants were analyzed for correct integration of the module by colony PCR; epitope tagging was in addition confirmed by Western Blot analysis of whole cell extracts.

N-terminal epitope taggings were performed so that the target genes were put back under their own promoters (Gauss et al., 2005). This is achieved by using marker cassettes that are flanked by loxP sites which are recognized by Cre recombinase. Upon expression of Cre recombinase from a galactose-inducible vector (pSH47), the marker cassette is excised via recombination and the expression of the target gene from its own promoter is restored.

Gene deletions and taggings were checked by PCR using oligos annealing in the respective marker cassette and in the UTR or coding region of the gene.

6.2.4. Preparation of nucleic acids and cell extracts

6.2.4.1. Preparation of RNA

For the preparation of RNA, at least 4 OD₆₀₀ of cells were harvested by centrifugation, resuspended in 1 ml cold TE buffer, and transferred to 2 ml safe-lock Eppendorf tubes. After a short spin and removal of the supernatant, the cell pellet was resuspended in 500 µl Cross RNA buffer I (stored at 4°C). 200 µl of acid-washed glass beads and 400 µl of Phenol/Chloroform/Isoamyl alcohol (25:24:1, Roth) were added, followed by 10 min vigorous shaking of the samples at 4°C. Samples were spun for 5 min at 13.000 rpm and 4°C and 400 µl of supernatant were transferred to a fresh Eppendorf cup. Precipitation of the RNA was achieved by addition of 1 ml 96% ethanol and at least 20 min incubation at -20°C, upon which the RNA was pelleted by centrifugation (20 min, 13.000 rpm, 4°C). Pellets were washed with 70% ethanol, dried and resuspended in 84 µl DEPC-treated water. For digestion of genomic DNA, 10 µl of DNase buffer, 4 µl of RQ DNase, and 2 µl of RNasin (all from Promega) were added and the reactions were incubated at 37°C for 15 min. For standard applications (e.g. qPCR), samples were extracted again with Phenol/Chloroform/Isoamyl alcohol and RNA was precipitated from the aqueous phase by addition of 1/10 volume 3 M sodium acetate, pH 5.2, and 3 volumes 96% ethanol. To prepare highly pure RNA for microarray analysis, DNase-treated samples were purified using a spin column-based cleanup kit (NucleoSpin RNA Clean-up, Macherey-Nagel) according to the manufacturer's directions.

6.2.4.2. Preparation of DNA

Genomic DNA was prepared from 10 ml of dense overnight cultures. Cells were harvested by centrifugation, washed once with water and resuspended in 200 µl of breaking buffer (2% Triton X-100, 1% SDS, 100 mM NaCl, 10 mM Tris pH 8.0, 1 mM EDTA pH 8.0). 200 µl of acid-washed glass beads (425-600 µm diameter; Sigma) and 200 µl phenol/chloroform/isoamyl alcohol (24:24:1 v/v/v; Roth) were added and the samples were vortexed vigorously for 4 min. Then, 400 µl of TE buffer was added followed by centrifugation for 5 min at 13.000 rpm and 4°C. The aqueous phase was transferred to a new tube and DNA was precipitated by addition of 1 ml 96% ethanol and centrifugation for 5 min. The pellet was washed once with 70% ethanol, dried at 37°C (4 min) and resuspended in 200 µl water. To remove RNA, samples were incubated with 7 µl RNase A (Roche) at 37°C for 15 min. Samples were then supplemented with 20 µl 3 M sodium acetate, pH 5.2, and 500 µl ethanol. DNA was pelleted by centrifugation (5 min, 13.000

rpm, 4°C) and washed as before. After resuspension in 50 µl water, the quality of the purified DNA was monitored by agarose gel electrophoresis.

6.2.4.3. Alkaline lysis

Protein samples for Western blotting, e.g. to check for successful integration of epitope tags or for efficient depletion of Scp160, were prepared by alkaline lysis. 2-10 OD₆₀₀ of cells, alternatively one inoculation loop full of cells scraped from a fresh plate, were resuspended in 1 ml of water. Cell lysis was achieved by addition of 150 µl of a solution containing 1.85 M NaOH and 7.5% β-mercaptoethanol, followed by 15 min incubation on ice. Proteins were then precipitated by adding 150 µl of 50% trichloroacetic acid and incubating 10 min on ice. Then, proteins were pelleted by centrifugation (15 min, 13000 rpm, 4°C) and resuspended in 50 µl Laemmli buffer. To ensure complete denaturation, samples were heated for 10 min at 65°C.

6.2.4.4. Preparation of native whole cell extracts

Protein samples in which epitope-tagged Pry3 protein variants were to be detected by Western blotting were prepared by native instead of alkaline cell lysis since this method yielded clearer Pry3 signals. 20 OD₆₀₀ of logarithmically growing cells were harvested by centrifugation, washed once with water and resuspended in 500 µl of low-salt buffer (20 mM HEPES-KOH pH 7.6, 100 mM potassium acetate, 5 mM magnesium acetate, 1 mM EDTA, 2 mM DTT, 0.5 mM PMSF and 0.25 mM benzamidine) and vortexed for 5 min with 400 µl glass beads. After centrifugation (2 min, 100 × g), the supernatant was collected, Laemmli buffer was added and samples were incubated at 65°C for 10 min.

6.2.5. Sucrose density gradients

6.2.5.1. Sucrose density gradient fractionation

Whole cell extracts for fractionation experiments were prepared as follows. To 180 ml of logarithmically growing cells, CHX was added to a final concentration of 0.1 mg/ml and incubated for 10 min at 30°C on a shaking platform. Cells were harvested and the pellet was resuspended in 400 µl polysome buffer (20 mM HEPES/KOH pH 7.5, 75 mM KCl, 2.5 mM MgCl₂, 1 mM EGTA, 0.1 mg/ml CHX, 1 mM DTT) supplemented with 2.5 µl SUPERase-In (Ambion). 200 µl of glass beads were added and the samples were vortexed

vigorously for 5 min at 4°C. After centrifugation (5 min, 16000 × g, 4°C), the supernatant was collected, snap-frozen and stored at -80°C until use.

Extract corresponding to 600 µg of RNA was loaded onto a 12 ml 20-60% linear sucrose gradient in polysome buffer and centrifuged for 2 h at 155000 × g and 4°C in an SW40 rotor. 750 µl fractions were collected from top to bottom using a Biocomp Gradient Station (Fredericton) with continuous UV absorption measurement at 256 nm.

6.2.5.2. RNA purification from gradient fractions

For the preparation of RNA for microarray analyses, gradient fractions containing mRNPs, ribosomal subunits and monosomes (light fractions) and fractions containing three or more polysomes (heavy fractions) were pooled. Then, the samples were phenol-chloroform extracted, and RNA was precipitated with isopropanol from the 1:4 diluted aqueous phase. Pellets were washed once with 70% ethanol, dried at 37°C and redissolved in 154 µl water (total volume per sample pool).

For digestion of genomic DNA, 10 µl DNase buffer, 10 µl RQ1 DNase, and 4 µl RNasin (all from Promega) were added and the reactions were incubated at 37°C for 25 min. DNase-treated samples were purified using a spin column-based cleanup kit (NucleoSpin RNA Clean-up, Macherey-Nagel) according to the manufacturer's directions. Samples were snap-frozen and stored at -80°C until further use. RNA integrity was monitored by running 1 µg of RNA on a 1% agarose TAE gel and staining with ethidium bromide.

6.2.6. Subcellular fractionation

Subcellular fractionation experiments were performed as described elsewhere (Frey et al., 2001). 180 ml cultures were grown to OD₆₀₀ 0.5-0.6 and CHX was added to a final concentration of 100 µg/ml. Cells were harvested by centrifugation and washed once with water containing 100 µg/ml CHX. Pellets were resuspended in 1 ml of ice-cold low-salt buffer (20 mM HEPES-KOH pH 7.6, 100 mM KAc, 5 mM Mg acetate, 1 mM EDTA, 2 mM DTT, 100 µg/ml CHX, 0.5 mM PMSF and 0.25 mM benzamidine) and vibrated with 400 µl glass beads at top speed for 5 min at 4°C. Cell debris was pelleted by centrifugation (2 min, 1200 rpm) and the supernatant (whole cell extract, WCE) was transferred to a new tube. These lysates were fractionated by consecutive centrifugation steps at 6000 (pellet P6), 18000 (pellet P18) and 200000 g (pellet P200, supernatant S200) for 20 min at 4°C. After each centrifugation step, pellets were rinsed twice

with ice-cold water and resuspended in 100-150 μ l low-salt buffer. For Western blot analysis, Laemmli buffer was added to the respective samples. RNA was extracted by vortexing with an equivalent volume of Phenol/Chloroform/Isoamyl alcohol (25:24:1, Roth). After 5 min centrifugation at 13000 rpm, RNA was precipitated from the aqueous phase by incubation with 1/10 Vol 3 M sodium acetate pH 5.2 and 3 Vol 96% ethanol. Upon centrifugation (30 min, 13000 rpm), the pellet was washed with 70% ethanol, dried at 37°C and resuspended in DEPC-treated water. DNase treatment was carried out as described in section 6.2.5.2.

6.2.7. Tet-off depletion system

Plasmid RJP1463, used to control *SCP160* expression by the repressible tetracycline operator (Gari et al., 1997), was generated as described in section 6.1.7. *SCP160* expression in *scp160* Δ strains complemented with RJP1463 was shut down by addition of 2 μ g/ml doxycycline to the respective growth medium. Depletion efficiencies were tested by Western analysis of time course samples.

6.2.8. FACS analysis

For FACS analysis, 2 OD₆₀₀ units of logarithmically growing cells were harvested, washed twice with 50 mM Tris/HCl pH 8.0 and resuspended in the same buffer containing 70% ethanol. Samples were incubated at least 1 h up to several days at 4°C, before 100 μ l of the suspension was spun down, washed twice with 50 mM Tris/HCl pH 8.0 and resuspended in the same buffer supplemented with 2 mg/ml RNaseA (Roche). Upon incubation at 50°C for 2 h on a turning wheel, Proteinase K (Roche) was added to a final concentration of 0.8 mg/ml and samples were incubated for additional 60 min at 50°C. Cells were pelleted by centrifugation, washed twice with FACS buffer (200 mM Tris/HCl pH 7.5, 211 mM NaCl, 78 mM MgCl₂) and taken up in 500 μ l FACS-PI buffer (180 mM Tris/HCl pH 7.5, 190 mM NaCl, 70 mM MgCl₂, 50 μ g/ml propidium iodide). Samples were then incubated in the dark for 1-2 h on a turning wheel. Prior to analysis, samples were briefly sonicated in a water bath and diluted 1:4 in 50 mM Tris/HCl pH 8.0 buffer.

Samples were analyzed in a FACS Calibur™ flow cytometer (Becton Dickinson) fitted with an argon laser (15 mW, 488 nm). Propidium iodide fluorescence was detected in the FL2 channel (585/42 nm). 20000 events were observed for each sample. Data collection was performed using CellQuest™ software (Becton Dickinson), and data analysis was carried out with WinMDI version 2.8, provided by Joseph Trotter (Scripps Research Institute, La Jolla, CA).

6.2.9. Microarray analysis

6.2.9.1. Sample preparation and microarray hybridization

RNA samples for microarray analysis were prepared as described in sections 6.2.4.1. (preparation of total RNA) and 6.2.5.2. (preparation of RNA from gradient fractions). All subsequent steps were conducted by the Kompetenzzentrum für Fluoreszente Bioanalytik, Regensburg (<http://www.kfb-regensburg.de>). Quality and quantity of the RNA were determined using an Agilent 2100 bioanalyzer (Agilent Technologies). For the preparation of biotinylated probes, the MessageAmp II Biotin Enhanced Kit (Ambion) was used. Biological sample duplicates were hybridized to Affymetrix Yeast Genome 2.0 Arrays.

6.2.9.2. Microarray data analysis

Raw signal intensities for each probe in the .CEL files were analyzed using version 6.4 of the PARTEK GENOMICS SUITE software (Partek Inc.). Data were filtered by application of an expanded mask file that was based on the *s_cerevisiae.msk* file of Affymetrix, to mask the *S. pombe* probe sets, unspecific probe sets, and replicate probe sets of *S. cerevisiae*. The robust multiarray average (RMA) normalization method was used for background correction (Irizarry et al., 2003), quantile normalization and medianpolish probe set summarization.

For the analysis of total RNA, the final gene list was filtered with a p-value cut-off of 0.05 and a fold change threshold of ≥ 2.5 or ≤ 0.4 . Genes listed as “dubious open reading frames (ORFs)” in the Saccharomyces Genome Database (SGD) were removed.

For the arrays that were hybridized with samples from gradient fractions, a principal component analysis (PCA) revealed a batch effect due to different scanning days. This effect was removed by the batch effect removal tool implemented in the PARTEK software package. In a first step, the translational state (= mRNA abundance in heavy versus light fractions) was calculated for all mRNAs in control and Scp160 depleted cells. This was done with one-way analysis of variance (ANOVA) applying a linear contrast to compare heavy (“H”) with baseline light (“L”) samples. In a second step, the translational state change was calculated for all mRNAs as follows: $(H_{\text{dox}}/L_{\text{dox}}) / (H_{\text{wt}}/L_{\text{wt}})$. The translational state of mRNAs of Scp160 depleted cells were compared to baseline control cells. Genes listed as “dubious open reading frames (ORFs)” in the Saccharomyces Genome Database (SGD) were removed. The final gene list was further filtered by a translational state change cut-off value of ≥ 1.8 or ≤ 0.56 in order to reveal mRNAs with stronger shifts in their translation efficiency.

6.2.9.3. Systematic classification of proteins

For systematic classification of significantly over-represented biological processes and subcellular localizations, gene lists were analyzed on the basis of the MIPS Functional Catalogue Database (FunCatDB) (Ruepp et al., 2004).

6.2.10. Quantitative real-time PCR (qPCR)

Quantitative RT-PCR (qRT-PCR) was performed using the StepOnePlus™ Real-Time PCR System (Applied Biosystems). Reaction mixtures (10 µl final volume) contained 2.5 µl of 1:8 dilutions of the individual cDNA samples, 5 pmol forward and reverse primers (see section 6.1.6.) and Power SYBR® Green PCR Master Mix (Applied Biosystems) as prescribed by the manufacturer. Primers were designed using Primer3 software version 0.4.0 (<http://frodo.wi.mit.edu/primer3/input.htm>) and tested for mispriming or formation of primer-dimers by melting curve analysis of the individual amplification products. The thermocycling profile included an initial denaturation for 10 min at 95°C, followed by 35 cycles of amplification, comprising denaturation at 95°C for 15 sec and annealing/elongation at 60°C for 1 min. After each cycle, a single fluorescence measurement was taken. For melting curve analysis of the amplification products, the temperature was increased in 0.3°C fractions to a final temperature of 95°C (continuous fluorescence measurement). All reactions were run in duplicates and included a negative control (H₂O). Relative quantifications were performed by the comparative CT method (Livak & Schmittgen, 2001).

6.2.11. Immunoprecipitation

6.2.11.1. Covalent coupling of α myc antibody to Protein G beads

For immunoprecipitation experiments, monoclonal mouse α myc antibody 9E11 (Evan et al., 1985) was coupled to magnetic Dynabeads® Protein G (Invitrogen Dynal). 1 ml beads slurry was washed twice with 1 ml 0.1 M sodium phosphate pH 7.0 and divided into four samples. To each sample, 1.25 ml hybridoma supernatant was added and incubated for 40 min at RT on a wheel. Beads were then washed twice with 1 ml 0.1 M sodium phosphate pH 7.0 and twice with 1 ml 0.2 M triethanolamin pH 8.2, pooled and incubated for 30 min at RT in 1 ml 20 mM dimethyl pimelimidate in 0.2 M triethanolamin on a wheel. The supernatant was removed and replaced by 1 ml 50 mM Tris/HCl pH 7.5. After 15 min incubation, beads were washed as follows:

3× in 1 ml 1× PBS/0.1% Tween

2× in 1 ml 1× TBS pH 7.4

1× in 1 ml 0.1 M Glycine/HCl pH 2.5

2× in 1 ml 0.1 M Tris/HCl pH 8.8

2× in 1 ml 1× TBS pH 7.4

Then, beads were taken up in 1 ml of the last buffer (50% slurry) and stored at 4°C.

6.2.11.2. Immunoprecipitation and preparation of RNA

Immunoprecipitation of C-terminally myc9-tagged Scp160 variants, She2 and Khd1 was carried out essentially as described previously (Bohl et al., 2000). 30 OD₆₀₀ units of logarithmically growing cells were harvested and resuspended in 200 µl breaking buffer (50 mM HEPES/KOH pH 7.3, 20 mM potassium acetate, 2 mM EDTA pH 8.0, 0.1% Triton X-100, 5% glycerol, 0.8 U/µl RNasin, 0.5 mM PMSF, 0.25 mM benzamidine). Glass bead lysis was performed by vortexing vigorously four times for 3 min with 1 min pause on ice between the cycles. 100 µl of breaking buffer was added and samples were centrifuged for 2 min at 0.8 × g. The supernatant (T, total extract) was added to Protein G magnetic beads coupled to anti myc antibody (see section 6.4.11.1) (blocked three times for 10 min in breaking buffer containing 0.1 mg/ml tRNA) and incubated for 1 h 15 min on a turning wheel at 4°C. Then, the flowthrough (FT) was removed and beads were washed three times with wash buffer (50 mM Hepes/KOH, 50 mM KOAc, 2 mM magnesium acetate, 0.1% Triton X-100, 5% glycerol). One-third of the beads was resuspended in SDS-PAGE loading buffer for Western analysis (IP). RNA bound to the remaining beads was extracted with phenol-chloroform, ethanol precipitated, resuspended in RQ1 DNase buffer, and treated with RQ1 DNase (Promega). For reverse transcription, the High Capacity cDNA Reverse Transcription Kit (Applied Biosystems) was used with random hexamers as primers and 250 ng RNA input per 20 µl reaction.

6.2.12. Tandem Affinity Purification (TAP)

6.2.12.1. Cell culture and lysis

For TAP purifications, cultures were grown in 2 l YEPD medium to OD₆₀₀ 3.5-4.0. Cells were harvested by centrifugation, washed once with water and resuspended in once cell volume (10-15 ml) cold TAP buffer (100 mM NaCl, 50 mM Tris/HCl pH 7.5, 1.5 mM MgCl₂, 0.15% NP-40) containing 1 mM DTT, 0.5 mM PMSF and 0.25 mM benzamidine. Two cell volumes of

acid-washed glass beads were added, and cells were lysed in a bead mill (Fritsch) using the following milling protocol: 3 x [4 min, 500 rpm, 2 min break]. To remove glass beads and cell debris, lysates were passed through a 50 ml syringe and centrifuged for 10 min at 4000 rpm and 4°C. For preclearing, the extract was subsequently spun for 30 min at 20000 g and 4°C in an SS-34 rotor. The fatty top phase was removed by aspiration, the cleared extract was collected, supplemented with glycerol to a final concentration of 5% and snap-frozen in liquid nitrogen.

6.2.12.2. Purification and TCA precipitation

400 µl IgG Sepharose beads (Amersham Biosciences) were washed three times with cold TAP buffer supplemented with 1 mM DTT and added to the cell lysate. After 1 h incubation on a turning wheel at 4°C, beads were pelleted and transferred to a Mobicol spin column (MoBiTec). Using a syringe and gravity flow, beads were washed with 10 ml TAP buffer containing 0.5 mM DTT. For purifications of Scp160, IgG beads were washed with 20 ml of the same buffer and the second purification step (binding to calmodulin beads) was omitted. To cleave off specifically bound protein complexes, 10 µl TEV protease were added in 150 µl TAP-buffer plus 0.5 mM DTT and incubated for 1 h 20 min on a turning wheel at 16°C. For elution, the column was centrifuged in a table top centrifuge for 1 min at 2000 rpm.

During TEV cleavage, 250 µl calmodulin affinity resin (Stratagene) was washed three times with TAP buffer containing 1 mM DTT and 2 mM CaCl₂, once with the same buffer plus 4 mM CaCl₂, and transferred with 150 µl of the last buffer to a new Mobicol column. TEV cleaved material was eluted from the first column by centrifugation (1 min, 2000 rpm, 4°C) and added to the washed calmodulin beads. After 1 h rotation at 4°C, beads were washed with 5 ml TAP buffer supplemented with 2 mM CaCl₂. 600 µl of elution buffer (10 mM Tris/HCl pH 8.0, 5 mM EDTA, pH 8.0) was added and the samples were incubated for 10 min at 37°C while shaking with 600 rpm. The eluate was collected by centrifugation (1 min, 2000 rpm) and proteins were precipitated with trichloroacetic acid (10% final concentration). To identify interaction partners of the TAP-tagged protein, samples were run on an SDS-PAGE gel; bands of interest were excised and send for mass spec analysis to the protein analysis unit of the university (ZfP; <http://proteinanalytik.web.med.uni-muenchen.de>).

7. Abbreviations

aa	amino acid
Amp	ampicillin
ATP	adenosine triphosphate
bp	basepair
°C	degree centigrade
<i>C. elegans</i>	<i>Caenorhabditis elegans</i>
CHX	cycloheximide
CIP	calf intestine phosphatase
clonNAT	nourseothricin
CSM	complete supplement mix
C-terminal	carboxy terminal
kDa	kilo dalton
<i>D. melanogaster</i>	<i>Drosophila melanogaster</i>
DEPC	diethylpyrocarbonate
DNA	deoxyribonucleic acid
DNase	deoxyribonuclease
dNTP	deoxyribonucleosid triphosphate
DTT	dithiothreitol
dox	doxycycline
ECL	enhanced chemoluminescence
<i>E. coli</i>	<i>Escherichia coli</i>
EDTA	ethylenediaminetetraacetic acid
eEF	eukaryotic elongation factor
eIF	eukaryotic initiation factor
ER	endoplasmic reticulum
et al.	<i>et alii</i> (from Latin, “and others”)
g	gram
x g	relative centrifugal force (rcf)
<i>G. gallus</i>	<i>Gallus gallus</i>
GEF	guanine nucleotide exchange factor
h	hour
<i>H. sapiens</i>	<i>Homo sapiens</i>
HA	hemagglutinin
Hepes	4-(2-hydroxyethyl)-1-piperazineethanesulfonic acid
k	kilo
kb	kilo basepairs
KH-domain	heterogeneous nuclear (hn)RNP K-homology domain
l	litre
LB	Luria Bertani
μ	micro
m	milli
M	molar
mA	milliampere
min	minutes
mRNA	messenger ribonucleic acid
n	nano
NES	nuclear export sequence
NLS	nuclear localization sequence
NP-40	Nonidet P-40 (Igepal-CA-630)

ABBREVIATIONS

NTP	nucleoside triphosphate
nt	nucleotide
OD	optical density
ORF	open reading frame
PAGE	polyacrylamide gelelectrophoresis
PBS	phosphate-buffered saline
PCR	polymerase chain reaction
PEG	polyethylene glycol
pH	potential of hydrogen
P _i	pyrophosphate
RNA	ribonucleic acid
RBD	RNA-binding domain
RBP	RNA-binding protein
RNP	ribonucleoprotein
rpm	revolutions per minute
RT	room temperature
<i>S. cerevisiae</i>	<i>Saccharomyces cerevisiae</i>
SDS	sodium dodecyl sulfate
s	second
S	sedimentation coefficient (Svedberg)
TAP	tandem affinity purification
TCA	trichloroacetic acid
tet	tetracycline
TEV	tobacco etch virus
Tris	trishydroxymethylaminomethane
tRNA	transfer ribonucleic acid
UTR	untranslated region
V	volt
WCE	whole cell extract
wt	wild type
<i>X. laevis</i>	<i>Xenopus laevis</i>
YEP	yeast extract peptone
YNB	yeast nitrogen base

8. References

- Akimitsu N, Tanaka J & Pelletier J (2007)** Translation of nonSTOP mRNA is repressed post-initiation in mammalian cells. *EMBO J* 26:2327-2338.
- Andersen CB, Becker T, Blau M, Anand M, Halic M, et al. (2006)** Structure of eEF3 and the mechanism of transfer RNA release from the E-site. *Nature* 443:663-668.
- Ashley CT, Jr., Wilkinson KD, Reines D & Warren ST (1993)** FMR1 protein: conserved RNP family domains and selective RNA binding. *Science* 262:563-566.
- Ausubel FM, Brent, R., Kingston, R. E., Moore, D. D., Seidman, J. G., Smith, J. A., and Struhl, K. (2000)** Current Protocols in Molecular Biology. Green and Wiley: New York.
- Ayala A, Parrado J, Bougria M & Machado A (1996)** Effect of oxidative stress, produced by cumene hydroperoxide, on the various steps of protein synthesis. Modifications of elongation factor-2. *J Biol Chem* 271:23105-23110.
- Bashirullah A, Halsell SR, Cooperstock RL, Kloc M, Karaiskakis A, et al. (1999)** Joint action of two RNA degradation pathways controls the timing of maternal transcript elimination at the midblastula transition in *Drosophila melanogaster*. *EMBO J* 18:2610-2620.
- Baum S, Bittins M, Frey S & Seedorf M (2004)** Asc1p, a WD40-domain containing adaptor protein, is required for the interaction of the RNA-binding protein Scp160p with polysomes. *Biochem J* 380:823-830.
- Beuth B, Pennell S, Arnvig KB, Martin SR & Taylor IA (2005)** Structure of a Mycobacterium tuberculosis NusA-RNA complex. *EMBO J* 24:3576-3587.
- Bohl F, Kruse C, Frank A, Ferring D & Jansen RP (2000)** She2p, a novel RNA-binding protein tethers ASH1 mRNA to the Myo4p myosin motor via She3p. *EMBO J* 19:5514-5524.
- Braddock DT, Baber JL, Levens D & Clore GM (2002)** Molecular basis of sequence-specific single-stranded DNA recognition by KH domains: solution structure of a complex between hnRNP K KH3 and single-stranded DNA. *EMBO J* 21:3476-3485.
- Brock ML & Shapiro DJ (1983)** Estrogen stabilizes vitellogenin mRNA against cytoplasmic degradation. *Cell* 34:207-214.
- Brykailo MA, Corbett AH & Fridovich-Keil JL (2007a)** Functional overlap between conserved and diverged KH domains in *Saccharomyces cerevisiae* SCP160. *Nucleic Acids Res* 35:1108-1118.
- Brykailo MA, McLane LM, Fridovich-Keil J & Corbett AH (2007b)** Analysis of a predicted nuclear localization signal: implications for the intracellular localization and function of the *Saccharomyces cerevisiae* RNA-binding protein Scp160. *Nucleic Acids Res* 35:6862-6869.
- Ceci M, Gaviraghi C, Gorrini C, Sala LA, Offenhauser N, Marchisio PC & Biffo S (2003)** Release of eIF6 (p27BBP) from the 60S subunit allows 80S ribosome assembly. *Nature* 426:579-584.
- Chang YW & Traugh JA (1998)** Insulin stimulation of phosphorylation of elongation factor 1 (eEF-1) enhances elongation activity. *Eur J Biochem* 251:201-207.
- Chapman R, Sidrauski C & Walter P (1998)** Intracellular signaling from the endoplasmic reticulum to the nucleus. *Annu Rev Cell Dev Biol* 14:459-485.
- Chen JY, Chen JC & Wu JL (2003)** Molecular cloning and functional analysis of zebrafish high-density lipoprotein-binding protein. *Comp Biochem Physiol B Biochem Mol Biol* 136:117-130.

- Cherkasova VA & Hinnebusch AG (2003)** Translational control by TOR and TAP42 through dephosphorylation of eIF2 α kinase GCN2. *Genes Dev* 17:859-872.
- Chial HJ, Giddings TH, Jr., Siewert EA, Hoyt MA & Winey M (1999)** Altered dosage of the *Saccharomyces cerevisiae* spindle pole body duplication gene, *NDC1*, leads to aneuploidy and polyploidy. *Proc Natl Acad Sci U S A* 96:10200-10205.
- Chmiel NH, Rio DC & Doudna JA (2006)** Distinct contributions of KH domains to substrate binding affinity of *Drosophila* P-element somatic inhibitor protein. *RNA* 12:283-291.
- Cho PF, Poulin F, Cho-Park YA, Cho-Park IB, Chicoine JD, Lasko P & Sonenberg N (2005)** A new paradigm for translational control: inhibition via 5'-3' mRNA tethering by Bicoid and the eIF4E cognate 4EHP. *Cell* 121:411-423.
- Cortes A, Huertas D, Fanti L, Pimpinelli S, Marsellach FX, Pina B & Azorin F (1999)** DDP1, a single-stranded nucleic acid-binding protein of *Drosophila*, associates with pericentric heterochromatin and is functionally homologous to the yeast Scp160p, which is involved in the control of cell ploidy. *EMBO J* 18:3820-3833.
- Cuesta R, Hinnebusch AG & Tamame M (1998)** Identification of GCD14 and GCD15, novel genes required for translational repression of GCN4 mRNA in *Saccharomyces cerevisiae*. *Genetics* 148:1007-1020.
- Cunningham KS, Dodson RE, Nagel MA, Shapiro DJ & Schoenberg DR (2000)** Vigilin binding selectively inhibits cleavage of the vitellogenin mRNA 3'-untranslated region by the mRNA endonuclease polysomal ribonuclease 1. *Proc Natl Acad Sci U S A* 97:12498-12502.
- Currie JR & Brown WT (1999)** KH domain-containing proteins of yeast: absence of a fragile X gene homologue. *Am J Med Genet* 84:272-276.
- D'Hulst C & Kooy RF (2009)** Fragile X syndrome: from molecular genetics to therapy. *J Med Genet* 46:577-584.
- Dodson RE & Shapiro DJ (1997)** Vigilin, a ubiquitous protein with 14 K homology domains, is the estrogen-inducible vitellogenin mRNA 3'-untranslated region-binding protein. *J Biol Chem* 272:12249-12252.
- Dubowy J & Macdonald PM (1998)** Localization of mRNAs to the oocyte is common in *Drosophila* ovaries. *Mech Dev* 70:193-195.
- Eberwine J, Miyashiro K, Kacharina JE & Job C (2001)** Local translation of classes of mRNAs that are targeted to neuronal dendrites. *Proc Natl Acad Sci U S A* 98:7080-7085.
- Eisenhaber B, Schneider G, Wildpaner M & Eisenhaber F (2004)** A sensitive predictor for potential GPI lipid modification sites in fungal protein sequences and its application to genome-wide studies for *Aspergillus nidulans*, *Candida albicans*, *Neurospora crassa*, *Saccharomyces cerevisiae* and *Schizosaccharomyces pombe*. *J Mol Biol* 337:243-253.
- Eissenberg JC & Elgin SC (2000)** The HP1 protein family: getting a grip on chromatin. *Curr Opin Genet Dev* 10:204-210.
- Evan GI, Lewis GK, Ramsay G & Bishop JM (1985)** Isolation of monoclonal antibodies specific for human c-myc proto-oncogene product. *Mol Cell Biol* 5:3610-3616.
- Fasken MB & Corbett AH (2009)** Mechanisms of nuclear mRNA quality control. *RNA Biol* 6:237-241.
- Fasken MB, Stewart M & Corbett AH (2008)** Functional significance of the interaction between the mRNA-binding protein, Nab2, and the nuclear pore-associated protein, Mlp1, in mRNA export. *J Biol Chem* 283:27130-27143.
- Fields S (1990)** Pheromone response in yeast. *Trends Biochem Sci* 15:270-273.

REFERENCES

- Frey S (2002)** Charakterisierung von Scp160p, einem mRNA- und ribosomenassoziierten Protein in *Saccharomyces cerevisiae*. *PhD thesis*, University of Heidelberg.
- Frey S, Pool M & Seedorf M (2001)** Scp160p, an RNA-binding, polysome-associated protein, localizes to the endoplasmic reticulum of *Saccharomyces cerevisiae* in a microtubule-dependent manner. *J Biol Chem* 276:15905-15912.
- Galy V, Gadal O, Fromont-Racine M, Romano A, Jacquier A & Nehrbass U (2004)** Nuclear retention of unspliced mRNAs in yeast is mediated by perinuclear Mlp1. *Cell* 116:63-73.
- Gari E, Piedrafita L, Aldea M & Herrero E (1997)** A set of vectors with a tetracycline-regulatable promoter system for modulated gene expression in *Saccharomyces cerevisiae*. *Yeast* 13:837-848.
- Gauss R, Trautwein M, Sommer T & Spang A (2005)** New modules for the repeated internal and N-terminal epitope tagging of genes in *Saccharomyces cerevisiae*. *Yeast* 22:1-12.
- Gautschi M, Lilie H, Funfschilling U, Mun A, Ross S, Lithgow T, Rucknagel P & Rospert S (2001)** RAC, a stable ribosome-associated complex in yeast formed by the DnaK-DnaJ homologs Ssz1p and zuotin. *Proc Natl Acad Sci U S A* 98:3762-3767.
- Gavin AC, Aloy P, Grandi P, Krause R, Boesche M, et al. (2006)** Proteome survey reveals modularity of the yeast cell machinery. *Nature* 440:631-636.
- Gebauer F & Hentze MW (2004)** Molecular mechanisms of translational control. *Nat Rev Mol Cell Biol* 5:827-835.
- Gerbasi VR, Weaver CM, Hill S, Friedman DB & Link AJ (2004)** Yeast Asc1p and mammalian RACK1 are functionally orthologous core 40S ribosomal proteins that repress gene expression. *Mol Cell Biol* 24:8276-8287.
- Gerber AP, Herschlag D & Brown PO (2004)** Extensive association of functionally and cytologically related mRNAs with Puf family RNA-binding proteins in yeast. *PLoS Biol* 2:E79.
- Gerber AP & Keller W (2001)** RNA editing by base deamination: more enzymes, more targets, new mysteries. *Trends Biochem Sci* 26:376-384.
- Gibbs GM, Roelants K & O'Bryan MK (2008)** The CAP superfamily: cysteine-rich secretory proteins, antigen 5, and pathogenesis-related 1 proteins--roles in reproduction, cancer, and immune defense. *Endocr Rev* 29:865-897.
- Gingras AC, Raught B & Sonenberg N (1999)** eIF4 initiation factors: effectors of mRNA recruitment to ribosomes and regulators of translation. *Annu Rev Biochem* 68:913-963.
- Goolsby KM & Shapiro DJ (2003)** RNAi-mediated depletion of the 15 KH domain protein, vigilin, induces death of dividing and non-dividing human cells but does not initially inhibit protein synthesis. *Nucleic Acids Res* 31:5644-5653.
- Grishin NV (2001)** KH domain: one motif, two folds. *Nucleic Acids Res* 29:638-643.
- Groppo R & Richter JD (2009)** Translational control from head to tail. *Curr Opin Cell Biol* 21:444-451.
- Guo M, Aston C, Burchett SA, Dyke C, Fields S, et al. (2003)** The yeast G protein alpha subunit Gpa1 transmits a signal through an RNA binding effector protein Scp160. *Mol Cell* 12:517-524.
- Halbeisen RE, Galgano A, Scherrer T & Gerber AP (2008)** Post-transcriptional gene regulation: from genome-wide studies to principles. *Cell Mol Life Sci* 65:798-813.
- Hasegawa Y, Irie K & Gerber AP (2008)** Distinct roles for Khd1p in the localization and expression of bud-localized mRNAs in yeast. *RNA* 14:2333-2347.
- Hieronimus H & Silver PA (2004)** A systems view of mRNP biology. *Genes Dev* 18:2845-2860.

REFERENCES

- Hinnebusch AG (2005)** Translational regulation of GCN4 and the general amino acid control of yeast. *Annu Rev Microbiol* 59:407-450.
- Hirayama T, Maeda T, Saito H & Shinozaki K (1995)** Cloning and characterization of seven cDNAs for hyperosmolarity-responsive (HOR) genes of *Saccharomyces cerevisiae*. *Mol Gen Genet* 249:127-138.
- Hogan DJ, Riordan DP, Gerber AP, Herschlag D & Brown PO (2008)** Diverse RNA-binding proteins interact with functionally related sets of RNAs, suggesting an extensive regulatory system. *PLoS Biol* 6:e255.
- Huertas D, Cortes A, Casanova J & Azorin F (2004)** *Drosophila* DDP1, a multi-KH-domain protein, contributes to centromeric silencing and chromosome segregation. *Curr Biol* 14:1611-1620.
- Irie K, Tadauchi T, Takizawa PA, Vale RD, Matsumoto K & Herskowitz I (2002)** The Khd1 protein, which has three KH RNA-binding motifs, is required for proper localization of ASH1 mRNA in yeast. *EMBO J* 21:1158-1167.
- Irizarry RA, Hobbs B, Collin F, Beazer-Barclay YD, Antonellis KJ, Scherf U & Speed TP (2003)** Exploration, normalization, and summaries of high density oligonucleotide array probe level data. *Biostatistics* 4:249-264.
- Jackson CL & Kepes F (1994)** BFR1, a multicopy suppressor of brefeldin A-induced lethality, is implicated in secretion and nuclear segregation in *Saccharomyces cerevisiae*. *Genetics* 137:423-437.
- Jackson RJ, Hellen CU & Pestova TV (2010)** The mechanism of eukaryotic translation initiation and principles of its regulation. *Nat Rev Mol Cell Biol* 11:113-127.
- Janke C, Magiera MM, Rathfelder N, Taxis C, Reber S, et al. (2004)** A versatile toolbox for PCR-based tagging of yeast genes: new fluorescent proteins, more markers and promoter substitution cassettes. *Yeast* 21:947-962.
- Jin P & Warren ST (2000)** Understanding the molecular basis of fragile X syndrome. *Hum Mol Genet* 9:901-908.
- Jones AR & Schedl T (1995)** Mutations in *gld-1*, a female germ cell-specific tumor suppressor gene in *Caenorhabditis elegans*, affect a conserved domain also found in Src-associated protein Sam68. *Genes Dev* 9:1491-1504.
- Kanamori H, Dodson RE & Shapiro DJ (1998)** In vitro genetic analysis of the RNA binding site of vigilin, a multi-KH-domain protein. *Mol Cell Biol* 18:3991-4003.
- Kaufman RJ (1999)** Stress signaling from the lumen of the endoplasmic reticulum: coordination of gene transcriptional and translational controls. *Genes Dev* 13:1211-1233.
- Kedersha N, Stoecklin G, Ayodele M, Yacono P, Lykke-Andersen J, et al. (2005)** Stress granules and processing bodies are dynamically linked sites of mRNP remodeling. *J Cell Biol* 169:871-884.
- Keene JD (2007)** RNA regulons: coordination of post-transcriptional events. *Nat Rev Genet* 8:533-543.
- Knop M, Siegers K, Pereira G, Zachariae W, Winsor B, Nasmyth K & Schiebel E (1999)** Epitope tagging of yeast genes using a PCR-based strategy: more tags and improved practical routines. *Yeast* 15:963-972.
- Kress TL, Krogan NJ & Guthrie C (2008)** A single SR-like protein, Npl3, promotes pre-mRNA splicing in budding yeast. *Mol Cell* 32:727-734.
- Kruse C, Grunweller A, Notbohm H, Kugler S, Purschke WG & Muller PK (1996)** Evidence for a novel cytoplasmic tRNA-protein complex containing the KH-multidomain protein vigilin. *Biochem J* 320 (Pt 1):247-252.
- Kruse C, Grunweller A, Willkomm DK, Pfeiffer T, Hartmann RK & Muller PK (1998)** tRNA is entrapped in similar, but distinct, nuclear and cytoplasmic ribonucleoprotein complexes, both of which contain vigilin and elongation factor 1 alpha. *Biochem J* 329 (Pt 3):615-621.

REFERENCES

- Kruse C, Willkomm D, Gebken J, Schuh A, Stossberg H, Vollbrandt T & Muller PK (2003)** The multi-KH protein vigilin associates with free and membrane-bound ribosomes. *Cell Mol Life Sci* 60:2219-2227.
- Kruse C, Willkomm DK, Grunweller A, Vollbrandt T, Sommer S, et al. (2000)** Export and transport of tRNA are coupled to a multi-protein complex. *Biochem J* 346 Pt 1:107-115.
- Laemmli UK (1970)** Cleavage of structural proteins during the assembly of the head of bacteriophage T4. *Nature* 227:680-685.
- Lang BD & Fridovich-Keil JL (2000)** Scp160p, a multiple KH-domain protein, is a component of mRNP complexes in yeast. *Nucleic Acids Res* 28:1576-1584.
- Lang BD, Li A, Black-Brewster HD & Fridovich-Keil JL (2001)** The brefeldin A resistance protein Bfr1p is a component of polyribosome-associated mRNP complexes in yeast. *Nucleic Acids Res* 29:2567-2574.
- Lee B, Udagawa T, Singh CR & Asano K (2007)** Yeast phenotypic assays on translational control. *Methods Enzymol* 429:105-137.
- Lesage G & Bussey H (2006)** Cell wall assembly in *Saccharomyces cerevisiae*. *Microbiol Mol Biol Rev* 70:317-343.
- Levin DE (2005)** Cell wall integrity signaling in *Saccharomyces cerevisiae*. *Microbiol Mol Biol Rev* 69:262-291.
- Li AM, Vargas CA, Brykailo MA, Openo KK, Corbett AH & Fridovich-Keil JL (2004)** Both KH and non-KH domain sequences are required for polyribosome association of Scp160p in yeast. *Nucleic Acids Res* 32:4768-4775.
- Li AM, Watson A & Fridovich-Keil JL (2003)** Scp160p associates with specific mRNAs in yeast. *Nucleic Acids Res* 31:1830-1837.
- Liu Z, Luyten I, Bottomley MJ, Messias AC, Houngninou-Molango S, Sprangers R, Zanier K, Kramer A & Sattler M (2001)** Structural basis for recognition of the intron branch site RNA by splicing factor 1. *Science* 294:1098-1102.
- Livak KJ & Schmittgen TD (2001)** Analysis of relative gene expression data using real-time quantitative PCR and the 2(-Delta Delta C(T)) Method. *Methods* 25:402-408.
- Lund MK & Guthrie C (2005)** The DEAD-box protein Dbp5p is required to dissociate Mex67p from exported mRNPs at the nuclear rim. *Mol Cell* 20:645-651.
- Lunde BM, Moore C & Varani G (2007)** RNA-binding proteins: modular design for efficient function. *Nat Rev Mol Cell Biol* 8:479-490.
- Mahoney WC & Duksin D (1979)** Biological activities of the two major components of tunicamycin. *J Biol Chem* 254:6572-6576.
- Mangus DA, Evans MC & Jacobson A (2003)** Poly(A)-binding proteins: multifunctional scaffolds for the post-transcriptional control of gene expression. *Genome Biol* 4:223.
- Marsellach FX, Huertas D & Azorin F (2006)** The multi-KH domain protein of *Saccharomyces cerevisiae* Scp160p contributes to the regulation of telomeric silencing. *J Biol Chem* 281:18227-18235.
- McKee AE & Silver PA (2007)** Systems perspectives on mRNA processing. *Cell Res* 17:581-590.
- Meisenberg G SW (1998)** Principles of medical biochemistry. Mosby: St. Louis, Missouri.
- Melamed D & Arava Y (2007)** Genome-wide analysis of mRNA polysomal profiles with spotted DNA microarrays. *Methods Enzymol* 431:177-201.
- Melamed D, Eliyahu E & Arava Y (2009)** Exploring translation regulation by global analysis of ribosomal association. *Methods* 48:301-305.

- Mendelsohn BA, Li AM, Vargas CA, Riehm K, Watson A & Fridovich-Keil JL (2003)** Genetic and biochemical interactions between SCP160 and EAP1 in yeast. *Nucleic Acids Res* 31:5838-5847.
- Moore MJ (2005)** From birth to death: the complex lives of eukaryotic mRNAs. *Science* 309:1514-1518.
- Morita K, Flemming AJ, Sugihara Y, Mochii M, Suzuki Y, et al. (2002)** A *Caenorhabditis elegans* TGF-beta, DBL-1, controls the expression of LON-1, a PR-related protein, that regulates polyploidization and body length. *EMBO J* 21:1063-1073.
- Moukadiri I, Armero J, Abad A, Sentandreu R & Zueco J (1997)** Identification of a mannoprotein present in the inner layer of the cell wall of *Saccharomyces cerevisiae*. *J Bacteriol* 179:2154-2162.
- Mugnier P & Tuite MF (1999)** Translation termination and its regulation in eukaryotes: recent insights provided by studies in yeast. *Biochemistry (Mosc)* 64:1360-1366.
- Nelson MR, Luo H, Vari HK, Cox BJ, Simmonds AJ, Krause HM, Lipshitz HD & Smibert CA (2007)** A multiprotein complex that mediates translational enhancement in *Drosophila*. *J Biol Chem* 282:34031-34038.
- Nielsen DA & Shapiro DJ (1990)** Estradiol and estrogen receptor-dependent stabilization of a minivitellogenin mRNA lacking 5,100 nucleotides of coding sequence. *Mol Cell Biol* 10:371-376.
- Nilsson J, Sengupta J, Frank J & Nissen P (2004)** Regulation of eukaryotic translation by the RACK1 protein: a platform for signalling molecules on the ribosome. *EMBO Rep* 5:1137-1141.
- O'Rourke SM & Herskowitz I (2002)** A third osmosensing branch in *Saccharomyces cerevisiae* requires the Msb2 protein and functions in parallel with the Sho1 branch. *Mol Cell Biol* 22:4739-4749.
- Paquin N & Chartrand P (2008)** Local regulation of mRNA translation: new insights from the bud. *Trends Cell Biol* 18:105-111.
- Parker R & Sheth U (2007)** P bodies and the control of mRNA translation and degradation. *Mol Cell* 25:635-646.
- Parker R & Song H (2004)** The enzymes and control of eukaryotic mRNA turnover. *Nat Struct Mol Biol* 11:121-127.
- Peters HI, Chang YW & Traugh JA (1995)** Phosphorylation of elongation factor 1 (EF-1) by protein kinase C stimulates GDP/GTP-exchange activity. *Eur J Biochem* 234:550-556.
- Petersen CP, Bordeleau ME, Pelletier J & Sharp PA (2006)** Short RNAs repress translation after initiation in mammalian cells. *Mol Cell* 21:533-542.
- Preiss T & Hentze MW (2003)** Starting the protein synthesis machine: eukaryotic translation initiation. *Bioessays* 25:1201-1211.
- Puig O, Caspary F, Rigaut G, Rutz B, Bouveret E, Bragado-Nilsson E, Wilm M & Seraphin B (2001)** The tandem affinity purification (TAP) method: a general procedure of protein complex purification. *Methods* 24:218-229.
- Raychaudhuri S, Fontanes V, Banerjee R, Bernavichute Y & Dasgupta A (2006)** Zuo1in, a DnaJ molecular chaperone, stimulates cap-independent translation in yeast. *Biochem Biophys Res Commun* 350:788-795.
- Rhoads RE (1999)** Signal transduction pathways that regulate eukaryotic protein synthesis. *J Biol Chem* 274:30337-30340.
- Rhoads RE (2009)** eIF4E: new family members, new binding partners, new roles. *J Biol Chem* 284:16711-16715.
- Rigaut G, Shevchenko A, Rutz B, Wilm M, Mann M & Seraphin B (1999)** A generic protein purification method for protein complex characterization and proteome exploration. *Nat Biotechnol* 17:1030-1032.

REFERENCES

- Rodriguez MM, Ron D, Touhara K, Chen CH & Mochly-Rosen D (1999)** RACK1, a protein kinase C anchoring protein, coordinates the binding of activated protein kinase C and select pleckstrin homology domains in vitro. *Biochemistry* 38:13787-13794.
- Roy A, Lu CF, Marykwas DL, Lipke PN & Kurjan J (1991)** The AGA1 product is involved in cell surface attachment of the *Saccharomyces cerevisiae* cell adhesion glycoprotein a-agglutinin. *Mol Cell Biol* 11:4196-4206.
- Rozen F, Edery I, Meerovitch K, Dever TE, Merrick WC & Sonenberg N (1990)** Bidirectional RNA helicase activity of eucaryotic translation initiation factors 4A and 4F. *Mol Cell Biol* 10:1134-1144.
- Ruegsegger U, Leber JH & Walter P (2001)** Block of HAC1 mRNA translation by long-range base pairing is released by cytoplasmic splicing upon induction of the unfolded protein response. *Cell* 107:103-114.
- Ruepp A, Zollner A, Maier D, Albermann K, Hani J, et al. (2004)** The FunCat, a functional annotation scheme for systematic classification of proteins from whole genomes. *Nucleic Acids Res* 32:5539-5545.
- Sambrook J, Russel, D. W. (2001)** Molecular Cloning. A Laboratory Manual. Cold Spring Harbor Laboratory Press: New York.
- Sanchez-Diaz P & Penalva LO (2006)** Post-transcription meets post-genomic: the saga of RNA binding proteins in a new era. *RNA Biol* 3:101-109.
- Schmid M & Jensen TH (2008)** The exosome: a multipurpose RNA-decay machine. *Trends Biochem Sci* 33:501-510.
- Sengupta J, Nilsson J, Gursky R, Spahn CM, Nissen P & Frank J (2004)** Identification of the versatile scaffold protein RACK1 on the eukaryotic ribosome by cryo-EM. *Nat Struct Mol Biol* 11:957-962.
- Sezen B, Seedorf M & Schiebel E (2009)** The SESA network links duplication of the yeast centrosome with the protein translation machinery. *Genes Dev* 23:1559-1570.
- Shatkin AJ & Manley JL (2000)** The ends of the affair: capping and polyadenylation. *Nat Struct Biol* 7:838-842.
- Shepard KA, Gerber AP, Jambhekar A, Takizawa PA, Brown PO, Herschlag D, DeRisi JL & Vale RD (2003)** Widespread cytoplasmic mRNA transport in yeast: identification of 22 bud-localized transcripts using DNA microarray analysis. *Proc Natl Acad Sci U S A* 100:11429-11434.
- Sikorski RS & Hieter P (1989)** A system of shuttle vectors and yeast host strains designed for efficient manipulation of DNA in *Saccharomyces cerevisiae*. *Genetics* 122:19-27.
- Siomi H, Choi M, Siomi MC, Nussbaum RL & Dreyfuss G (1994)** Essential role for KH domains in RNA binding: impaired RNA binding by a mutation in the KH domain of FMR1 that causes fragile X syndrome. *Cell* 77:33-39.
- Siomi H, Matunis MJ, Michael WM & Dreyfuss G (1993)** The pre-mRNA binding K protein contains a novel evolutionarily conserved motif. *Nucleic Acids Res* 21:1193-1198.
- Sivan G, Kedersha N & Elroy-Stein O (2007)** Ribosomal slowdown mediates translational arrest during cellular division. *Mol Cell Biol* 27:6639-6646.
- Svitkin YV, Herdy B, Costa-Mattioli M, Gingras AC, Raught B & Sonenberg N (2005)** Eukaryotic translation initiation factor 4E availability controls the switch between cap-dependent and internal ribosomal entry site-mediated translation. *Mol Cell Biol* 25:10556-10565.
- Tarun SZ, Jr., Wells SE, Deardorff JA & Sachs AB (1997)** Translation initiation factor eIF4G mediates in vitro poly(A) tail-dependent translation. *Proc Natl Acad Sci U S A* 94:9046-9051.
- Taylor DJ FJ, Kinzy TG (2007)** Structure and function of the eukaryotic ribosome and elongation factors. In: Mathews MB SN, Hershey JWB, ed. *Translational Control in Biology and Medicine*. Cold Spring Harbor Laboratory Press. 59-86.

- Tran EJ, Zhou Y, Corbett AH & Wentz SR (2007)** The DEAD-box protein Dbp5 controls mRNA export by triggering specific RNA:protein remodeling events. *Mol Cell* 28:850-859.
- Travers KJ, Patil CK, Wodicka L, Lockhart DJ, Weissman JS & Walter P (2000)** Functional and genomic analyses reveal an essential coordination between the unfolded protein response and ER-associated degradation. *Cell* 101:249-258.
- Uknes S, Mauch-Mani B, Moyer M, Potter S, Williams S, et al. (1992)** Acquired resistance in Arabidopsis. *Plant Cell* 4:645-656.
- Valverde R, Edwards L & Regan L (2008)** Structure and function of KH domains. *FEBS J* 275:2712-2726.
- Van Dyke N, Baby J & Van Dyke MW (2006)** Stm1p, a ribosome-associated protein, is important for protein synthesis in *Saccharomyces cerevisiae* under nutritional stress conditions. *J Mol Biol* 358:1023-1031.
- Van Dyke N, Pickering BF & Van Dyke MW (2009)** Stm1p alters the ribosome association of eukaryotic elongation factor 3 and affects translation elongation. *Nucleic Acids Res* 37:6116-6125.
- Vollbrandt T, Willkomm D, Stossberg H & Kruse C (2004)** Vigilin is co-localized with 80S ribosomes and binds to the ribosomal complex through its C-terminal domain. *Int J Biochem Cell Biol* 36:1306-1318.
- Wang Q, Zhang Z, Blackwell K & Carmichael GG (2005)** Vigilins bind to promiscuously A-to-I-edited RNAs and are involved in the formation of heterochromatin. *Curr Biol* 15:384-391.
- Warner JR (1999)** The economics of ribosome biosynthesis in yeast. *Trends Biochem Sci* 24:437-440.
- Weber V, Wernitznig A, Hager G, Harata M, Frank P & Wintersberger U (1997)** Purification and nucleic-acid-binding properties of a *Saccharomyces cerevisiae* protein involved in the control of ploidy. *Eur J Biochem* 249:309-317.
- Wells SE, Hillner PE, Vale RD & Sachs AB (1998)** Circularization of mRNA by eukaryotic translation initiation factors. *Mol Cell* 2:135-140.
- Wiedmann B, Sakai H, Davis TA & Wiedmann M (1994)** A protein complex required for signal-sequence-specific sorting and translocation. *Nature* 370:434-440.
- Wintersberger U, Kuhne C & Karwan A (1995)** Scp160p, a new yeast protein associated with the nuclear membrane and the endoplasmic reticulum, is necessary for maintenance of exact ploidy. *Yeast* 11:929-944.
- Wishart JA, Hayes A, Wardleworth L, Zhang N & Oliver SG (2005)** Doxycycline, the drug used to control the tet-regulatable promoter system, has no effect on global gene expression in *Saccharomyces cerevisiae*. *Yeast* 22:565-569.
- Wotton D, Freeman K & Shore D (1996)** Multimerization of Hsp42p, a novel heat shock protein of *Saccharomyces cerevisiae*, is dependent on a conserved carboxyl-terminal sequence. *J Biol Chem* 271:2717-2723.
- Yan W, Schilke B, Pfund C, Walter W, Kim S & Craig EA (1998)** Zuo1p, a ribosome-associated DnaJ molecular chaperone. *EMBO J* 17:4809-4817.
- Yin QY, de Groot PW, Dekker HL, de Jong L, Klis FM & de Koster CG (2005)** Comprehensive proteomic analysis of *Saccharomyces cerevisiae* cell walls: identification of proteins covalently attached via glycosylphosphatidylinositol remnants or mild alkali-sensitive linkages. *J Biol Chem* 280:20894-20901.
- Zhang M & Green MR (2001)** Identification and characterization of yUAP/Sub2p, a yeast homolog of the essential human pre-mRNA splicing factor hUAP56. *Genes Dev* 15:30-35.
- Zhao J, Hyman L & Moore C (1999)** Formation of mRNA 3' ends in eukaryotes: mechanism, regulation, and interrelationships with other steps in mRNA synthesis. *Microbiol Mol Biol Rev* 63:405-445.

REFERENCES

Zhou J, Wang Q, Chen LL & Carmichael GG (2008) On the mechanism of induction of heterochromatin by the RNA-binding protein vigilin. *RNA* 14:1773-1781.

Zhou Y, Mah TF, Greenblatt J & Friedman DI (2002) Evidence that the KH RNA-binding domains influence the action of the E. coli NusA protein. *J Mol Biol* 318:1175-1188.

9. Appendix

Parts of this work have been submitted for publication:

Schreck H, Mayer A, Cramer P, Jansen R-P (2010) Translational control by the yeast multi-KH domain protein Scp160 contributes to control of ploidy. *Nucleic Acids Res* (submitted)

10. Curriculum Vitae

Name	Heidrun Schreck
Geburtsdatum	26.05.1981
Geburtsort	Engelskirchen
Nationalität	deutsch
Familienstand	ledig

seit 07.2006 **Promotion**
bei Prof. Dr. Ralf-Peter Jansen, Genzentrum,
Ludwig-Maximilians-Universität München (LMU)
im Rahmen der International Max Planck Research School for Molecular
and Cellular Life Sciences (IMPRS-LS), Martinsried

08.2000 – 06.2006 **Studium Diplom-Biotechnologie**
Westfälische Wilhelms-Universität Münster
Diplomarbeit bei Prof. Dr. Paul Tudzynski, Institut für Botanik

08.1991 – 05.2000 **Freiherr-vom-Stein-Gymnasium Rösrath**
Allgemeine Hochschulreife

Conferences/Posters:

Schreck H, Mayer A, Jansen RP. Yeast Scp160 - A ploidy maintenance factor involved in translational control. Translational Control. Cold Spring Harbor Laboratories, New York, USA. 09/2008

Schreck H, Jansen RP. Yeast Scp160 – From mRNA binding to translational control. EMBO Conference on Protein Synthesis and Translational Control - partnered with Cold Spring Harbor Laboratories. EMBL Heidelberg, Germany. 09/2007

11. Acknowledgement

Allen, die zum Gelingen dieser Arbeit beigetragen haben, möchte ich ganz herzlich danken, insbesondere...

... meinem Doktorvater Ralf-Peter Jansen dafür, dass ich dieses spannende und vielseitige Projekt bearbeiten durfte. Danke, dass du immer ein offenes Ohr für mich hattest. Ich kann dir gar nicht genug für das Vertrauen danken, das du mir dadurch erwiesen hast, dass ich meine Arbeit auf mich selbst gestellt in München beenden durfte. Die vergangenen eineinhalb Jahre hätten für mich sonst anders ausgesehen.

... meinem Thesis Advisory Committee-Mitglied Klaus Förstemann für angeregte und hilfreiche Diskussionen über mein Projekt, für deine Bereitschaft, mir nach dem Wegzug der AG Jansen in Laborangelegenheiten zur Seite zu stehen, und die Erstellung des Zweitgutachtens.

... dem zweiten Mitglied meines Thesis Advisory Committees, Gunter Meister, für hilfreiche Vorschläge zu meiner Arbeit.

... den alten und neuen Mitgliedern der AG Jansen für die gemeinsame Zeit im Labor und für sonstige, weniger Labor-bezogene Aktivitäten. Es hat immer Spaß gemacht mit euch. Susi, danke für deine Unterstützung und gemeinsames Herunterwürgen des Mensa-Essens; du bist die Beste! Stephan, danke für das gemeinsame Bewältigen der ersten Post-AG-Jansen-Zeit und viele Gespräche über Mountain Bikes und TransAlp. Maria, danke für gemeinsame sportliche Aktivitäten, diverse Feiern, schlechte-Filme-Gucken, und für deine Freundschaft.

... Katja Strässer und allen Mitgliedern des Strässer Labs für gemeinsame Laborseminare und schöne Weihnachtsfeiern. Lina, danke für die Einführung in die Geheimnisse der real-time PCR, interessante Diskussionen über das Schicksal als PhD student und Quatschen in gemeinsamen Pausen.

... Petra, Kai und Malte für die "Wiederbelebung" meines Labors und regelmässige Kuchenzufuhr.

... Andreas Mayer für unermüdliche Neu- und Re-Analysen meiner Microarray-Daten. Ohne deine Hilfe wäre alles viel schwieriger gewesen.

... Eli van der Sluis für Hilfe im Kampf gegen die Gradientenmaschine.

~~~    ~~~    ~~~

... meinen Eltern: danke für eure immerwährende Unterstützung, euer Interesse, euer Engagement und eure Liebe. Ich weiß, dass ich mich immer auf euch verlassen kann.

... meinem Jens. Danke, dass du mir beim Durchhalten geholfen und meine wechselhaften Stimmungen geduldig ertragen hast. Mit dir ist alles schön, und ich wünsche mir, dass das auf Ewig so bleibt. Ich liebe dich.